



Measurement of the W -boson mass and width with the ATLAS detector using proton–proton collisions at $\sqrt{s} = 7$ TeV

The ATLAS Collaboration

Proton–proton data recorded by the ATLAS detector in 2011, at a centre-of-mass energy of 7 TeV, have been used for an improved determination of the W -boson mass and a first measurement of the W -boson width at the LHC. Recent fits to the proton parton distribution functions are incorporated in the measurement procedure and an improved statistical method is used to increase the measurement precision. The measurement of the W -boson mass yields a value of $m_W = 80366.5 \pm 9.8$ (stat.) ± 12.5 (syst.) MeV = 80366.5 ± 15.9 MeV, and the width is measured as $\Gamma_W = 2202 \pm 32$ (stat.) ± 34 (syst.) MeV = 2202 ± 47 MeV. The first uncertainty components are statistical and the second correspond to the experimental and physics-modelling systematic uncertainties. Both results are consistent with the expectation from fits to electroweak precision data. The present measurement of m_W is compatible with and supersedes the previous measurement performed using the same data.

Contents

1	Introduction	2
2	ATLAS detector	3
3	Measurement overview and analysis strategy	4
3.1	Data samples and event simulation	4
3.2	Selection of electrons and muons and reconstruction of the recoil	5
3.3	W -boson kinematics and event selection	5
3.4	W -boson mass analysis updates	6
3.5	Statistical analysis	7
4	Experimental corrections and uncertainties	9
4.1	Uncertainty propagation	9
4.2	Sources of uncertainty	9
5	Physics corrections and uncertainties	10
5.1	Electroweak uncertainties	10
5.2	QCD model and uncertainties	10
6	Improved measurement of the W-boson mass	11
6.1	Results with CT10nnlo and consistency tests	11
6.2	Impact of updated parton distribution functions	12
6.3	Results and discussion	15
6.4	Combination	20
7	Measurement of the W-boson width	21
7.1	Overview	21
7.2	Results and discussion	22
7.3	Combination	24
8	Simultaneous determination of the W-boson mass and width	26
9	Conclusion	27

1 Introduction

At lowest order in the Standard Model (SM) electroweak theory [1–3] the W -boson mass, m_W , can be expressed solely as a function of the Z -boson mass, m_Z , the fine-structure constant, α , and the Fermi constant, G_F . Higher-order corrections introduce an additional dependence of the W -boson mass on the gauge couplings and the masses of the heavy particles of the SM, such as the top-quark mass, m_t , and the Higgs boson mass, m_H [4, 5]. In extended theories, the loop corrections receive contributions from additional particles and interactions. The consistency of the SM and potential effects of new physics can therefore be probed by comparing the measured values of m_W with the results of global fits to the relevant physical parameters [6–8]. The SM fit yields $m_W^{\text{SM}} = 80355 \pm 6$ MeV [6, 7]. The present

experimental situation is characterised by a significant tension between the precise measurement from the CDF Collaboration, $m_W = 80433.5 \pm 9.4$ MeV [9], and the average of the LEP [10], D0 [11], ATLAS [12] and LHCb [13] measurements, $m_W = 80369.2 \pm 13.3$ MeV [14].

The electroweak theory also predicts the total decay width of the W boson, Γ_W . It is expected to be equal to the sum of the partial widths over three generations of lepton doublets and two generations of quark doublets, yielding an expected value of $\Gamma_W^{\text{SM}} = 2088 \pm 1$ MeV [6]. New particle candidates that couple to the W boson and are lighter than m_W would open a new decay channel and alter Γ_W [15]. Examples are supersymmetric models in which the W boson decays into the lightest super-partner of the charged gauge bosons and the lightest super-partner of the neutral gauge bosons [16]. The current world average of W -boson width determinations yields a value of $\Gamma_W = 2085 \pm 42$ MeV [17], and is based on measurements at LEP-2 [10] and the Tevatron [18, 19]. No measurement of Γ_W has been previously performed at the Large Hadron Collider (LHC).

In this paper, an improved measurement of the W -boson mass as well as a first measurement of its width is presented, which is based on data from $\sqrt{s} = 7$ TeV recorded by the ATLAS detector in 2011, i.e., the same data as was used for the first measurement of m_W at the LHC [12]. This was based on a χ^2 considering statistical uncertainties only, where systematic uncertainties were included a posteriori through variations of the physics and calibration models within their uncertainties (the so-called ‘offset’ method).

The present analysis uses an improved statistic based on the profile likelihood (PLH) [20]. This technique performs a simultaneous determination of m_W together with a set of nuisance parameters describing the experimental and modelling uncertainties. The nuisance parameters are adjusted to optimally describe the data, yielding an overall improved model and some reduction in uncertainty compared with the fitting technique used previously. With few sub-dominant exceptions, the sources of uncertainty considered in this measurement are either of experimental nature, or phenomenological, with model parameters derived from the data. A nuisance parameter representation is therefore adequate and the PLH technique can be applied. The measurement of Γ_W relies on the same PLH statistic and on the same physics, detector and background model as those used for the determination of m_W .

Recent parton distribution functions (PDFs) are studied within this work, and the dependence of the measurement results on the assumed PDF set is presented and discussed. The present analysis also aims at consolidating the earlier result of ATLAS, in the perspective of the latest measurement by CDF.

2 ATLAS detector

The ATLAS experiment [21] is a multipurpose particle detector with a forward–backward symmetric cylindrical geometry. It consists of an inner tracking detector surrounded by a thin superconducting solenoid, electromagnetic and hadronic calorimeters, and a muon spectrometer incorporating three large superconducting toroid magnets¹.

The inner-detector system (ID) is immersed in a 2 T axial magnetic field and provides charged-particle tracking in the range of $|\eta| < 2.5$. At small radii, a high-granularity silicon pixel detector covers the vertex

¹ ATLAS uses a right-handed coordinate system with its origin at the nominal interaction point (IP) in the centre of the detector and the z -axis along the beam pipe. The x -axis points from the IP to the centre of the LHC ring, and the y -axis points upwards. Cylindrical coordinates (r, ϕ) are used in the transverse plane, ϕ being the azimuthal angle around the z -axis. The pseudorapidity is defined in terms of the polar angle θ as $\eta = -\ln \tan(\theta/2)$. Angular distance is measured in units of $\Delta R \equiv \sqrt{(\Delta\eta)^2 + (\Delta\phi)^2}$.

region and typically provides three measurements per track. It is followed by the silicon microstrip tracker, which usually provides eight measurement points per track. These silicon detectors are complemented by a gas-filled straw-tube transition radiation tracker, which enables radially extended track reconstruction within $|\eta| = 2.0$. The transition radiation tracker also provides electron identification information based on the fraction of hits (typically 35 in total) above a higher energy-deposit threshold corresponding to transition radiation.

The calorimeter system covers the pseudorapidity range $|\eta| < 4.9$. Within the region $|\eta| < 3.2$, electromagnetic (EM) calorimetry is provided by high-granularity lead/liquid-argon (LAr) calorimeters, with an additional thin LAr presampler covering $|\eta| < 1.8$ to correct for upstream energy-loss fluctuations. The EM calorimeter is divided into a barrel section covering $|\eta| < 1.475$ and two endcap sections covering $1.375 < |\eta| < 3.2$. For $|\eta| < 2.5$, it is divided into three layers in depth, which are finely segmented in η and ϕ . Hadronic calorimetry is provided by a steel/scintillator-tile calorimeter, segmented into three barrel structures within $|\eta| = 1.7$ and two copper/LAr hadronic endcap calorimeters covering $1.5 < |\eta| < 3.2$. The solid-angle coverage is completed with forward copper/LAr and tungsten/LAr calorimeter modules in $3.1 < |\eta| < 4.9$, optimised for electromagnetic and hadronic measurements, respectively.

The muon spectrometer (MS) comprises separate trigger and high-precision tracking chambers measuring the deflection of muons in a magnetic field generated by superconducting air-core toroids. The precision chamber system covers the region $|\eta| < 2.7$ with three layers of monitored drift tubes, complemented by cathode strip chambers in the forward region. The muon trigger system covers the range $|\eta| < 2.4$ with resistive plate chambers in the barrel, and thin gap chambers in the endcap regions.

A three-level trigger system is used to select events for offline analysis [22]. The level-1 trigger is implemented in hardware and uses a subset of detector information to reduce the event rate to a design value of at most 75 kHz. This is followed by two software-based trigger levels that together reduce the event rate to about 300 Hz. A software suite [23] is used in data simulation, in the reconstruction and analysis of real and simulated data, in detector operations, and in the trigger and data acquisition systems of the experiment.

3 Measurement overview and analysis strategy

3.1 Data samples and event simulation

The data sample consists of $W \rightarrow e\nu$ and $W \rightarrow \mu\nu$ candidate events, collected in 2011 with the ATLAS detector in proton–proton collisions at the LHC, at a centre-of-mass energy of $\sqrt{s} = 7$ TeV. The data collected with all relevant detector systems operational correspond to approximately 4.6 fb^{-1} and 4.1 fb^{-1} of integrated luminosity in the electron and muon channels, respectively.

The POWHEG Monte Carlo (MC) generator (v1/r1556) [24–26] is used for the simulation of W - and Z -boson production and decay in the electron, muon, and τ -lepton channels, and is interfaced to PYTHIA 8 (v8.170) for the modelling of the parton shower, hadronisation, and underlying event [27, 28]. Parton shower and underlying event parameters are set according to the AZNLO tune [29]. The CT10 PDF set [30] is used for the hard process, and the CTEQ6L1 PDF set [31] is used in the parton shower. The Z -boson simulation includes the effect of virtual photon exchange. The W - and Z -boson rapidity and p_T distributions are reweighted to optimise the description of the data, as described in Section 5.2. The change in the final-state distributions from updating the distributions to more recent PDFs is evaluated using POWHEG.

QED final-state radiation (FSR) is simulated using PHOTOS (v2.154) [32]. Decays of τ -leptons are handled by PYTHIA 8, taking into account polarisation effects. The W - and Z -boson event yields are normalised according to their measured cross sections, and the experimental uncertainties of 1.8% and 2.3% are assigned to the W^+/Z and W^-/Z production cross-section ratios, respectively [33]. The W -boson production samples assume $m_W = 80399$ MeV and $\Gamma_W = 2085$ MeV.

Background processes such as top-quark pair and single-top-quark production are modelled using the MC@NLO MC generator (v4.01) [34–36], interfaced to HERWIG and JIMMY for the parton shower. Gauge-boson pair production (WW , WZ , ZZ) is simulated with HERWIG (v6.520). The CT10 PDF set is used in all these samples.

The response of the ATLAS detector is simulated using a software suite [37] based on GEANT4 [38]. The hard-scattering process is overlaid with additional proton–proton interactions, simulated with PYTHIA 8 (v8.165) using the A2 tune [39]. The distribution of the average number of interactions per bunch crossing $\langle\mu\rangle$ spans the range 2.5–16.0, with a mean value of approximately 9.0.

3.2 Selection of electrons and muons and reconstruction of the recoil

Object definitions are unchanged compared to Ref. [12]. Electron candidates are reconstructed from clusters of energy deposited in the electromagnetic calorimeter and associated with at least one track in the ID [40, 41]. Quality requirements are applied to the associated tracks in order to reject poorly reconstructed charged-particle trajectories. The energy of the electron is reconstructed from the energy collected in calorimeter cells within an area of size $\Delta\eta \times \Delta\phi = 0.075 \times 0.175$ in the barrel, and 0.125×0.125 in the endcaps. The energy measurement relies on a multivariate regression algorithm developed and optimised on simulated events. The kinematic properties of the reconstructed electron are inferred from the energy measured in the EM calorimeter and from the pseudorapidity and azimuth of the associated track. Electron candidates are required to fulfil tight identification requirements [40], and their transverse momentum, p_T^ℓ , and pseudorapidity should satisfy $p_T^\ell > 15$ GeV and $|\eta| < 2.4$. As in the previous result, the pseudorapidity range $1.2 < |\eta| < 1.8$ is excluded from the measurement. Background from jets misidentified as electrons is reduced using additional isolation requirements using the activity in the ID and calorimeter nearby the electron candidates passing the kinematic and identification selections [12].

Muon candidates are reconstructed independently in the ID and in the MS, and a combined muon candidate is formed from the statistical combination of the ID and MS track parameters [42]. The kinematic properties of the reconstructed muon are defined using the ID track parameters alone, which allows a simpler calibration procedure. Muon candidates are required to have $p_T^\ell > 20$ GeV and $|\eta| < 2.4$ [12]. Similarly to the electrons, the multijet background is reduced by applying an isolation requirement [12].

The recoil, \vec{u}_T , is an estimator of the W - or Z -boson transverse momentum. It is reconstructed from the vector sum of the transverse energy of all clusters measured in the calorimeters, excluding clusters located at a distance $\Delta R < 0.2$ from electron or muon candidates. The definition of \vec{u}_T does not involve the explicit reconstruction of jets to avoid possible p_T threshold effects.

3.3 W -boson kinematics and event selection

The transverse momentum vector of charged leptons from the W -boson decay, \vec{p}_T^ℓ , is measured as summarised in the previous section. The transverse momentum of the decay neutrino is inferred

from the missing transverse momentum vector, \vec{p}_T^{miss} , defined as $\vec{p}_T^{\text{miss}} = -(\vec{p}_T^\ell + \vec{u}_T)$. The W -boson transverse mass, m_T , is derived from p_T^{miss} and from the transverse momentum of the charged lepton as $m_T = \sqrt{2p_T^\ell p_T^{\text{miss}}(1 - \cos \Delta\phi)}$, where $\Delta\phi$ is the azimuthal opening angle between the charged lepton and the missing transverse momentum.

The W -boson sample is collected using triggers requiring at least one muon candidate with transverse momentum larger than 18 GeV or at least one electron candidate with transverse momentum larger than 20 GeV. The transverse-momentum requirement for the electron candidate was raised to 22 GeV in later data-taking periods to cope with the increased instantaneous luminosity delivered by the LHC. Selected events are required to have a reconstructed primary vertex with at least three associated tracks.

The sample of W -boson candidate events is selected by requiring exactly one reconstructed electron or muon candidate with $p_T^\ell > 30$ GeV. The leptons are required to match the corresponding trigger signal. The magnitude of the recoil is required to satisfy $u_T < 30$ GeV, the missing transverse momentum $p_T^{\text{miss}} > 30$ GeV and the transverse mass $m_T > 60$ GeV. Approximately 5.89×10^6 candidate events are selected in the $W \rightarrow e\nu$ channel and 7.84×10^6 events in the $W \rightarrow \mu\nu$ channel.

3.4 W -boson mass analysis updates

The selected W -boson event sample includes events from various background processes. Background contributions from Z -boson, $W \rightarrow \tau\nu$, boson pair, and top-quark production are estimated using simulation, and represent about 6.4% of the total sample in the muon channels, and about 3.1% in the electron channels. Contributions from multijet production are estimated with data-driven techniques, and are detailed in Ref. [12]. Compared with that reference, the multijet background yield was re-evaluated using the final luminosity calibration for Run 1 [43], resulting in a 1–2% decrease of the contamination of multijet background control regions by electroweak processes, and a corresponding 20% increase in the estimated multijet background yield in the electron channel. This background now represents 1.2% of the total sample, and agrees with the previous measurement within uncertainties. The multijet background in the muon channel is unaffected, due to the smaller contamination in this case. In addition, uncertainties in the multijet distributions were previously propagated to the m_W measurement through fluctuations of the extrapolation parameters; an eigenvector decomposition is used in the present analysis.

The results of Ref. [12] were obtained using the CT10nnlo PDF set and compared with results using the CT14 [44] and MMHT2014 PDF sets [45]. The present analysis extends the study of the PDF dependence of the fit results to the ATLASpdf21 [46], CT18, CT18A [47], MSHT20 [48], NNPDF3.1 [49] and NNPDF4.0 [50] sets.

In the previous measurement, m_W was determined with the W -boson width fixed to the SM prediction. In the present analysis, this assumption is relaxed by treating Γ_W as a source of systematic uncertainty, considering the SM value and uncertainty of $\Gamma_W^{\text{SM}} = 2088 \pm 1$ MeV. The W -boson width is also extracted assuming the SM prediction and uncertainty of the W -boson mass, $m_W^{\text{SM}} = 80355 \pm 6$ MeV.

Finally, an improved statistic is used for the fit as described in the following section.

Table 1: Summary of the 28 categories and kinematic distributions used in the m_W measurement for the electron and muon decay channels.

Decay channel	$W \rightarrow e\nu$	$W \rightarrow \mu\nu$
Kinematic distributions	p_T^ℓ, m_T	p_T^ℓ, m_T
Charge categories	W^+, W^-	W^+, W^-
$ \eta_\ell $ categories	[0, 0.6], [0.6, 1.2], [1.8, 2.4]	[0, 0.8], [0.8, 1.4], [1.4, 2.0], [2.0, 2.4]

3.5 Statistical analysis

The previous measurement used separate template fits to the p_T^ℓ and m_T distributions observed in different event categories. The W -boson candidate events were classified according to the charge, flavour and pseudorapidity of the final state lepton, as summarised in Table 1. In the fit, the χ^2 of the comparison between data and simulation was minimised considering statistical uncertainties only; systematic uncertainties were included by varying the parameters determining the templates within their uncertainties, and repeating the fits.

The present analysis performs a simultaneous optimisation of m_W or Γ_W , and of nuisance parameters describing systematic uncertainties, through a global profile likelihood fit in all event categories for a given kinematic distribution. The likelihood function, which describes how compatible with each other the data and MC distributions are, is given by

$$\mathcal{L}(\vec{n}|\mu, \vec{\theta}) = \prod_j \prod_i \text{Poisson}(n_{ji} | v_{ji}(\mu, \vec{\theta})) \cdot \text{Gauss}(\vec{\theta}), \quad (1)$$

where \vec{n} represents the observed distributions in data, and n_{ji} is the number of events observed in data in bin i of the distribution in a given category j . It is the input to the Poisson distribution with expectation $v_{ji}(\mu, \vec{\theta}) = S_{ji}(\mu, \vec{\theta}) + B_{ji}(\vec{\theta})$, of S_{ji} events from signal and B_{ji} events from background contributions. The parameter of interest, μ , represents variations in m_W or Γ_W with respect to a conventional reference, μ_{ref} . Uncertainties of the signal and background distributions are encapsulated as nuisance parameters (NPs), denoted by $\vec{\theta}$ in Eq. (1), for which a normal probability distribution is assumed. The expected number of events v_{ji} is parameterised as

$$v_{ji}(\mu, \vec{\theta}) = \Phi \times \left[S_{ji}^{\text{nom}} + \mu \times (S_{ji}^\mu - S_{ji}^{\text{nom}}) \right] + \sum_s \theta_s \times (S_{ji}^s - S_{ji}^{\text{nom}}) \\ + B_{ji}^{\text{nom}} + \sum_b \theta_b \times (B_{ji}^b - B_{ji}^{\text{nom}}), \quad (2)$$

where Φ is an overall, unconstrained normalisation factor ensuring that the total W^\pm signal rate always adjusts to the number of events in data, S_{ji}^{nom} and B_{ji}^{nom} are the nominal distributions of signal and background, respectively, while s and b represent nuisance parameters acting on signal and background contributions.

Changes in μ and $\vec{\theta}$ lead to changes in the expected signal and background distributions, which are interpolated using a polynomial morphing procedure. Signal templates for arbitrary values of m_W or Γ_W are obtained from the same simulation sample through a reweighting of the W -boson Breit–Wigner

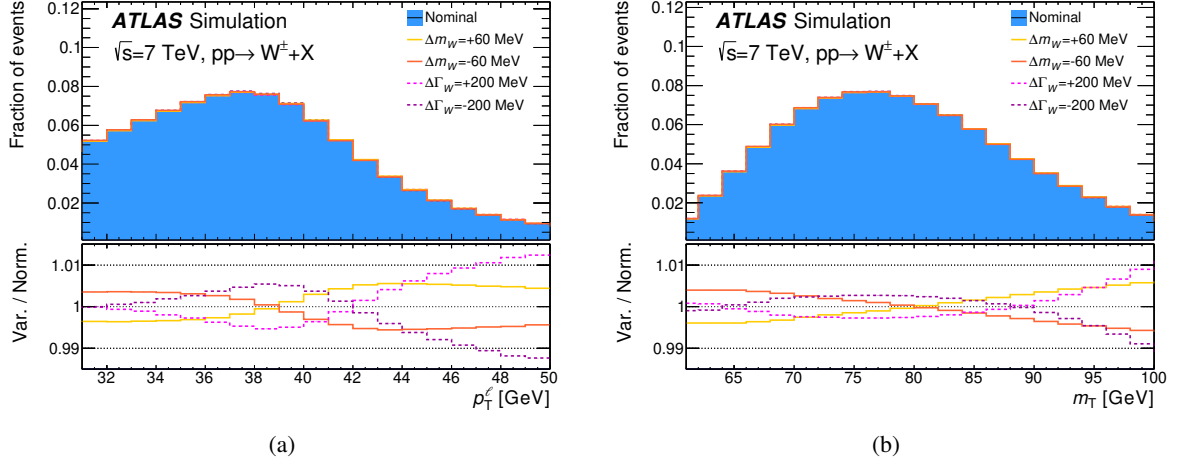


Figure 1: Simulated kinematic distributions of (a) p_T^ℓ and (b) m_T in $W^\pm \rightarrow \mu^\pm \nu$ events, for W -boson mass and width values of $m_W = 80399$ MeV and $\Gamma_W = 2085$ MeV. The ratio panels represent the relative effect of varying these parameters by ± 60 MeV and ± 200 MeV, respectively.

distribution. Templates representing systematic variations are determined from two-sided one- and two-sigma variations of the corresponding sources of uncertainty. The effect of varying m_W or Γ_W on the p_T^ℓ and m_T distributions is illustrated in Figure 1. The procedure to interpolate between these points during the PLH fit was extensively tested, and excellent closure was observed.

As the new fitting method allows to better optimise the total uncertainty of the measurement due to the inclusion of NPs in the likelihood, the nominal fit ranges for the m_W measurement are re-evaluated. The updated optimal fit ranges are $30 < p_T^\ell < 50$ GeV and $60 < m_T < 100$ GeV, in contrast with $32 < p_T^\ell < 45$ GeV and $66 < m_T < 99$ GeV used in the previous measurement. For the determination of Γ_W , the same ranges are used as in the m_W measurement.

The baseline results rely on a numerical minimisation of the likelihood from Eq. (2). For ancillary studies, such as the decomposition of uncertainties, fit range variations, and to estimate the correlation between the m_T and p_T^ℓ fits, the following assumptions are made: in the limit where all uncertainties are Gaussian and the dependence of $v_{ji}(\mu, \vec{\theta})$ on μ and $\vec{\theta}$ is linear, the likelihood can be written as

$$-2 \ln \mathcal{L}(\vec{n} | \mu, \vec{\theta}) = \sum_j \sum_i \left(\frac{n_{ji} - v_{ji}(\mu_{\text{ref}}, \vec{0}) - \frac{\partial v_{ij}}{\partial \mu}(\mu - \mu_{\text{ref}}) - \sum_t \frac{\partial v_{ij}}{\partial \theta_t} \theta_t}{\sigma_{ji}} \right)^2 + \sum_t \theta_t^2, \quad (3)$$

and the minimisation and uncertainty estimation can be performed analytically [51]. This approach gives results within 2 MeV from the nominal fits and is much faster.

The decomposition of the post-fit uncertainties is performed according to the methods of Ref. [51]. The uncertainty components are defined to represent the contribution of the pre-fit uncertainty in the corresponding sources to the total uncertainty of the measurement, consistently with standard error propagation.

4 Experimental corrections and uncertainties

The p_T^ℓ and m_T distributions are affected by the lepton energy calibration and by the calibration of the recoil. Lepton momentum corrections are derived exploiting $Z \rightarrow \ell\ell$ event samples and the precisely measured value of m_Z [52], and the recoil response is calibrated using the expected momentum balance between u_T and $p_T^{\ell\ell}$ [12]. Lepton identification and reconstruction efficiency corrections are determined from W - and Z -boson events using the tag-and-probe method [40, 42].

A precision on the energy and momentum scale for electrons and muons of $O(10^{-4})$ is achieved, with somewhat larger uncertainty for the muons in the high- η region. The response and resolution of $u_T = |\vec{u}_T|$ is determined with a precision of a few percent. The experimental precision is limited by the finite size of the Z -boson sample, and by systematic uncertainties in the modelling of the distributions used in the calibration procedures.

4.1 Uncertainty propagation

Systematic uncertainties in the determination of m_W and Γ_W are evaluated by varying the calibration model parameters within their uncertainty. For two-sided systematic uncertainties, separate templates are produced for 68% confidence level (CL) upwards and downwards variations. Systematic uncertainties that are estimated independently in many kinematic bins are propagated through simultaneous random variations of the corresponding parameters within their uncertainty and generating templates for each variation. A principal component analysis (PCA) [53, 54] is used to transform these variations into a set of uncorrelated two-sided uncertainties, preserving the total uncertainty. This approach is used for the statistical uncertainties of the electron and muon efficiencies, as well as for the recoil calibration, and allows a faithful representation of these uncertainties using a reduced set of nuisance parameters.

Because of the finite size of the MC samples, some systematic variations contribute significant statistical fluctuations in the final-state distributions. A smoothing procedure is applied to remove such fluctuations, preserving the normalisation of each variation. For calibration systematic uncertainties, the effect of the upwards and downwards variations are symmetrised. The impact of the smoothing and symmetrisation procedures on the best-fit values and uncertainties are below 1 and 0.1 MeV, respectively.

The effect of each systematic variation is decomposed into corresponding uncertainties in the normalisation and in the shape of the final state distributions. Systematic uncertainties that yield differences smaller than 0.01% in the normalised p_T^ℓ distribution and smaller than 0.02% in the normalised m_T distribution are removed, reducing the number of shape systematic variations by a factor of two, for a change in the total measurement uncertainty by less than 1% of itself. This pruning procedure simplifies the likelihood, stabilising and accelerating the fit procedure.

4.2 Sources of uncertainty

The electron calibration and selection efficiencies account for 75 sources of uncertainty in the p_T^ℓ distribution and 58 in the m_T distribution, including the energy scale and resolution as well as the electron identification, isolation, and trigger efficiencies. Of these uncertainties, 23 originate from the energy calibration and are treated as two-sided systematic uncertainties, while 52 (p_T^ℓ) and 35 (m_T) systematic variations come from the trigger, reconstruction, identification and isolation efficiencies. PCA is utilised to handle those

systematic variations. Similarly, the muon response and efficiencies contribute 83 (p_T^ℓ) and 76 (m_T) sources of uncertainty, of which 6 are treated as two-sided uncertainties.

The calibration of the hadronic recoils yields 36 sources of systematic uncertainties for the m_T distributions, but only 7 sources for the p_T^ℓ distributions since the impact on the latter are only due to the hadronic recoil requirement in the signal selection. Of these uncertainties, 3 are two-sided uncertainties, while 4 (p_T^ℓ) and 33 (m_T) PCA variations are taken into account.

5 Physics corrections and uncertainties

5.1 Electroweak uncertainties

The dominant source of electroweak corrections to W -boson production originates from QED final-state radiation, and is simulated with `PHOTOS`. The effect of QED initial-state radiation (ISR) is also included through the `PYTHIA 8` parton shower (PS). Other sources of electroweak corrections are not included in the simulated event samples, and their full effects are considered as systematic uncertainties. Systematic uncertainties from missing higher-order electroweak corrections are estimated considering the same sources of uncertainty as in Ref. [12]. An improvement of the present analysis is that the corresponding uncertainties are evaluated at detector level instead of generator level, which was a simplification used in the previous analysis as these are not leading uncertainties. The detector-level systematic variations are obtained by applying detector response and efficiency migration matrices derived from samples of simulated signal events described in Section 3.1. Their impact on m_W is larger than for generator-level variations by typically 20%.

5.2 QCD model and uncertainties

The rapidity, transverse momentum and decay distributions of the simulated W - and Z -boson samples are reweighted to include the effects of higher-order QCD corrections, which improves the agreement between the data and simulation. The differential cross section as a function of the boson rapidity, $d\sigma(y)/dy$, and the coefficients describing angular distributions of decay leptons, A_i [55], are calculated at $O(\alpha_s^2)$ in fixed-order QCD. The transverse-momentum spectrum at a given rapidity, $d\sigma(p_T, y)/(dp_T dy) \cdot (d\sigma(y)/dy)^{-1}$, is modelled using the `PYTHIA 8` MC generator, with parameters adjusted to reproduce the measured Z -boson p_T distribution at $\sqrt{s} = 7$ TeV [29]. The resulting tune, called `AZ` in the following, predicts W -boson p_T distributions that agree with measurements at $\sqrt{s} = 5.02$ and 13 TeV [56].

PDF uncertainties are calculated for the CT10, CT14, CT18, CT18A, MMHT2014, MSHT20, NNPDF3.1, NNPDF4.0 and ATLASpdf21 sets using the Hessian method [57], where each eigenvector of the PDF fit covariance matrix defines a pair of PDF uncertainty variations and a corresponding nuisance parameter in the PLH fit. The CT10, CT14, CT18 and CT18A variations correspond to 90% CL, and are rescaled to match the 68% CL. Given the precisely measured p_T^Z distribution, PDF uncertainty variations are constrained to leave the predicted p_T^Z distribution unchanged, and propagate only the part of the PDF uncertainty in the p_T^W distribution that is uncorrelated to p_T^Z . The uncertainties in the `AZ` tune parameters are propagated separately, as described below.

The `PYTHIA 8` parton shower model contributes additional sources of uncertainty in the p_T^W distribution. The `AZ` tune parameters are assumed universal between Z - and W -boson production, and their uncertainties

are propagated to the W -boson final-state distributions. The initial-state charm and bottom quark masses affect the p_T spectrum, and the corresponding uncertainties are estimated by varying their respective masses by ± 0.5 GeV and ± 0.8 GeV, respectively. Uncertainties in the shower evolution are parameterised through variations of the factorisation scale, μ_F , by factors of 0.5 and 2.0 with respect to the central choice $\mu_F^2 = p_{T,0}^2 + p_T^2$, where $p_{T,0}$ is an infrared cut-off, and p_T is the evolution variable of the parton shower [58]. The variations are applied independently to the light-quark, charm-quark and bottom-quark-induced processes, and are propagated considering only the relative impact on the p_T^W and p_T^Z distributions. Differences between the PYTHIA 8 and HERWIG 7 predictions for this ratio were found to be negligible.

The accuracy of the next-to-next-to-leading-order (NNLO) predictions for the angular coefficients A_0 – A_7 is validated by comparing to the corresponding measured values in Z -boson production [55]. The Z -boson data uncertainties are propagated to the W -boson predictions, which assumes that NNLO predictions have similar accuracy for the W - and Z -boson processes, and are validated within the experimental precision of the Z -boson data. The observed disagreement between data and prediction for the A_2 coefficient is taken as additional uncertainty. Similarly to some experimental uncertainties, random angular coefficient variations are treated with a PCA to produce uncorrelated two-sided uncertainties.

The effect of missing higher-order corrections on the NNLO predictions of the normalised rapidity distributions and the effect of the LHC beam-energy uncertainty of 0.65% were both found to be negligible.

6 Improved measurement of the W -boson mass

The improvements to the previous m_W measurement described in Sections 3.4 and 3.5 are implemented in several steps. The impact of the analysis updates is evaluated using the same statistical method as in the previous measurement, and yields a change of the measured W -boson mass from 80369.5 ± 18.5 MeV to 80371.9 ± 18.7 MeV, corresponding to a shift of 2.4 MeV and a minimal increase of the total uncertainty. The analysis is then repeated using the CT10nnlo PDF set and unchanged systematic uncertainties but implementing the PLH approach. This provides a test of the stability of the measurement under the change of statistic used in the fit. The final step consists of updating the measurement to more recent PDF sets, one of which is used to define a new baseline.

6.1 Results with CT10nnlo and consistency tests

The PLH fits using the CT10nnlo PDF set are first performed with statistical uncertainties only. Excellent consistency with the previous results is obtained, which provides a basic validation for the technical aspects of the fit. The comparison is repeated for fits including all systematic uncertainties, with the results summarised in Figure 2. The results of the PLH fits combining all categories yield $m_W = 80357.0 \pm 15.8$ MeV and $m_W = 80388.2 \pm 23.8$ MeV for the p_T^ℓ and m_T distributions, respectively. Compared to the original ATLAS measurement, this corresponds to shifts of m_W of -12.4 MeV and $+12.5$ MeV, respectively, while the total uncertainties are reduced by about 3 MeV due to the profiling of some systematic uncertainties. Repeating the present analysis with the fit range used in Ref. [12] increases the difference by 3 MeV.

The compatibility between the present and previous results is tested by repeating the PLH fits for an ensemble of models where the preferred values of the nuisance parameters are varied randomly within their pre-fit uncertainties. As shown in Figure 3, the spread of fit results from pseudo-experiments with

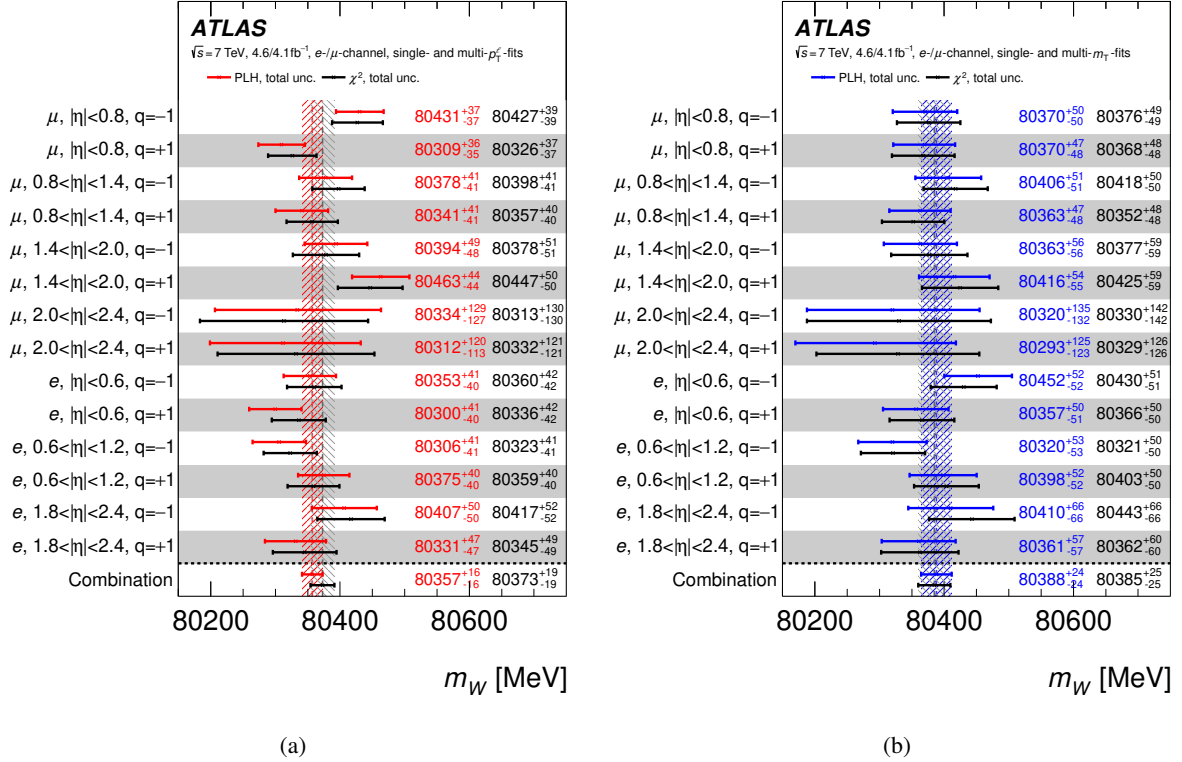


Figure 2: Overview of the m_W fit results in all categories for the (a) p_T^ℓ and (b) m_T distributions, with the CT10nnlo PDF set, where q denotes the charge of the decay lepton. The results of the PLH fit are compared with the χ^2 fit, where systematic uncertainties are propagated using the offset method [12]. The points labelled as ‘Combination’ correspond to the result of a joint PLH fit to all categories and to a combination of individual χ^2 fits.

varied nuisance parameters is about 16 MeV, confirming that the change in central value introduced by the new statistical method corresponds to about one standard deviation. The distribution of the nuisance parameter pulls² is consistent with a normal distribution, indicating an overall correct estimate of the pre-fit uncertainties.

6.2 Impact of updated parton distribution functions

The impact of a change in the PDFs on the final state distributions is evaluated using POWHEG, both to calculate the extrapolation from the central CT10nnlo set to CT14, CT18, CT18A, MMHT2014, MSHT20, NNPDF3.1, NNPDF4.0 and ATLASpdf21, and to calculate the PDF uncertainty variations. All calculations are performed at generator level in full phase space, and the impact on the final-state distributions is evaluated using migration matrices as in Section 5.1. As in Section 5.2, the PDF extrapolations are constrained to leave p_T^Z unchanged. The impact of the extrapolations on the detector-level p_T^ℓ distributions is illustrated in Figure 4.

² For a given nuisance parameter θ , the pull is defined as $\hat{\theta}/\sqrt{1-\sigma_\theta}$, where $\hat{\theta}$ and σ_θ are the nuisance parameter post-fit value and uncertainty, respectively.

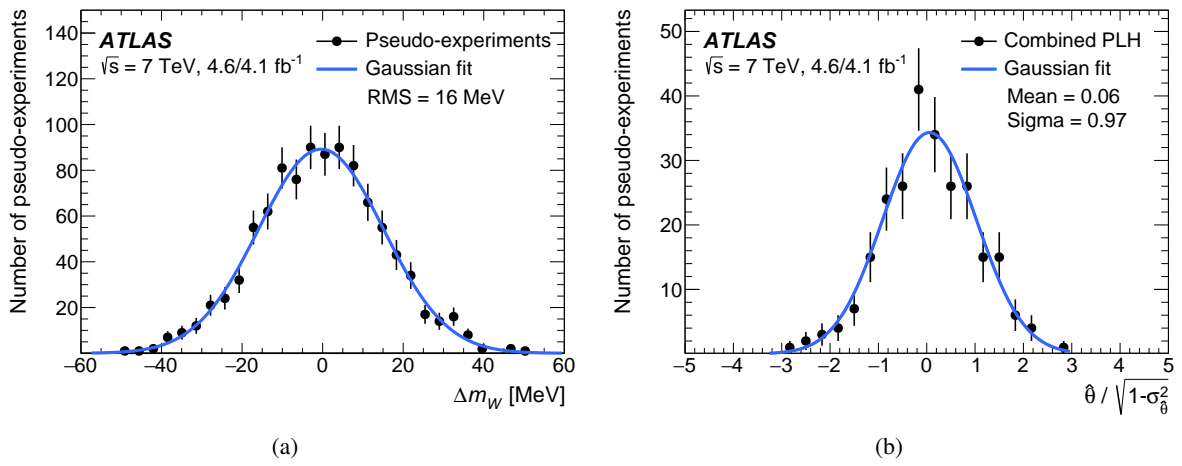


Figure 3: (a) Distribution of the difference Δm_W between the nominal m_W PLH fit result and results obtained for pseudo-experiments using random variations of the sources of systematic uncertainty. The p_T^ℓ distribution is used. (b) Distribution of pull significances for the NPs in the combined PLH fit to the p_T^ℓ distribution.

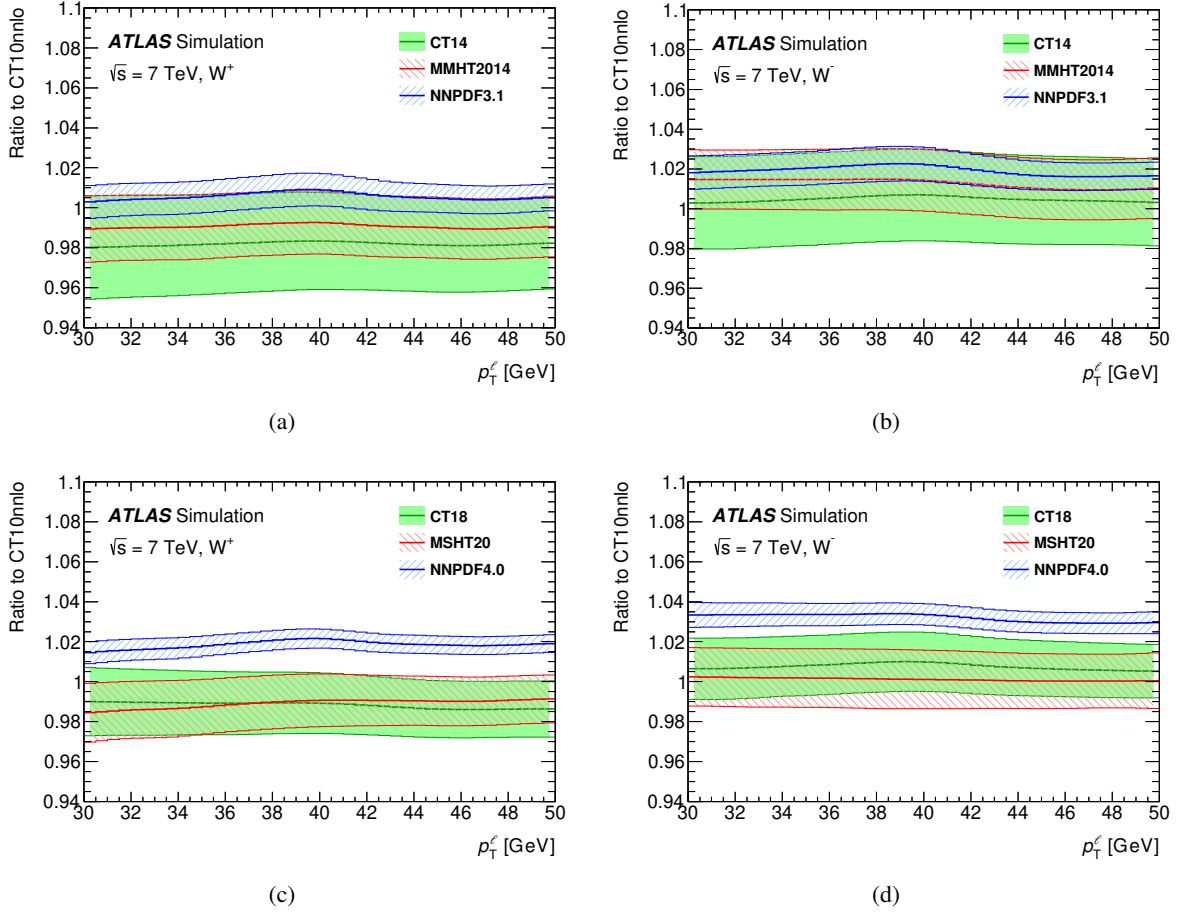


Figure 4: Relative effect, with respect to CT10nnlo, of the indicated PDF extrapolations on the detector-level, η -inclusive p_T^ℓ distributions in (a,c) W^+ events and (b,d) W^- events. The thick lines show the central PDF set, and the envelopes show the associated 68% CL uncertainty.

Table 2: Best-fit value of m_W , total and PDF uncertainties, in MeV, and goodness-of-fit for the p_T^ℓ and m_T distributions and the PDF sets described in the text. Each fit uses 14 event categories with 40 bins, for 558 degrees of freedom.

PDF set	p_T^ℓ fit				m_T fit			
	m_W	σ_{tot}	σ_{PDF}	$\chi^2/\text{n.d.f.}$	m_W	σ_{tot}	σ_{PDF}	$\chi^2/\text{n.d.f.}$
CT14	80358.3	+16.1 -16.2	4.6	543.3/558	80401.3	+24.3 -24.5	11.6	557.4/558
CT18	80362.0	+16.2 -16.2	4.9	529.7/558	80394.9	+24.3 -24.5	11.7	549.2/558
CT18A	80353.2	+15.9 -15.8	4.8	525.3/558	80384.8	+23.5 -23.8	10.9	548.4/558
MMHT2014	80361.6	+16.0 -16.0	4.5	539.8/558	80399.1	+23.2 -23.5	10.0	561.5/558
MSHT20	80359.0	+13.8 -15.4	4.3	550.2/558	80391.4	+23.6 -24.1	10.0	557.3/558
ATLASpdf21	80362.1	+16.9 -16.9	4.2	526.9/558	80405.5	+28.2 -27.7	13.2	544.9/558
NNPDF3.1	80347.5	+15.2 -15.7	4.8	523.1/558	80368.9	+22.7 -22.9	9.7	556.6/558
NNPDF4.0	80343.7	+15.0 -15.0	4.2	539.2/558	80363.1	+21.4 -22.1	7.7	558.8/558

6.3 Results and discussion

Fit results with updated PDF sets are listed in Table 2. A satisfactory fit quality is obtained for all PDF sets. Separate fits are performed to the p_T^ℓ and m_T distributions as they are projections of the same data, and the corresponding statistical correlations cannot be accounted for in the framework of Eq. (1) in a straightforward way. Moreover, the PCA treatment applied for some classes of systematic uncertainties leads to different sets of nuisance parameters for the two distributions.

The best-fit values of m_W obtained with different PDF sets span a range of about 18 MeV for the p_T^ℓ fits, and about 42 MeV for the m_T fits. This envelope is dominated by the NNPDF3.1 and NNPDF4.0 fits, which yield the lowest fit values; the range spanned by the other sets is only 9 MeV for p_T^ℓ and 21 MeV for m_T .

The influence of the size of the initial PDF uncertainties on the best-fit values is studied in Figure 5, where the fits are repeated with pre-fit PDF uncertainties scaled by factors 1–3. Enlarged uncertainties allow the models to better adapt to the data, resulting in a reduced PDF model dependence. For scale factors of 2 and above, the residual model dependence is below 5 MeV for the p_T^ℓ fits, and 25 MeV for m_T fits, with the total uncertainty increased by less than 1.5 MeV.

The baseline result is defined using CT18, which is compatible with the previous exercise and yields the most conservative uncertainty among the PDF sets considered except for ATLASpdf21. CT18 is also the only recent PDF set that does not include the W - and Z -boson cross sections measured by ATLAS at 7 TeV [33], which represent the same data as those used in the present analysis. The results for all measurement categories and for the CT18 PDF set are summarised in Figure 6. The post-fit, $|\eta|$ -inclusive p_T^ℓ distributions obtained with CT18 are shown in Figure 7, and agree with the data within the uncertainties. Similarly to CT10nnlo, the distribution of the nuisance parameter pulls is consistent with a normal distribution.

The compatibility of the results for m_W in the different measurement categories is verified by repeating the fit assuming independent parameters of interest in each category. The differences to the baseline fit are small compared with the measurement uncertainties. Partial fits are performed to the electron and muon channels separately. The electron and muon fit results are found to agree within one standard deviation. A similar exercise is performed for the W^+ and W^- channels, and the same conclusion is obtained. Finally,

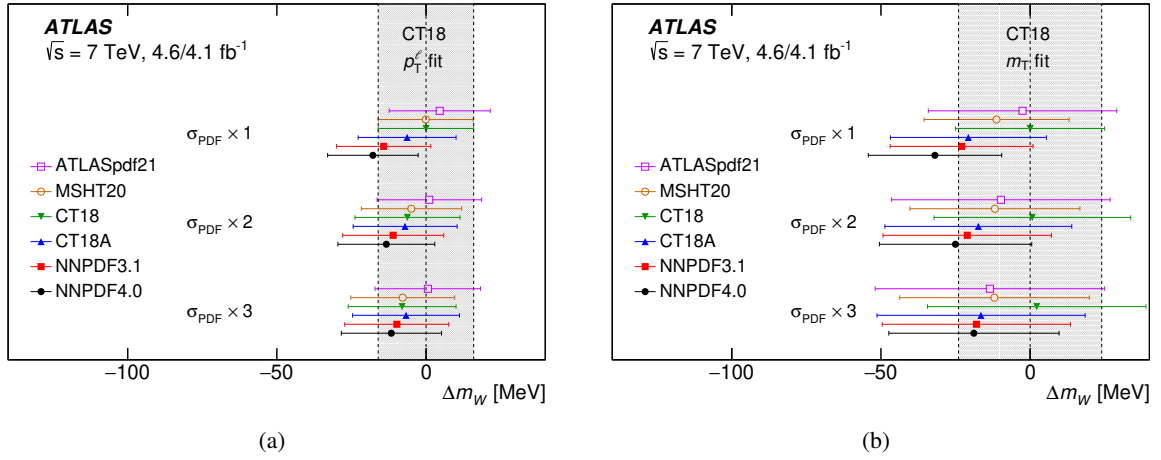


Figure 5: Variation of the fitted value of m_W with the PDF set used in the fit, for the (a) p_T^{ℓ} and (b) m_T distributions and different scalings of the pre-fit PDF uncertainties. The reference value is defined by the CT18 PDF set.

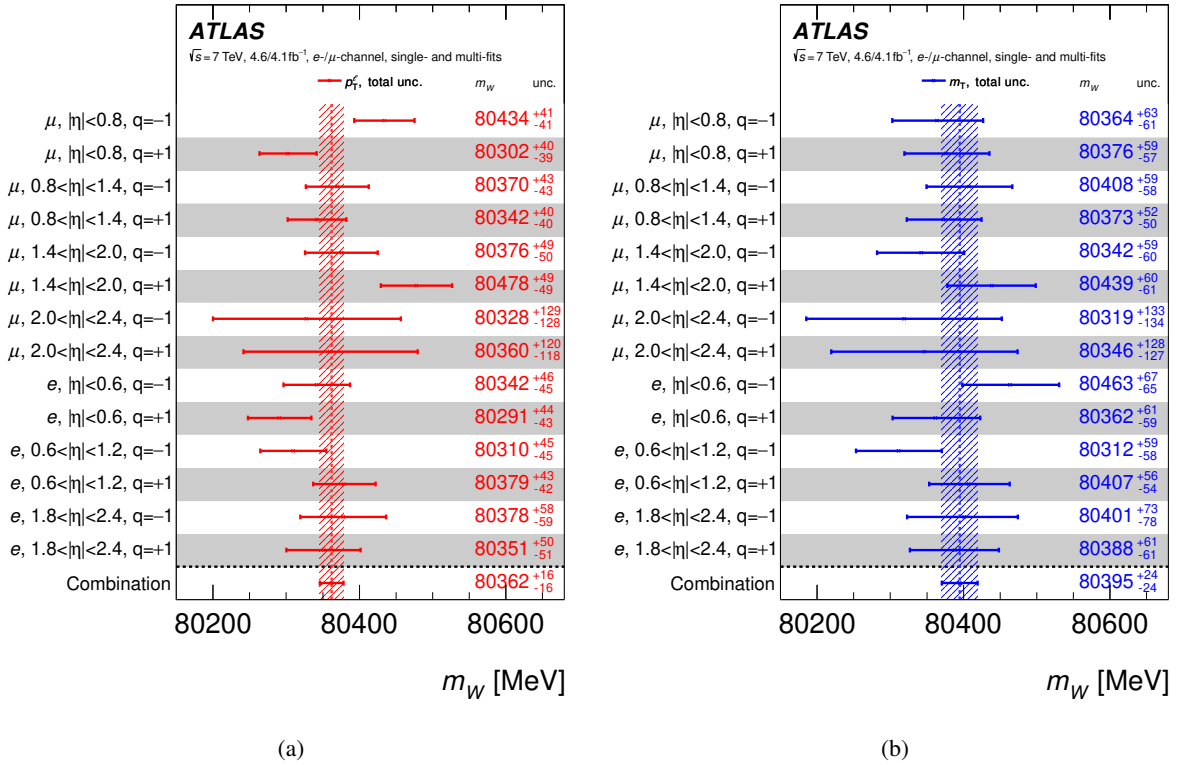


Figure 6: Overview of the m_W PLH fit results in all categories for the (a) p_T^{ℓ} and (b) m_T distributions, with the CT18 PDF set. The points labelled as 'Combination' correspond to the result of a joint PLH fit to all categories.

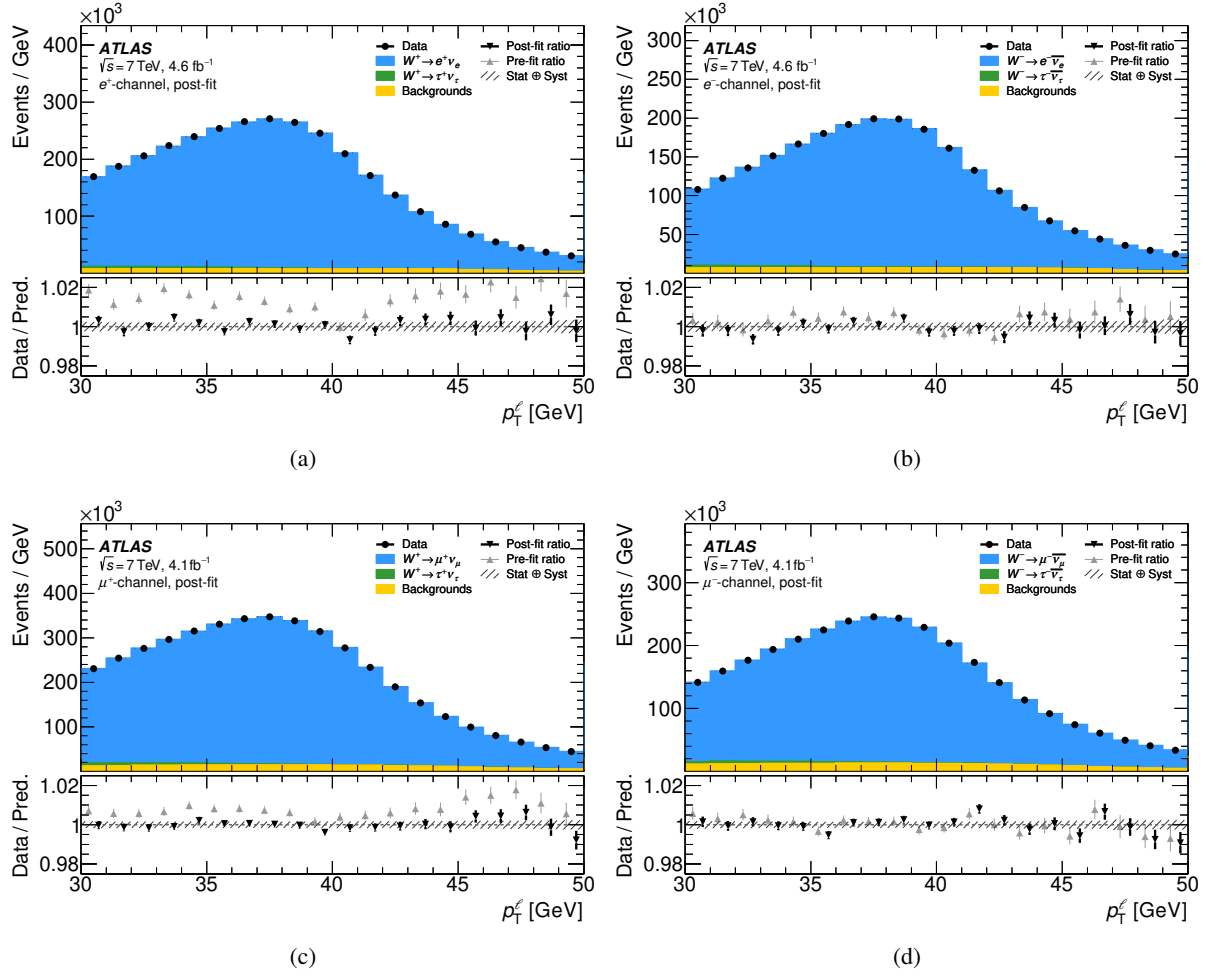


Figure 7: Post-fit distributions of p_T^l with data and MC for (a) $W^+ \rightarrow e^+ \nu_e$, (b) $W^- \rightarrow e^- \bar{\nu}_e$, (c) $W^+ \rightarrow \mu^+ \nu_\mu$ and (d) $W^- \rightarrow \mu^- \bar{\nu}_\mu$, inclusive over all η regions, and using the CT18 PDF set. In the bottom panels, the darker points represent the post-fit ratio of data to MC, while the lighter points indicate the ratio before the fit. The hatched band represents the total uncertainty of the data.

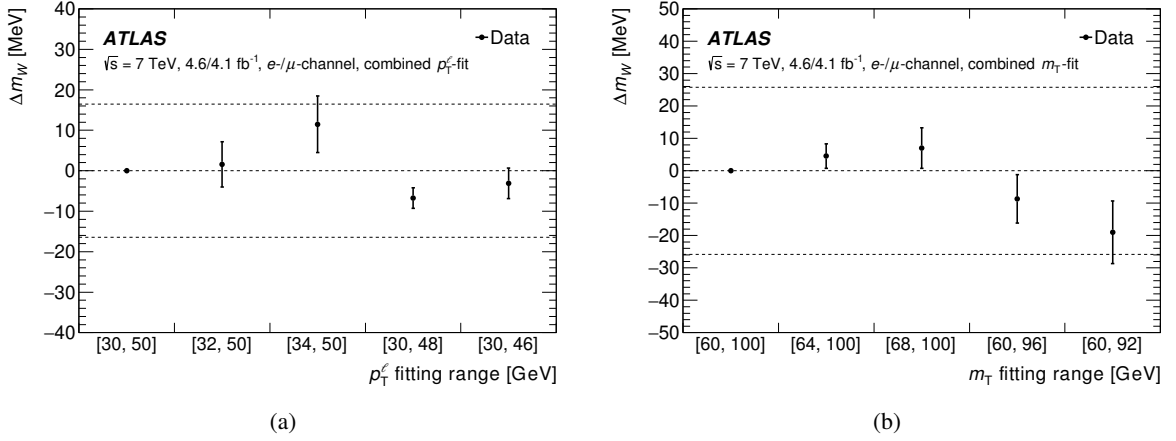


Figure 8: Difference Δm_W between the W -boson mass measured using the (a) p_T^ℓ and (b) m_T distribution fit ranges indicated in the figure and the nominal fit range. The nominal ranges are $30 < p_T^\ell < 50$ GeV and $60 < m_T < 100$ GeV, respectively. The outer dashed lines indicate the total measurement uncertainty for the nominal range. Results are shown for the combined fit over all categories, and for the CT18 PDF set.

the dependence of the fit result on the p_T^ℓ and m_T ranges used for the fit is shown in Figure 8, with good stability.

Figure 9 summarises the ten nuisance parameters that induce the largest shift of m_W in fits to the p_T^ℓ and m_T distributions. They are related to electron and muon calibration uncertainties, to the uncertainty in charm-induced production for the p_T^W description, to specific eigenvectors (EV) of the CT18 PDF set, and to missing higher-order electroweak corrections. The corresponding nuisance parameter pulls are also shown. By construction, the PLH fits induce shifts of the nuisance parameters from their nominal value and significant deviations would indicate an underestimation of systematic uncertainties. All observed pulls are within the expectation.

While uncertainties in the PDFs and in the AZ tune parameters have well defined confidence intervals and can be treated as nuisance parameters, this is more questionable for the other uncertainties in the W -boson p_T distribution, i.e., the factorisation scale and quark-mass variations. It was verified that the impact of the latter on the final-state distributions is very similar, in shape, to that of the AZ tune parameters, and that these effects are thus not different from the other sources of uncertainty in this respect, and can be treated accordingly. The small post-fit value of the corresponding uncertainty is due to the strong discrimination between the effects of m_W and p_T^W variations on the p_T^ℓ distribution.

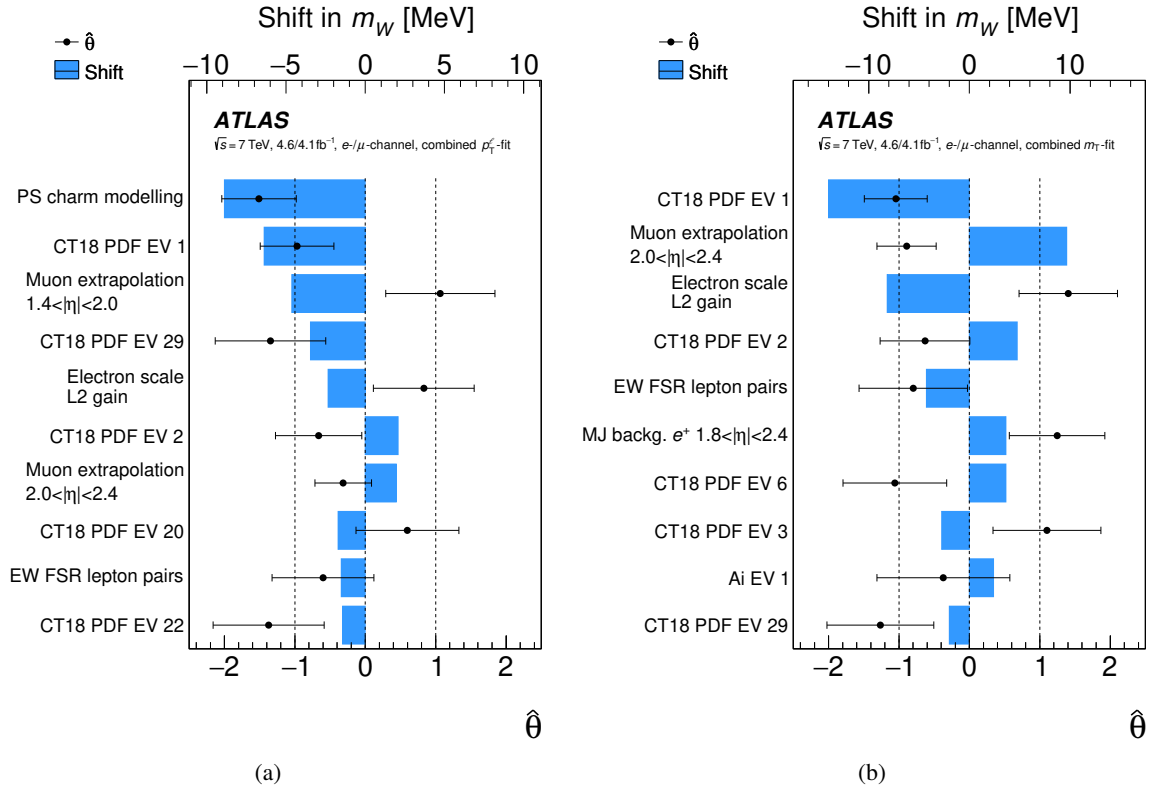


Figure 9: The ten nuisance parameters inducing the largest shifts on the fitted value of m_W in the combined PLH fits, using the (a) p_T^ℓ and (b) m_T distributions and the CT18 PDF set. For a given NP θ , the shift is defined as the product of its post-fit value $\hat{\theta}$ and its pre-fit impact on m_W . The points, which are plotted according to the bottom horizontal scale, show $\hat{\theta}$ for each of the nuisance parameters. The error bars show the corresponding post-fit uncertainties, $\sigma_{\hat{\theta}}$. The nuisance parameters are ranked according to the shift induced on m_W , the NPs with the largest shifts at the top.

Table 3: Uncertainty correlation between the p_T^ℓ and m_T fits, combination weights and combination results for m_W and the indicated PDF sets.

PDF set	Correlation	weight (p_T^ℓ)	weight (m_T)	Combined m_W [MeV]
CT14	52.2%	88%	12%	80363.6 ± 15.9
CT18	50.4%	86%	14%	80366.5 ± 15.9
CT18A	53.4%	88%	12%	80357.2 ± 15.6
MMHT2014	56.0%	88%	12%	80366.2 ± 15.8
MSHT20	57.6%	97%	3%	80359.3 ± 14.6
ATLASpdf21	42.8%	87%	13%	80367.6 ± 16.6
NNPDF3.1	56.8%	89%	11%	80349.6 ± 15.3
NNPDF4.0	59.5%	90%	10%	80345.6 ± 14.9

6.4 Combination

All event categories are statistically independent as long as only the p_T^ℓ or only the m_T distributions are considered. The correlation between the final p_T^ℓ - and m_T -based results for m_W is determined from an ensemble of fit results obtained by fluctuating the data and the most probable values of the nuisance parameters within their respective uncertainties. The p_T^ℓ and m_T results are then combined using the BLUE prescription [59]. The results of this procedure are given in Table 3. The weight of the p_T^ℓ fit ranges from 86% to 97%, depending on the PDF set, and dominates the final result. For the CT18 PDF set, the final result is:

$$m_W = 80366.5 \pm 9.8 \text{ (stat.)} \pm 12.5 \text{ (syst.) MeV} = 80366.5 \pm 15.9 \text{ MeV,}$$

where the first uncertainty component is statistical and the second corresponds to the total systematic uncertainties.

The decomposition of the post-fit uncertainties is performed according to Ref. [51] and shown in Table 4. Statistical uncertainties contribute about 10 MeV in the present fit. This is in contrast with 6 MeV obtained from fits considering statistical uncertainties only, with all nuisance parameters fixed to their best-fit values. The increase reflects the larger number of parameters determined from the same data. Correspondingly, the systematic uncertainty components are smaller than systematic ‘impacts’ conventionally reported for PLH fits.³ Systematic uncertainties contribute about 13 MeV, dominated by PDF uncertainties, missing higher-order electroweak corrections, and electron and muon calibration uncertainties.

The fits are performed assuming the SM value for the W -boson width, $\Gamma_W^{\text{SM}} = 2088 \pm 1$ MeV [6]. The fitted value of m_W varies with the assumed value for Γ_W following $\Delta m_W = -0.06 \Delta \Gamma_W$. Assuming an alternate SM prediction of $\Gamma_W^{\text{SM}} = 2091 \pm 1$ MeV, as obtained in Ref. [7], does not change the measured value of the W -boson mass significantly.

The compatibility of the measured value of the W -boson mass using the CT18 PDF set with the Standard Model expectation is illustrated in Figure 10(a), together with selected previous measurements. The two-dimensional 68% and 95% confidence limits for the predictions of m_W and m_t in the context of the

³ Impacts are obtained from the quadratic subtraction between the total fit uncertainty and the uncertainty of a fit with selected nuisance parameters removed and overestimate the genuine systematic uncertainty.

Table 4: Uncertainty components for the p_T^ℓ , m_T and combined m_W measurements using the CT18 PDF set. The first columns give the total, statistical and overall systematic uncertainty in the measurements. The following columns show the contributions of modelling and experimental systematic uncertainties, grouped into categories.

Unc. [MeV]	Total	Stat.	Syst.	PDF	A_i	Backg.	EW	e	μ	u_T	Lumi	Γ_W	PS
p_T^ℓ	16.2	11.1	11.8	4.9	3.5	1.7	5.6	5.9	5.4	0.9	1.1	0.1	1.5
m_T	24.4	11.4	21.6	11.7	4.7	4.1	4.9	6.7	6.0	11.4	2.5	0.2	7.0
Combined	15.9	9.8	12.5	5.7	3.7	2.0	5.4	6.0	5.4	2.3	1.3	0.1	2.3

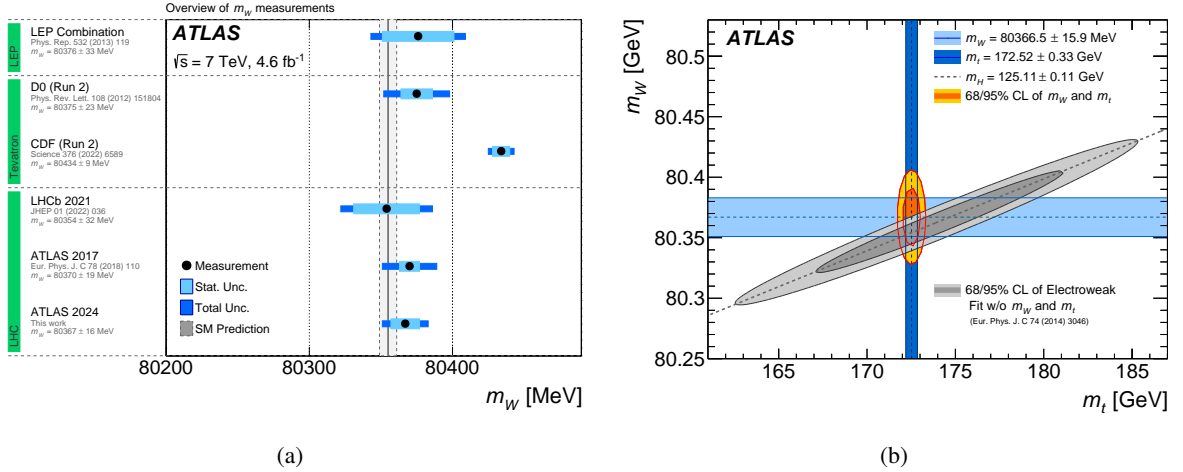


Figure 10: (a) Present measured value of m_W , compared to SM prediction from the global electroweak fit [6], and to the measurements of LEP [10], Tevatron [18, 19] and the LHC [12, 13]. (b) The 68% and 95% confidence level contours of the m_W and m_t indirect determinations from the global electroweak fit [7], compared to the 68% and 95% confidence-level contours of the present ATLAS measurement of m_W , the ATLAS measurement of m_H [61] and the LHC measurement of m_t [60].

Standard Model electroweak fit are shown in Figure 10(b), and are compared to the present measurement of m_W and to the combined value of the LHC top-quark mass determinations at 7 and 8 TeV [60].

7 Measurement of the W -boson width

7.1 Overview

The p_T^ℓ and m_T distributions are not only sensitive to m_W but also to Γ_W , as shown in Figure 1. In particular, the high tails of the p_T^ℓ and m_T distributions are sensitive to changes of Γ_W . The fit to the m_T distribution is expected to be more sensitive, because events with high m_T are more likely to come from the tail of the W -boson Breit–Wigner distribution than events with high p_T^ℓ . The measurement of Γ_W relies on the same statistical framework, the same calibration, and the same distributions as the previously presented measurement of m_W . However, Γ_W is left free in the fit, while the W -boson mass is treated as NP and set to its SM expectation within the global electroweak fit, $m_W^{\text{SM}} = 80355 \pm 6$ MeV [6]. The templates are generated with different values of Γ_W , centred around the reference value used in the Monte Carlo signal

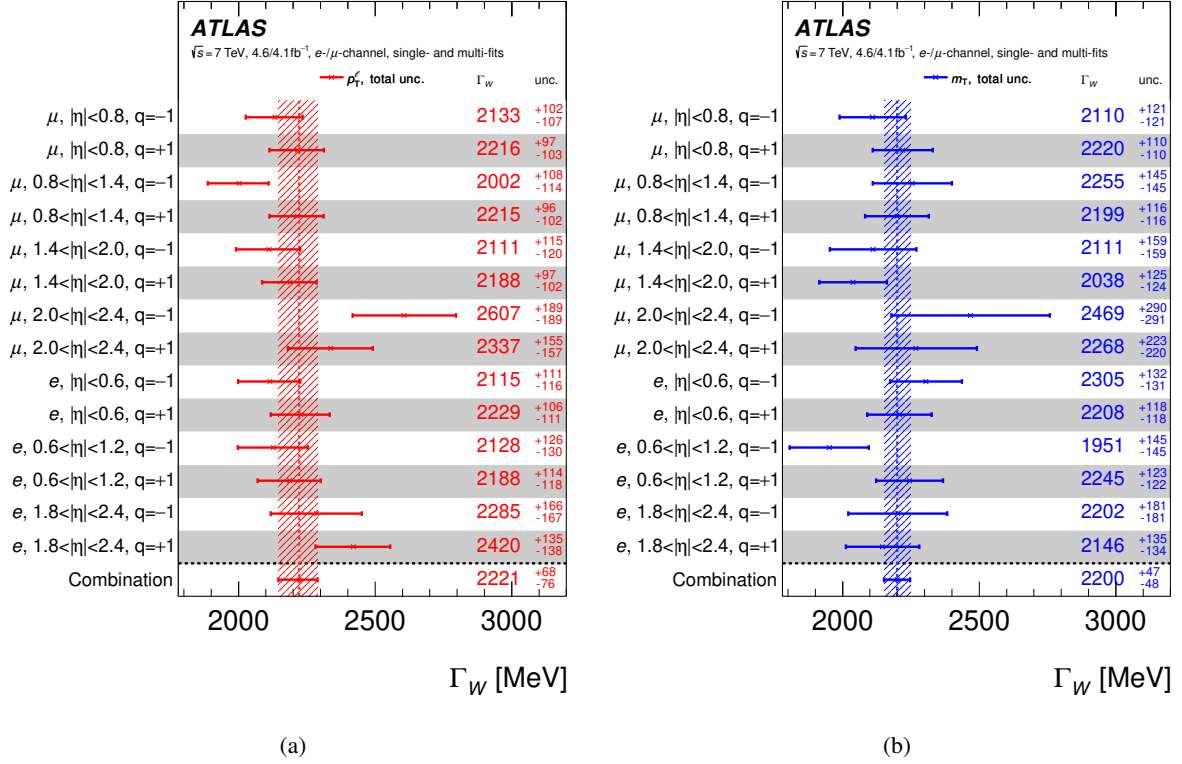


Figure 11: Overview of the Γ_W PLH fit results in all categories for the (a) p_T^ℓ and (b) m_T distributions, with the CT18 PDF set. The points labelled as ‘Combination’ correspond to the result of a joint PLH fit to all categories.

samples. All results are obtained using the same fit ranges as in the m_W measurement: $60 < m_T < 100$ GeV and $30 < p_T^\ell < 50$ GeV. The choice of fitting range is driven by the uncertainties in the lepton performance and the hadronic recoil.

7.2 Results and discussion

The results for each measurement category including all systematic uncertainties for the CT18 PDF set are summarised in Figure 11 yielding the values of $\Gamma_W = 2221^{+68}_{-76}$ MeV and $\Gamma_W = 2200^{+47}_{-48}$ MeV for p_T^ℓ and m_T distributions respectively. Good agreement between the categories can be observed.

Contrary to m_W , the fitted value of Γ_W depends more strongly on the assumed value of the mass. The fitted value of Γ_W varies with the assumed value for m_W following $\Delta\Gamma_W = -1.25 \Delta m_W$. In the Standard Model, the predicted value of m_W mainly depends on the assumed value of m_t . The present result is based on Ref. [6], which uses $m_t = 172.6$ GeV and is close to the LHC combined value used in Figure 10(b). Using $m_t = 171.8$ GeV [62] or $m_t = 173.1$ GeV [63] yields $m_W^{\text{SM}} = 80350$ MeV or 80360 MeV, respectively, with corresponding variations of Γ_W by ± 6 MeV.

The impact of different PDF sets (CT14, CT18, CT18A, MMHT2014, MSHT20, ATLASpdf21, NNPDF3.1, NNPDF4.0) on the Γ_W measurement is also studied. The results of full fits for all considered PDF sets are summarised in Table 5, with again a satisfactory fit quality for all PDF sets. The PDF dependence of the fit

Table 5: Best-fit value of Γ_W , total and PDF uncertainties, in MeV, and goodness-of-fit for the p_T^ℓ and m_T distributions and the PDF sets described in the text. Each fit uses 14 event categories with 40 bins, for 558 degrees of freedom.

PDF set	p_T^ℓ fit				m_T fit			
	Γ_W	σ_{tot}	σ_{PDF}	$\chi^2/\text{n.d.f.}$	Γ_W	σ_{tot}	σ_{PDF}	$\chi^2/\text{n.d.f.}$
CT14	2228	+67 -83	24	550.0/558	2202	+48 -48	5	556.8/558
CT18	2221	+68 -76	21	534.5/558	2200	+47 -48	5	548.8/558
CT18A	2207	+68 -75	18	533.0/558	2181	+47 -48	5	550.6/558
MMHT2014	2155	+71 -78	19	546.0/558	2186	+48 -48	5	562.2/558
MSHT20	2206	+66 -79	15	556.5/558	2179	+47 -48	4	559.4/558
ATLASpdf21	2213	+67 -73	18	531.3/558	2190	+47 -48	6	545.6/558
NNPDF31	2203	+65 -78	20	531.7/558	2180	+47 -47	6	560.4/558
NNPDF40	2182	+69 -68	12	550.5/558	2184	+47 -47	4	564.0/558

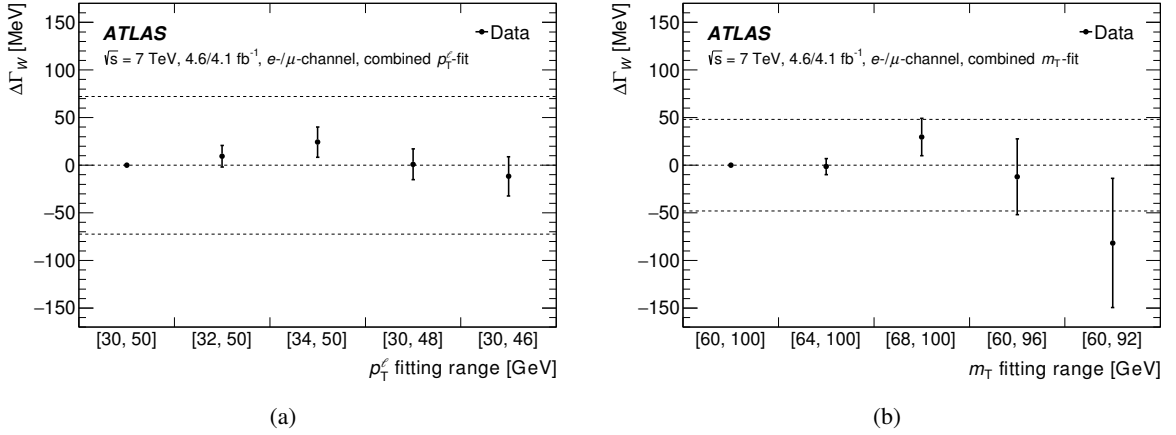


Figure 12: Difference $\Delta\Gamma_W$ between the W -boson width measured using the (a) p_T^ℓ and (b) m_T distribution fit ranges indicated in the figure and the nominal fit range. The nominal ranges are $30 < p_T^\ell < 50$ GeV and $60 < m_T < 100$ GeV, respectively. The outer dashed lines indicate the total measurement uncertainty for the nominal range. Results are shown for the combined fit over all categories, and for the CT18 PDF set.

result is weaker than for m_W , and all central values are well within the uncertainties obtained with CT18. The CT18 PDF set is chosen for the baseline result, consistently with the m_W measurement.

Partial fits are performed to the electron and muon channels separately. These fit results are found to agree within one standard deviation. Similarly, separate fits are performed in the W^+ and W^- channels. The results for the two charges are consistent within the 68% CL contour of the two-dimensional likelihood function for the m_T fits, while for the p_T^ℓ fits the consistency between the two charges is within two standard deviations. Finally, the dependence of the measurement result on the m_T and p_T^ℓ ranges used for the fit is studied in Figure 12, with stable results.

Figure 13 summarises the ten nuisance parameters that induce the largest shift of Γ_W in fits to the p_T^ℓ and m_T distributions. The largest shifts are related to the multijet (MJ) background, to the lepton calibration,

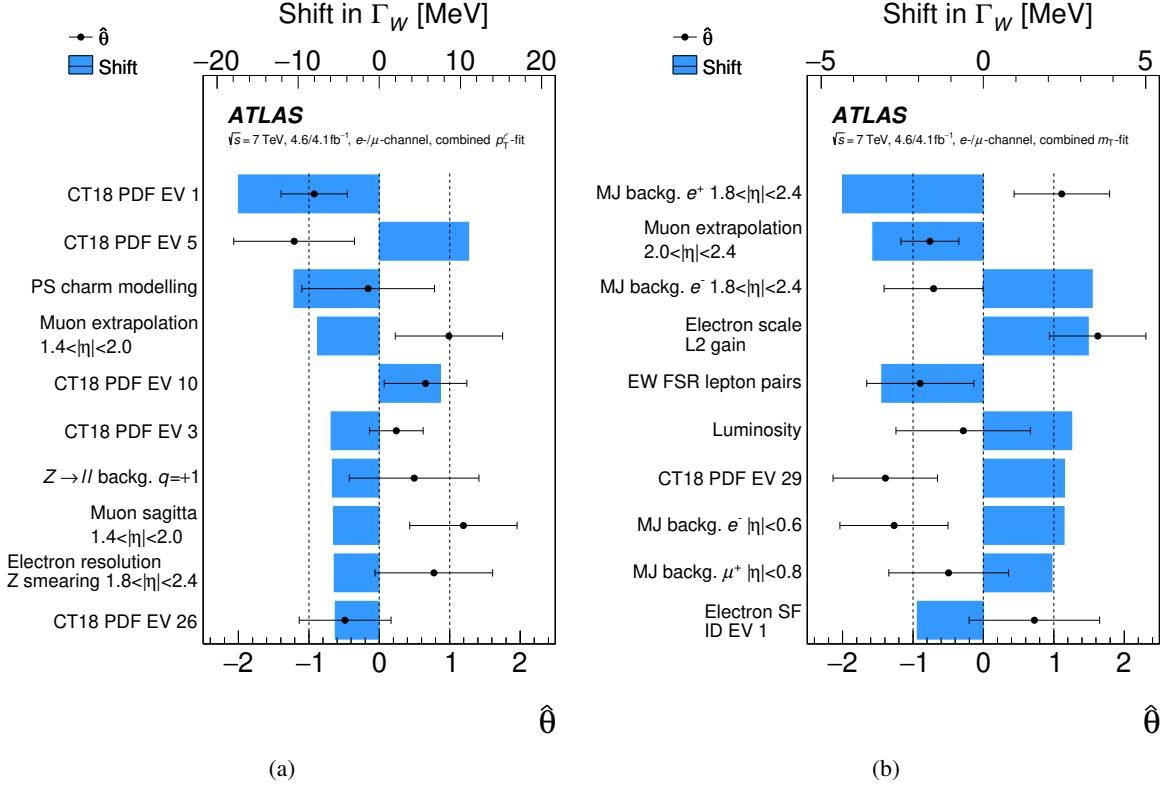


Figure 13: The ten nuisance parameters inducing the largest shifts on the fitted value of Γ_W in the combined PLH fits, using the (a) p_T^ℓ and (b) m_T distributions and the CT18 PDF set. For a given NP θ , the shift is defined as the product of its post-fit value $\hat{\theta}$ and its pre-fit impact on Γ_W . The points, which are plotted according to the bottom horizontal scale, show $\hat{\theta}$ for each of the nuisance parameters. The error bars show the corresponding post-fit uncertainties, $\sigma_{\hat{\theta}}$. The nuisance parameters are ranked according to the shift induced on Γ_W , the NPs with the largest shifts at the top.

to specific eigenvectors of the CT18 PDF set, to the luminosity, and to the uncertainty in charm-induced production for the p_T^W description.

The decomposition of post-fit uncertainties is done with the same method as in the m_W measurement, see Section 6.4. A summary of the uncertainties contributed by various sources is given in Table 6. The measurement is dominated by systematic uncertainties for the p_T^ℓ distribution, while for the m_T distribution statistical and systematic uncertainties are of similar magnitude. The dominant systematic uncertainties are due to the parton shower modelling for p_T^ℓ , and lepton and recoil performance for m_T , respectively.

An overview of selected pre- and post-fit distributions of m_T is shown in Figure 14, where a general better agreement can be observed for the post-fit case. The post-fit distributions use the final measured value of Γ_W .

7.3 Combination

The combination of results obtained from p_T^ℓ and m_T distributions follows the procedure described in Section 6.4. The p_T^ℓ and m_T results are fully compatible with each other. The results for all considered

Table 6: Uncertainty components for the p_T^ℓ , m_T and combined Γ_W measurements using the CT18 PDF set. The first columns give the total, statistical and overall systematic uncertainty in the measurements. The following columns show the contributions of modelling and experimental systematic uncertainties, grouped into categories.

Unc. [MeV]	Total	Stat.	Syst.	PDF	A_i	Backg.	EW	e	μ	u_T	Lumi	m_W	PS
p_T^ℓ	72	27	66	21	14	10	5	13	12	12	10	6	55
m_T	48	36	32	5	7	10	3	13	9	18	9	6	12
Combined	47	32	34	7	8	9	3	13	9	17	9	6	18

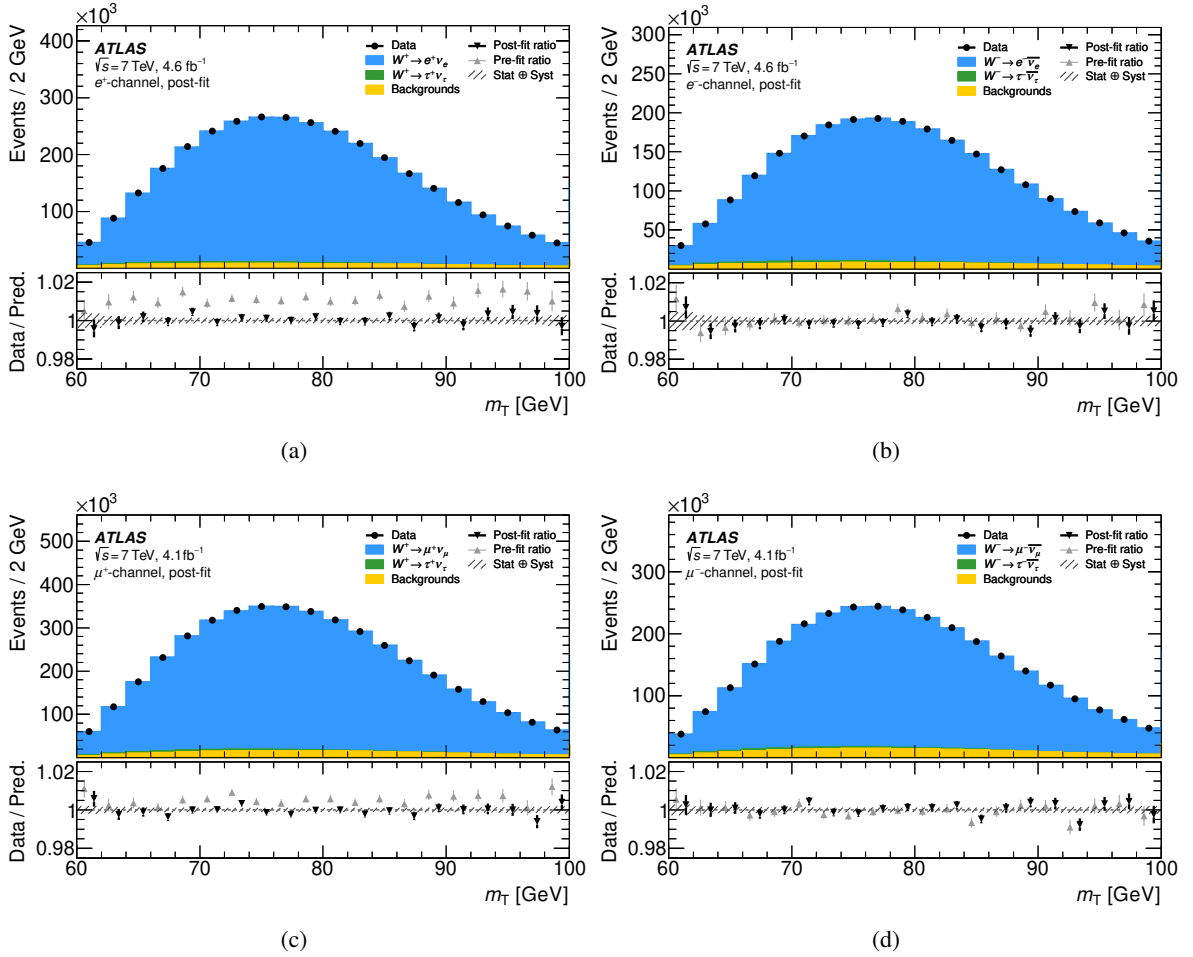


Figure 14: Post-fit distributions of m_T with data and MC for (a) $W^+ \rightarrow e^+ \nu_e$, (b) $W^- \rightarrow e^- \bar{\nu}_e$, (c) $W^+ \rightarrow \mu^+ \nu_\mu$ and (d) $W^- \rightarrow \mu^- \bar{\nu}_\mu$, inclusive over all η regions, and using the CT18 PDF set. In the bottom panels, the darker points represent the post-fit ratio of data to MC, while the lighter points indicate the ratio before the fit. The hatched band represents the total uncertainty of the data.

Table 7: Uncertainty correlation between the p_T^ℓ and m_T fits, combination weights and combination results for Γ_W and the indicated PDF sets.

PDF set	Correlation	weight (m_T)	weight (p_T^ℓ)	Combined Γ_W [MeV]
CT14	50.3%	88%	12%	2204 ± 47
CT18	51.5%	87%	13%	2202 ± 47
CT18A	50.0%	86%	14%	2184 ± 47
MMHT2014	50.8%	88%	13%	2182 ± 47
MSHT20	53.6%	89%	11%	2181 ± 47
ATLASpdf21	49.5%	84%	16%	2193 ± 46
NNPDF31	49.9%	86%	14%	2182 ± 46
NNPDF40	51.4%	85%	15%	2184 ± 46

PDF sets are presented in Table 7. The weight of the m_T fit ranges from 84% to 89%, depending on the PDF set, and dominates the final result. For CT18, the final result yields:

$$\Gamma_W = 2202 \pm 32 \text{ (stat.)} \pm 34 \text{ (syst.) MeV} = 2202 \pm 47 \text{ MeV,}$$

where the first uncertainty component is statistical and the second corresponds to the total systematic uncertainties. The compatibility of the measured value with the SM expectation is illustrated in Figure 15(a), together with selected previous measurements.

8 Simultaneous determination of the W -boson mass and width

The previously described determination of m_W assumes for the W -boson width its SM value and uncertainty, and similarly the Γ_W measurement uses the SM prediction for m_W . To further test the interplay between the two observables, the PLH fit is also performed with both m_W and Γ_W free in the fit. This fit with two parameters of interest relies on the same experimental calibrations and physics modelling. The fit yields values of $m_W = 80351.8 \pm 16.7$ MeV and $\Gamma_W = 2216 \pm 73$ MeV for the p_T^ℓ distributions and $m_W = 80369.4 \pm 26.8$ MeV and $\Gamma_W = 2186 \pm 53$ MeV for the m_T distributions using the CT18 PDF set. Compared with the separate m_W and Γ_W fits, the decrease of m_W by 10 MeV and 25 MeV for the p_T^ℓ and m_T distributions, respectively, is consistent with the larger measured value of Γ_W following the observed anti-correlation of m_W and Γ_W . The increase in total uncertainty is due to the removal of the constraints on Γ_W and m_W in the fit.

The combination of results obtained from p_T^ℓ and m_T distributions follows the procedure described in Section 6.4. The p_T^ℓ and m_T results are fully compatible with each other.

For the CT18 PDF set, the combination yields values of

$$m_W = 80354.8 \pm 16.1 \text{ MeV}$$

and

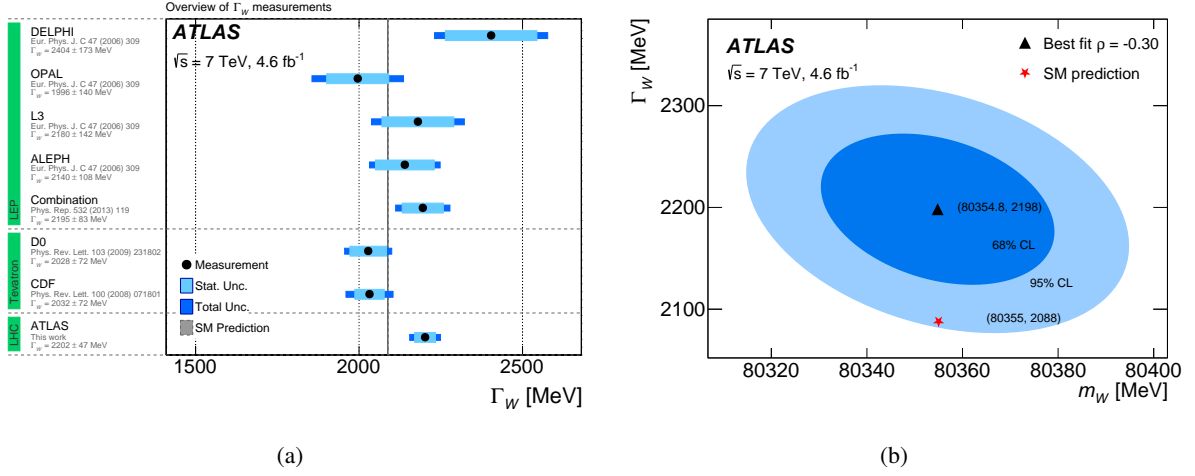


Figure 15: (a) Present measurement of Γ_W , compared to the SM prediction from the global electroweak fit [6], and to the measurements of LEP [10] and Tevatron [64]. (b) 68% and 95% CL uncertainty contours for the simultaneous determination of m_W and Γ_W using the CT18 PDF set and combining results from the p_T^ℓ and m_T distributions. The triangular marker represents the best fit, while the star corresponds to the SM prediction of Ref. [6].

$$\Gamma_W = 2198 \pm 49 \text{ MeV},$$

with a correlation of -30% that reflects the negative slope of the dependencies reported in Sections 6.4 and 7.2. The 68% and 95% CL uncertainty contours are shown in Figure 15(b).

9 Conclusion

This paper reports on a first measurement of the W -boson width at the LHC as well as the reanalysis of the data used in the published W -boson mass measurement, using an improved fitting technique and updated parton distribution functions. Both measurements are based on proton–proton collision data at a centre-of-mass energy of $\sqrt{s} = 7$ TeV recorded by the ATLAS detector at the LHC in 2011, and corresponding to an integrated luminosity of 4.6 fb^{-1} and 4.1 fb^{-1} in the electron and muon channels, respectively.

The measurements of m_W using the p_T^ℓ and m_T distributions are found to be consistent and their combination yields

$$m_W = 80366.5 \pm 9.8 \text{ (stat.)} \pm 12.5 \text{ (syst.) MeV} = 80366.5 \pm 15.9 \text{ MeV}.$$

The present result is compatible with and supersedes the previous measurement of m_W at ATLAS using the same data. No significant deviation from the SM expectation is observed. The PDF dependence of the m_W result is driven by the pre-fit PDF uncertainties, and is strongly reduced when allowing for enlarged uncertainties. The final results are obtained using the CT18 PDF set, which is the most conservative PDF set for these measurements and compatible with the fits using enlarged PDF uncertainties of other sets.

The measurements of Γ_W using the p_T^ℓ and m_T distributions are also found to be consistent and their combination yields a value of

$$\Gamma_W = 2202 \pm 32 \text{ (stat.)} \pm 34 \text{ (syst.) MeV} = 2202 \pm 47 \text{ MeV.}$$

It is the currently most precise single measurement of Γ_W and agrees with the SM expectation of $\Gamma_W^{\text{SM}} = 2088 \pm 1 \text{ MeV}$ within two standard deviations. The dependence of Γ_W on the assumed PDF set is weak compared with the measurement uncertainties.

Acknowledgements

We thank CERN for the very successful operation of the LHC and its injectors, as well as the support staff at CERN and at our institutions worldwide without whom ATLAS could not be operated efficiently.

The crucial computing support from all WLCG partners is acknowledged gratefully, in particular from CERN, the ATLAS Tier-1 facilities at TRIUMF/SFU (Canada), NDGF (Denmark, Norway, Sweden), CC-IN2P3 (France), KIT/GridKA (Germany), INFN-CNAF (Italy), NL-T1 (Netherlands), PIC (Spain), RAL (UK) and BNL (USA), the Tier-2 facilities worldwide and large non-WLCG resource providers. Major contributors of computing resources are listed in Ref. [65].

We gratefully acknowledge the support of ANPCyT, Argentina; YerPhI, Armenia; ARC, Australia; BMWFW and FWF, Austria; ANAS, Azerbaijan; CNPq and FAPESP, Brazil; NSERC, NRC and CFI, Canada; CERN; ANID, Chile; CAS, MOST and NSFC, China; Minciencias, Colombia; MEYS CR, Czech Republic; DNRF and DNSRC, Denmark; IN2P3-CNRS and CEA-DRF/IRFU, France; SRNSFG, Georgia; BMBF, HGF and MPG, Germany; GSRI, Greece; RGC and Hong Kong SAR, China; ISF and Benozziyo Center, Israel; INFN, Italy; MEXT and JSPS, Japan; CNRST, Morocco; NWO, Netherlands; RCN, Norway; MEiN, Poland; FCT, Portugal; MNE/IFA, Romania; MESTD, Serbia; MSSR, Slovakia; ARRS and MIZŠ, Slovenia; DSI/NRF, South Africa; MICINN, Spain; SRC and Wallenberg Foundation, Sweden; SERI, SNSF and Cantons of Bern and Geneva, Switzerland; MOST, Taipei; TENMAK, Türkiye; STFC, United Kingdom; DOE and NSF, United States of America.

Individual groups and members have received support from BCKDF, CANARIE, CRC and DRAC, Canada; PRIMUS 21/SCI/017, Czech Republic; COST, ERC, ERDF, Horizon 2020, ICSC-NextGenerationEU and Marie Skłodowska-Curie Actions, European Union; Investissements d’Avenir Labex, Investissements d’Avenir Idex and ANR, France; DFG and AvH Foundation, Germany; Herakleitos, Thales and Aristeia programmes co-financed by EU-ESF and the Greek NSRF, Greece; BSF-NSF and MINERVA, Israel; Norwegian Financial Mechanism 2014-2021, Norway; NCN and NAWA, Poland; La Caixa Banking Foundation, CERCA Programme Generalitat de Catalunya and PROMETEO and GenT Programmes Generalitat Valenciana, Spain; Göran Gustafssons Stiftelse, Sweden; The Royal Society and Leverhulme Trust, United Kingdom.

In addition, individual members wish to acknowledge support from CERN: European Organization for Nuclear Research (CERN PIAS); Chile: Agencia Nacional de Investigación y Desarrollo (FONDECYT 1190886, FONDECYT 1210400, FONDECYT 1230987); China: National Natural Science Foundation of China (NSFC - 12175119, NSFC 12275265); Czech Republic: Ministry of Education Youth and Sports (FORTE CZ.02.01.01/00/22_008/0004632); European Union: European Research Council (ERC - 948254, ERC 101089007), Horizon 2020 Framework Programme (MUCCA - CHIST-ERA-19-XAI-00), Italian Center for High Performance Computing, Big Data and Quantum Computing (ICSC, NextGenerationEU);

France: Agence Nationale de la Recherche (ANR-20-CE31-0013, ANR-21-CE31-0022), Investissements d’Avenir Labex (ANR-11-LABX-0012); Germany: Baden-Württemberg Stiftung (BW Stiftung-Postdoc Eliteprogramme), Deutsche Forschungsgemeinschaft (DFG - 469666862, DFG - CR 312/5-2); Italy: Istituto Nazionale di Fisica Nucleare (ICSC, NextGenerationEU); Japan: Japan Society for the Promotion of Science (JSPS KAKENHI 22H01227, JSPS KAKENHI 22KK0227, JSPS KAKENHI JP21H05085, JSPS KAKENHI JP22H04944); Netherlands: Netherlands Organisation for Scientific Research (NWO Veni 2020 - VI.Veni.202.179); Norway: Research Council of Norway (RCN-314472); Poland: Polish National Agency for Academic Exchange (PPN/PPO/2020/1/00002/U/00001), Polish National Science Centre (NCN 2021/42/E/ST2/00350, NCN OPUS nr 2022/47/B/ST2/03059, NCN UMO-2019/34/E/ST2/00393, UMO-2020/37/B/ST2/01043, UMO-2021/40/C/ST2/00187, UMO-2022/47/O/ST2/00148); Slovenia: Slovenian Research Agency (ARIS grant J1-3010); Spain: Generalitat Valenciana (Artemisa, FEDER, IDIFEDER/2018/048), Ministry of Science and Innovation (RYC2019-028510-I, RYC2020-030254-I), PROMETEO and GenT Programmes Generalitat Valenciana (CIDEAGENT/2019/023, CIDEAGENT/2019/027); Sweden: Swedish Research Council (VR 2022-03845, VR 2023-03403), Knut and Alice Wallenberg Foundation (KAW 2022.0358); Switzerland: Swiss National Science Foundation (SNSF - PCEFP2_194658); United Kingdom: Leverhulme Trust (Leverhulme Trust RPG-2020-004); United States of America: Neubauer Family Foundation.

References

- [1] S. L. Glashow, *Partial-symmetries of weak interactions*, *Nucl. Phys.* **22** (1961) 579.
- [2] A. Salam and J. C. Ward, *Electromagnetic and weak interactions*, *Phys. Lett.* **13** (1964) 168.
- [3] S. Weinberg, *A Model of Leptons*, *Phys. Rev. Lett.* **19** (1967) 1264.
- [4] A. Sirlin, *Radiative corrections in the $SU(2)_L \times U(1)$ theory: A simple renormalization framework*, *Phys. Rev. D* **22** (1980) 971.
- [5] M. Awramik, M. Czakon, A. Freitas and G. Weiglein, *Precise prediction for the W -boson mass in the standard model*, *Phys. Rev. D* **69** (2004) 053006, arXiv: [hep-ph/0311148](https://arxiv.org/abs/hep-ph/0311148).
- [6] J. de Blas et al., *Global analysis of electroweak data in the Standard Model*, *Phys. Rev. D* **106** (2022) 033003, arXiv: [2112.07274](https://arxiv.org/abs/2112.07274) [[hep-ph](#)].
- [7] The GFitter Group, J. Haller et al., *Update of the global electroweak fit and constraints on two-Higgs-doublet models*, *Eur. Phys. J. C* **78** (2018) 675, arXiv: [1803.01853](https://arxiv.org/abs/1803.01853) [[hep-ph](#)].
- [8] J. Erler, ‘Global Fits to Electroweak Data Using GAPP’, *QCD and weak boson physics in Run II. Proceedings, Batavia, IL, March 4-6, June 3-4, November 4-6, 1999*, arXiv: [hep-ph/0005084](https://arxiv.org/abs/hep-ph/0005084) [[hep-ph](#)].
- [9] CDF Collaboration, *High-precision measurement of the W boson mass with the CDF II detector*, *Science* **376** (2022) 170.
- [10] The ALEPH Collaboration, The DELPHI Collaboration, The L3 Collaboration, The OPAL Collaboration, The LEP Electroweak Working Group, *Electroweak measurements in electron-positron collisions at W -boson-pair energies at LEP*, *Phys. Rept.* **532** (2013) 119, arXiv: [1302.3415](https://arxiv.org/abs/1302.3415) [[hep-ex](#)].

- [11] D0 Collaboration, *Measurement of the W Boson Mass with the D0 Detector*, *Phys. Rev. Lett.* **108** (2012) 151804, arXiv: [1203.0293 \[hep-ex\]](#).
- [12] ATLAS Collaboration, *Measurement of the W-boson mass in pp collisions at $\sqrt{s} = 7$ TeV with the ATLAS detector*, *Eur. Phys. J. C* **78** (2018) 110, arXiv: [1701.07240 \[hep-ex\]](#),
Erratum: *Eur. Phys. J. C* **78** (2018) 898.
- [13] LHCb Collaboration, *Measurement of the W boson mass*, *JHEP* **01** (2022) 036, arXiv: [2109.01113 \[hep-ex\]](#).
- [14] S. Amoroso et al., *Compatibility and combination of world W-boson mass measurements*, (2023), arXiv: [2308.09417 \[hep-ex\]](#).
- [15] M. E. Peskin and T. Takeuchi, *Estimation of oblique electroweak corrections*, *Phys. Rev. D* **46** (1992) 381.
- [16] S. Heinemeyer, W. Hollik, G. Weiglein and L. Zeune, *Implications of LHC search results on the W boson mass prediction in the MSSM*, *JHEP* **12** (2013) 084, arXiv: [1311.1663 \[hep-ph\]](#).
- [17] Particle Data Group, R. L. Workman et al., *Review of Particle Physics*, *PTEP* **2022** (2022) 083C01.
- [18] CDF Collaboration, *Precise measurement of the W-boson mass with the CDF II detector*, *Phys. Rev. Lett.* **108** (2012) 151803, arXiv: [1203.0275 \[hep-ex\]](#).
- [19] D0 Collaboration, *Measurement of the W boson mass with the D0 detector*, *Phys. Rev. D* **89** (2014) 012005, arXiv: [1310.8628 \[hep-ex\]](#).
- [20] W. A. Rolke, A. M. López and J. Conrad, *Limits and confidence intervals in the presence of nuisance parameters*, *Nucl. Instrum. Meth. A* **551** (2005) 493, arXiv: [physics/0403059](#).
- [21] ATLAS Collaboration, *The ATLAS Experiment at the CERN Large Hadron Collider*, *JINST* **3** (2008) S08003.
- [22] ATLAS Collaboration, *Performance of the ATLAS Trigger System in 2010*, *Eur. Phys. J. C* **72** (2012) 1849, arXiv: [1110.1530 \[hep-ex\]](#).
- [23] ATLAS Collaboration, *The ATLAS Collaboration Software and Firmware*, ATL-SOFT-PUB-2021-001, 2021, URL: <https://cds.cern.ch/record/2767187>.
- [24] P. Nason, *A new method for combining NLO QCD with shower Monte Carlo algorithms*, *JHEP* **11** (2004) 040, arXiv: [hep-ph/0409146](#).
- [25] S. Frixione, P. Nason and C. Oleari, *Matching NLO QCD computations with parton shower simulations: the POWHEG method*, *JHEP* **11** (2007) 070, arXiv: [0709.2092 \[hep-ph\]](#).
- [26] S. Alioli, P. Nason, C. Oleari and E. Re, *A general framework for implementing NLO calculations in shower Monte Carlo programs: the POWHEG BOX*, *JHEP* **06** (2010) 043, arXiv: [1002.2581 \[hep-ph\]](#).
- [27] T. Sjöstrand, S. Mrenna and P. Skands, *PYTHIA 6.4 physics and manual*, *JHEP* **05** (2006) 026, arXiv: [hep-ph/0603175](#).
- [28] T. Sjöstrand, S. Mrenna and P. Skands, *A brief introduction to PYTHIA 8.1*, *Comput. Phys. Commun.* **178** (2008) 852, arXiv: [0710.3820 \[hep-ph\]](#).

- [29] ATLAS Collaboration, *Measurement of the Z/γ^* boson transverse momentum distribution in pp collisions at $\sqrt{s} = 7$ TeV with the ATLAS detector*, *JHEP* **09** (2014) 145, arXiv: [1406.3660 \[hep-ex\]](#).
- [30] H.-L. Lai et al., *New parton distributions for collider physics*, *Phys. Rev. D* **82** (2010) 074024, arXiv: [1007.2241 \[hep-ph\]](#).
- [31] J. Pumplin et al., *New Generation of Parton Distributions with Uncertainties from Global QCD Analysis*, *JHEP* **07** (2002) 012, arXiv: [hep-ph/0201195](#).
- [32] P. Golonka and Z. Was, *PHOTOS Monte Carlo: a precision tool for QED corrections in Z and W decays*, *Eur. Phys. J. C* **45** (2006) 97, arXiv: [hep-ph/0506026](#).
- [33] ATLAS Collaboration, *Precision measurement and interpretation of inclusive W^+ , W^- and Z/γ^* production cross sections with the ATLAS detector*, *Eur. Phys. J. C* **77** (2017) 367, arXiv: [1612.03016 \[hep-ex\]](#).
- [34] S. Frixione and B. R. Webber, *Matching NLO QCD computations and parton shower simulations*, *JHEP* **06** (2002) 029, arXiv: [hep-ph/0204244](#).
- [35] S. Frixione, P. Nason and B. R. Webber, *Matching NLO QCD and parton showers in heavy flavour production*, *JHEP* **08** (2003) 007, arXiv: [hep-ph/0305252](#).
- [36] S. Frixione, E. Laenen, P. Motylinski and B. R. Webber, *Single-top production in MC@NLO*, *JHEP* **03** (2006) 092, arXiv: [hep-ph/0512250](#).
- [37] ATLAS Collaboration, *The ATLAS Simulation Infrastructure*, *Eur. Phys. J. C* **70** (2010) 823, arXiv: [1005.4568 \[physics.ins-det\]](#).
- [38] S. Agostinelli et al., *GEANT4—a simulation toolkit*, *Nucl. Instrum. Meth. A* **506** (2003) 250.
- [39] ATLAS Collaboration, *Summary of ATLAS Pythia 8 tunes*, ATL-PHYS-PUB-2012-003, 2012, URL: <https://cds.cern.ch/record/1474107>.
- [40] ATLAS Collaboration, *Electron reconstruction and identification efficiency measurements with the ATLAS detector using the 2011 LHC proton–proton collision data*, *Eur. Phys. J. C* **74** (2014) 2941, arXiv: [1404.2240 \[hep-ex\]](#).
- [41] ATLAS Collaboration, *Electron and photon energy calibration with the ATLAS detector using LHC Run 1 data*, *Eur. Phys. J. C* **74** (2014) 3071, arXiv: [1407.5063 \[hep-ex\]](#).
- [42] ATLAS Collaboration, *Measurement of the muon reconstruction performance of the ATLAS detector using 2011 and 2012 LHC proton–proton collision data*, *Eur. Phys. J. C* **74** (2014) 3130, arXiv: [1407.3935 \[hep-ex\]](#).
- [43] ATLAS Collaboration, *Improved luminosity determination in pp collisions at $\sqrt{s} = 7$ TeV using the ATLAS detector at the LHC*, *Eur. Phys. J. C* **73** (2013) 2518, arXiv: [1302.4393 \[hep-ex\]](#).
- [44] S. Dulat et al., *New parton distribution functions from a global analysis of quantum chromodynamics*, *Phys. Rev. D* **93** (2016) 033006, arXiv: [1506.07443 \[hep-ph\]](#).

- [45] L. A. Harland-Lang, A. D. Martin, P. Motylinski and R. S. Thorne, *Parton distributions in the LHC era: MMHT 2014 PDFs*, *Eur. Phys. J. C* **75** (2015) 204, arXiv: [1412.3989 \[hep-ph\]](#).
- [46] ATLAS Collaboration, *Determination of the parton distribution functions of the proton using diverse ATLAS data from pp collisions at $\sqrt{s} = 7, 8$ and 13 TeV*, *Eur. Phys. J. C* **82** (2022) 438, arXiv: [2112.11266 \[hep-ex\]](#).
- [47] T.-J. Hou et al., *New CTEQ global analysis of quantum chromodynamics with high-precision data from the LHC*, *Phys. Rev. D* **103** (2021) 014013, arXiv: [1912.10053 \[hep-ph\]](#).
- [48] S. Bailey, T. Cridge, L. A. Harland-Lang, A. D. Martin and R. S. Thorne, *Parton distributions from LHC, HERA, Tevatron and fixed target data: MSHT20 PDFs*, *Eur. Phys. J. C* **81** (2021) 341, arXiv: [2012.04684 \[hep-ph\]](#).
- [49] NNPDF Collaboration, *Parton distributions from high-precision collider data*, *Eur. Phys. J. C* **77** (2017) 663, arXiv: [1706.00428 \[hep-ph\]](#).
- [50] NNPDF Collaboration, R. D. Ball et al., *The path to proton structure at 1% accuracy*, *Eur. Phys. J. C* **82** (2022) 428, arXiv: [2109.02653 \[hep-ph\]](#).
- [51] A. Pinto et al., *Uncertainty components in profile likelihood fits*, (2023), arXiv: [2307.04007 \[physics.data-an\]](#).
- [52] The ALEPH Collaboration, The DELPHI Collaboration, The L3 Collaboration, The OPAL Collaboration, The SLD Collaboration, The LEP Electroweak Working Group, The SLD Electroweak and Heavy Flavour Groups, *Precision electroweak measurements on the Z resonance*, *Phys. Rept.* **427** (2006) 257, arXiv: [hep-ex/0509008](#).
- [53] K. Pearson, *LIII. On lines and planes of closest fit to systems of points in space*, *London Edinburgh Dublin Philos. Mag. & J. Sci.* **2** (1901) 559.
- [54] H. Hotelling, *Analysis of a complex of statistical variables into principal components*, *J. Educ. Psychol.* (1933) 417.
- [55] ATLAS Collaboration, *Measurement of the angular coefficients in Z-boson events using electron and muon pairs from data taken at $\sqrt{s} = 8$ TeV with the ATLAS detector*, *JHEP* **08** (2016) 159, arXiv: [1606.00689 \[hep-ex\]](#).
- [56] ATLAS Collaboration, *Precise measurements of W and Z transverse momentum spectra with the ATLAS detector at $\sqrt{s} = 5.02$ TeV and 13 TeV*, CERN-EP-2024-080, 2024.
- [57] J. Pumplin et al., *Uncertainties of predictions from parton distribution functions. II. The Hessian method*, *Phys. Rev. D* **65** (2001) 014013, arXiv: [hep-ph/0101032](#).
- [58] T. Sjöstrand and P. Z. Skands, *Transverse-momentum-ordered showers and interleaved multiple interactions*, *Eur. Phys. J. C* **39** (2005) 129, arXiv: [hep-ph/0408302](#).
- [59] L. Lyons, D. Gibaut and P. Clifford, *How to combine correlated estimates of a single physical quantity*, *Nucl. Instrum. Meth. A* **270** (1988) 110.
- [60] ATLAS and CMS Collaborations, *Combination of measurements of the top quark mass from data collected by the ATLAS and CMS experiments at $\sqrt{s}=7$ and 8 TeV*, (2024), arXiv: [2402.08713 \[hep-ex\]](#).

- [61] ATLAS Collaboration, *Combined Measurement of the Higgs Boson Mass from the $H \rightarrow \gamma\gamma$ and $H \rightarrow ZZ^* \rightarrow 4\ell$ Decay Channels with the ATLAS Detector Using $\sqrt{s}=7, 8,$ and 13 TeV pp Collision Data*, *Phys. Rev. Lett.* **131** (2023) 251802, arXiv: [2308.04775](https://arxiv.org/abs/2308.04775) [[hep-ex](#)].
- [62] J. de Blas, M. Pierini, L. Reina and L. Silvestrini, *Impact of the Recent Measurements of the Top-Quark and W-Boson Masses on Electroweak Precision Fits*, *Phys. Rev. Lett.* **129** (2022) 271801, arXiv: [2204.04204](https://arxiv.org/abs/2204.04204) [[hep-ph](#)].
- [63] J. de Blas et al., *The Global Electroweak and Higgs Fits in the LHC era*, *PoS EPS-HEP2017* (2017) 467, ed. by P. Checchia et al., arXiv: [1710.05402](https://arxiv.org/abs/1710.05402) [[hep-ph](#)].
- [64] The Tevatron Electroweak Working Group, *Combination of CDF and D0 Results on the Width of the W boson*, 2010, arXiv: [1003.2826](https://arxiv.org/abs/1003.2826) [[hep-ex](#)].
- [65] ATLAS Collaboration, *ATLAS Computing Acknowledgements*, ATL-SOFT-PUB-2023-001, 2023, URL: <https://cds.cern.ch/record/2869272>.

The ATLAS Collaboration

G. Aad ¹⁰³, E. Aakvaag ¹⁶, B. Abbott ¹²¹, S. Abdelhameed ^{117a}, K. Abeling ⁵⁵, N.J. Abicht ⁴⁹, S.H. Abidi ²⁹, M. Aboeela ⁴⁴, A. Aboulhorma ^{35e}, H. Abramowicz ¹⁵², H. Abreu ¹⁵¹, Y. Abulaiti ¹¹⁸, B.S. Acharya ^{69a,69b,k}, A. Ackermann ^{63a}, C. Adam Bourdarios ⁴, L. Adamczyk ^{86a}, S.V. Addepalli ²⁶, M.J. Addison ¹⁰², J. Adelman ¹¹⁶, A. Adiguzel ^{21c}, T. Adye ¹³⁵, A.A. Affolder ¹³⁷, Y. Afik ³⁹, M.N. Agaras ¹³, J. Agarwala ^{73a,73b}, A. Aggarwal ¹⁰¹, C. Agheorghiesei ^{27c}, A. Ahmad ³⁶, F. Ahmadov ^{38,x}, W.S. Ahmed ¹⁰⁵, S. Ahuja ⁹⁶, X. Ai ^{62e}, G. Aielli ^{76a,76b}, A. Aikot ¹⁶⁴, M. Ait Tamliah ^{35e}, B. Aitbenchikh ^{35a}, M. Akbiyik ¹⁰¹, T.P.A. Åkesson ⁹⁹, A.V. Akimov ³⁷, D. Akiyama ¹⁶⁹, N.N. Akolkar ²⁴, S. Aktas ^{21a}, K. Al Houry ⁴¹, G.L. Alberghi ^{23b}, J. Albert ¹⁶⁶, P. Albicocco ⁵³, G.L. Albouy ⁶⁰, S. Alderweireldt ⁵², Z.L. Alegria ¹²², M. Aleksa ³⁶, I.N. Aleksandrov ³⁸, C. Alexa ^{27b}, T. Alexopoulos ¹⁰, F. Alfonsi ^{23b}, M. Algren ⁵⁶, M. Alhroob ¹⁶⁸, B. Ali ¹³³, H.M.J. Ali ⁹², S. Ali ³¹, S.W. Alibocus ⁹³, M. Aliev ^{33c}, G. Alimonti ^{71a}, W. Alkahi ⁵⁵, C. Allaire ⁶⁶, B.M.M. Allbrooke ¹⁴⁷, J.F. Allen ⁵², C.A. Allendes Flores ^{138f}, P.P. Allport ²⁰, A. Aloisio ^{72a,72b}, F. Alonso ⁹¹, C. Alpigiani ¹³⁹, Z.M.K. Alsolami ⁹², M. Alvarez Estevez ¹⁰⁰, A. Alvarez Fernandez ¹⁰¹, M. Alves Cardoso ⁵⁶, M.G. Alvigi ^{72a,72b}, M. Aly ¹⁰², Y. Amaral Coutinho ^{83b}, A. Ambler ¹⁰⁵, C. Amelung ³⁶, M. Amerl ¹⁰², C.G. Ames ¹¹⁰, D. Amidei ¹⁰⁷, K.J. Amirie ¹⁵⁶, S.P. Amor Dos Santos ^{131a}, K.R. Amos ¹⁶⁴, S. An ⁸⁴, V. Ananiev ¹²⁶, C. Anastopoulos ¹⁴⁰, T. Andeen ¹¹, J.K. Anders ³⁶, S.Y. Andrean ^{47a,47b}, A. Andreazza ^{71a,71b}, S. Angelidakis ⁹, A. Angerami ^{41,z}, A.V. Anisenkov ³⁷, A. Annovi ^{74a}, C. Antel ⁵⁶, E. Antipov ¹⁴⁶, M. Antonelli ⁵³, F. Anulli ^{75a}, M. Aoki ⁸⁴, T. Aoki ¹⁵⁴, M.A. Aparo ¹⁴⁷, L. Aperio Bella ⁴⁸, C. Appelt ¹⁸, A. Apyan ²⁶, S.J. Arbiol Val ⁸⁷, C. Arcangeletti ⁵³, A.T.H. Arce ⁵¹, E. Arena ⁹³, J-F. Arguin ¹⁰⁹, S. Argyropoulos ⁵⁴, J.-H. Arling ⁴⁸, O. Arnaez ⁴, H. Arnold ¹¹⁵, G. Artoni ^{75a,75b}, H. Asada ¹¹², K. Asai ¹¹⁹, S. Asai ¹⁵⁴, N.A. Asbah ³⁶, K. Assamagan ²⁹, R. Astalos ^{28a}, K.S.V. Astrand ⁹⁹, S. Atashi ¹⁶⁰, R.J. Atkin ^{33a}, M. Atkinson ¹⁶³, H. Atmani ^{35f}, P.A. Atmasiddha ¹²⁹, K. Augsten ¹³³, S. Auricchio ^{72a,72b}, A.D. Auriol ²⁰, V.A. Austrup ¹⁰², G. Avolio ³⁶, K. Axiotis ⁵⁶, G. Azuelos ^{109,ad}, D. Babal ^{28b}, H. Bachacou ¹³⁶, K. Bachas ^{153,o}, A. Bachi ³⁴, F. Backman ^{47a,47b}, A. Badea ³⁹, T.M. Baer ¹⁰⁷, P. Bagnaia ^{75a,75b}, M. Bahmani ¹⁸, D. Bahner ⁵⁴, K. Bai ¹²⁴, J.T. Baines ¹³⁵, L. Baines ⁹⁵, O.K. Baker ¹⁷³, E. Bakos ¹⁵, D. Bakshi Gupta ⁸, V. Balakrishnan ¹²¹, R. Balasubramanian ¹¹⁵, E.M. Baldin ³⁷, P. Balek ^{86a}, E. Ballabene ^{23b,23a}, F. Balli ¹³⁶, L.M. Baltos ^{63a}, W.K. Balunas ³², J. Balz ¹⁰¹, I. Bamwidhi ^{117b}, E. Banas ⁸⁷, M. Bandieramonte ¹³⁰, A. Bandyopadhyay ²⁴, S. Bansal ²⁴, L. Barak ¹⁵², M. Barakat ⁴⁸, E.L. Barberio ¹⁰⁶, D. Barberis ^{57b,57a}, M. Barbero ¹⁰³, M.Z. Barel ¹¹⁵, K.N. Barends ^{33a}, T. Barillari ¹¹¹, M-S. Barisits ³⁶, T. Barklow ¹⁴⁴, P. Baron ¹²³, D.A. Baron Moreno ¹⁰², A. Baroncelli ^{62a}, G. Barone ²⁹, A.J. Barr ¹²⁷, J.D. Barr ⁹⁷, F. Barreiro ¹⁰⁰, J. Barreiro Guimarães da Costa ^{14a}, U. Barron ¹⁵², M.G. Barros Teixeira ^{131a}, S. Barsov ³⁷, F. Bartels ^{63a}, R. Bartoldus ¹⁴⁴, A.E. Barton ⁹², P. Bartos ^{28a}, A. Basan ¹⁰¹, M. Baselga ⁴⁹, A. Bassalat ^{66,b}, M.J. Basso ^{157a}, R. Bate ¹⁶⁵, R.L. Bates ⁵⁹, S. Batlamous ¹⁰⁰, B. Batool ¹⁴², M. Battaglia ¹³⁷, D. Battulga ¹⁸, M. Baucé ^{75a,75b}, M. Bauer ³⁶, P. Bauer ²⁴, L.T. Bazzano Hurrell ³⁰, J.B. Beacham ⁵¹, T. Beau ¹²⁸, J.Y. Beaucamp ⁹¹, P.H. Beauchemin ¹⁵⁹, P. Bechtel ²⁴, H.P. Beck ^{19,n}, K. Becker ¹⁶⁸, A.J. Beddall ⁸², V.A. Bednyakov ³⁸, C.P. Bee ¹⁴⁶, L.J. Beemster ¹⁵, T.A. Beermann ³⁶, M. Begalli ^{83d}, M. Beger ²⁹, A. Behera ¹⁴⁶, J.K. Behr ⁴⁸, J.F. Beirer ³⁶, F. Beisiegel ²⁴, M. Belfkir ^{117b}, G. Bella ¹⁵², L. Bellagamba ^{23b}, A. Bellerive ³⁴, P. Bellos ²⁰, K. Beloborodov ³⁷, D. Benckekroun ^{35a}, F. Bendebba ^{35a}, Y. Benhammou ¹⁵²,

K.C. Benkendorfer ⁶¹, L. Beresford ⁴⁸, M. Beretta ⁵³, E. Bergeaas Kuutmann ¹⁶², N. Berger ⁴,
 B. Bergmann ¹³³, J. Beringer ^{17a}, G. Bernardi ⁵, C. Bernius ¹⁴⁴, F.U. Bernlochner ²⁴,
 F. Bernon ^{36,103}, A. Berrocal Guardia ¹³, T. Berry ⁹⁶, P. Berta ¹³⁴, A. Berthold ⁵⁰, S. Bethke ¹¹¹,
 A. Betti ^{75a,75b}, A.J. Bevan ⁹⁵, N.K. Bhalla ⁵⁴, M. Bhamjee ^{33c}, S. Bhatta ¹⁴⁶,
 D.S. Bhattacharya ¹⁶⁷, P. Bhattarai ¹⁴⁴, K.D. Bhide ⁵⁴, V.S. Bhopatkar ¹²², R.M. Bianchi ¹³⁰,
 G. Bianco ^{23b,23a}, O. Biebel ¹¹⁰, R. Bielski ¹²⁴, M. Biglietti ^{77a}, C.S. Billingsley ⁴⁴, M. Bindi ⁵⁵,
 A. Bingul ^{21b}, C. Bini ^{75a,75b}, A. Biondini ⁹³, C.J. Birch-sykes ¹⁰², G.A. Bird ³², M. Birman ¹⁷⁰,
 M. Biros ¹³⁴, S. Biryukov ¹⁴⁷, T. Bisanz ⁴⁹, E. Bisceglie ^{43b,43a}, J.P. Biswal ¹³⁵, D. Biswas ¹⁴²,
 I. Bloch ⁴⁸, A. Blue ⁵⁹, U. Blumenschein ⁹⁵, J. Blumenthal ¹⁰¹, V.S. Bobrovnikov ³⁷,
 M. Boehler ⁵⁴, B. Boehm ¹⁶⁷, D. Bogavac ³⁶, A.G. Bogdanchikov ³⁷, C. Bohm ^{47a},
 V. Boisvert ⁹⁶, P. Bokan ³⁶, T. Bold ^{86a}, M. Bomben ⁵, M. Bona ⁹⁵, M. Boonekamp ¹³⁶,
 C.D. Booth ⁹⁶, A.G. Borbély ⁵⁹, I.S. Bordulev ³⁷, H.M. Borecka-Bielska ¹⁰⁹, G. Borissov ⁹²,
 D. Bortoletto ¹²⁷, D. Boscherini ^{23b}, M. Bosman ¹³, J.D. Bossio Sola ³⁶, K. Bouaouda ^{35a},
 N. Bouchhar ¹⁶⁴, L. Boudet ⁴, J. Boudreau ¹³⁰, E.V. Bouhova-Thacker ⁹², D. Boumediene ⁴⁰,
 R. Bouquet ^{57b,57a}, A. Boveia ¹²⁰, J. Boyd ³⁶, D. Boye ²⁹, I.R. Boyko ³⁸, L. Bozianu ⁵⁶,
 J. Bracinik ²⁰, N. Brahimi ⁴, G. Brandt ¹⁷², O. Brandt ³², F. Braren ⁴⁸, B. Brau ¹⁰⁴,
 J.E. Brau ¹²⁴, R. Brenner ¹⁷⁰, L. Brenner ¹¹⁵, R. Brenner ¹⁶², S. Bressler ¹⁷⁰, D. Britton ⁵⁹,
 D. Britzger ¹¹¹, I. Brock ²⁴, G. Brooijmans ⁴¹, E. Brost ²⁹, L.M. Brown ¹⁶⁶, L.E. Bruce ⁶¹,
 T.L. Bruckler ¹²⁷, P.A. Bruckman de Renstrom ⁸⁷, B. Brüers ⁴⁸, A. Bruni ^{23b}, G. Bruni ^{23b},
 M. Bruschi ^{23b}, N. Bruscinò ^{75a,75b}, T. Buanes ¹⁶, Q. Buat ¹³⁹, D. Buchin ¹¹¹, A.G. Buckley ⁵⁹,
 O. Bulekov ³⁷, B.A. Bullard ¹⁴⁴, S. Burdin ⁹³, C.D. Burgard ⁴⁹, A.M. Burger ³⁶,
 B. Burghgrave ⁸, O. Burlayenko ⁵⁴, J.T.P. Burr ³², J.C. Burzynski ¹⁴³, E.L. Busch ⁴¹,
 V. Büscher ¹⁰¹, P.J. Bussey ⁵⁹, J.M. Butler ²⁵, C.M. Buttar ⁵⁹, J.M. Butterworth ⁹⁷,
 W. Buttinger ¹³⁵, C.J. Buxo Vazquez ¹⁰⁸, A.R. Buzykaev ³⁷, S. Cabrera Urbán ¹⁶⁴,
 L. Cadamuro ⁶⁶, D. Caforio ⁵⁸, H. Cai ¹³⁰, Y. Cai ^{14a,14e}, Y. Cai ^{14c}, V.M.M. Cairo ³⁶,
 O. Cakir ^{3a}, N. Calace ³⁶, P. Calafiura ^{17a}, G. Calderini ¹²⁸, P. Calfayan ⁶⁸, G. Callea ⁵⁹,
 L.P. Caloba ^{83b}, D. Calvet ⁴⁰, S. Calvet ⁴⁰, M. Calvetti ^{74a,74b}, R. Camacho Toro ¹²⁸,
 S. Camarda ³⁶, D. Camarero Munoz ²⁶, P. Camarri ^{76a,76b}, M.T. Camerlingo ^{72a,72b},
 D. Cameron ³⁶, C. Camincher ¹⁶⁶, M. Campanelli ⁹⁷, A. Camplani ⁴², V. Canale ^{72a,72b},
 A.C. Canbay ^{3a}, E. Canonero ⁹⁶, J. Cantero ¹⁶⁴, Y. Cao ¹⁶³, F. Capocasa ²⁶, M. Capua ^{43b,43a},
 A. Carbone ^{71a,71b}, R. Cardarelli ^{76a}, J.C.J. Cardenas ⁸, G. Carducci ^{43b,43a}, T. Carli ³⁶,
 G. Carlino ^{72a}, J.I. Carlotto ¹³, B.T. Carlson ^{130,p}, E.M. Carlson ^{166,157a}, J. Carmignani ⁹³,
 L. Carminati ^{71a,71b}, A. Carnelli ¹³⁶, M. Carnesale ^{75a,75b}, S. Caron ¹¹⁴, E. Carquin ^{138f},
 S. Carrá ^{71a}, G. Carratta ^{23b,23a}, A.M. Carroll ¹²⁴, T.M. Carter ⁵², M.P. Casado ^{13,h},
 M. Caspar ⁴⁸, F.L. Castillo ⁴, L. Castillo Garcia ¹³, V. Castillo Gimenez ¹⁶⁴, N.F. Castro ^{131a,131e},
 A. Catinaccio ³⁶, J.R. Catmore ¹²⁶, T. Cavaliere ⁴, V. Cavaliere ²⁹, N. Cavalli ^{23b,23a},
 Y.C. Cekmecelioglu ⁴⁸, E. Celebi ^{21a}, S. Cella ³⁶, F. Celli ¹²⁷, M.S. Centonze ^{70a,70b},
 V. Cepaitis ⁵⁶, K. Cerny ¹²³, A.S. Cerqueira ^{83a}, A. Cerri ¹⁴⁷, L. Cerrito ^{76a,76b}, F. Cerutti ^{17a},
 B. Cervato ¹⁴², A. Cervelli ^{23b}, G. Cesarini ⁵³, S.A. Cetin ⁸², D. Chakraborty ¹¹⁶, J. Chan ^{17a},
 W.Y. Chan ¹⁵⁴, J.D. Chapman ³², E. Chapon ¹³⁶, B. Chargeishvili ^{150b}, D.G. Charlton ²⁰,
 M. Chatterjee ¹⁹, C. Chauhan ¹³⁴, Y. Che ^{14c}, S. Chekanov ⁶, S.V. Chekulaev ^{157a},
 G.A. Chelkov ^{38,a}, A. Chen ¹⁰⁷, B. Chen ¹⁵², B. Chen ¹⁶⁶, H. Chen ^{14c}, H. Chen ²⁹,
 J. Chen ^{62c}, J. Chen ¹⁴³, M. Chen ¹²⁷, S. Chen ¹⁵⁴, S.J. Chen ^{14c}, X. Chen ^{62c,136},
 X. Chen ^{14b,ac}, Y. Chen ^{62a}, C.L. Cheng ¹⁷¹, H.C. Cheng ^{64a}, S. Cheong ¹⁴⁴, A. Cheplakov ³⁸,
 E. Cheremushkina ⁴⁸, E. Cherepanova ¹¹⁵, R. Cherkaoui El Moursli ^{35e}, E. Cheu ⁷, K. Cheung ⁶⁵,
 L. Chevalier ¹³⁶, V. Chiarella ⁵³, G. Chiarelli ^{74a}, N. Chiedde ¹⁰³, G. Chiodini ^{70a},
 A.S. Chisholm ²⁰, A. Chitan ^{27b}, M. Chitishvili ¹⁶⁴, M.V. Chizhov ³⁸, K. Choi ¹¹, Y. Chou ¹³⁹,

E.Y.S. Chow [id114](#), K.L. Chu [id170](#), M.C. Chu [id64a](#), X. Chu [id14a,14e](#), J. Chudoba [id132](#),
 J.J. Chwastowski [id87](#), D. Cieri [id111](#), K.M. Ciesla [id86a](#), V. Cindro [id94](#), A. Ciocio [id17a](#), F. Ciroto [id72a,72b](#),
 Z.H. Citron [id170](#), M. Citterio [id71a](#), D.A. Ciubotaru [id27b](#), A. Clark [id56](#), P.J. Clark [id52](#), C. Clarry [id156](#),
 J.M. Clavijo Columbie [id48](#), S.E. Clawson [id48](#), C. Clement [id47a,47b](#), J. Clercx [id48](#), Y. Coadou [id103](#),
 M. Cobal [id69a,69c](#), A. Coccaro [id57b](#), R.F. Coelho Barrue [id131a](#), R. Coelho Lopes De Sa [id104](#),
 S. Coelli [id71a](#), B. Cole [id41](#), J. Collot [id60](#), P. Conde Muiño [id131a,131g](#), M.P. Connell [id33c](#),
 S.H. Connell [id33c](#), E.I. Conroy [id127](#), F. Conventi [id72a,ae](#), H.G. Cooke [id20](#), A.M. Cooper-Sarkar [id127](#),
 F.A. Corchia [id23b,23a](#), A. Cordeiro Oudot Choi [id128](#), L.D. Corpe [id40](#), M. Corradi [id75a,75b](#),
 F. Corriveau [id105,v](#), A. Cortes-Gonzalez [id18](#), M.J. Costa [id164](#), F. Costanza [id4](#), D. Costanzo [id140](#),
 B.M. Cote [id120](#), J. Couthures [id4](#), G. Cowan [id96](#), K. Cranmer [id171](#), D. Cremonini [id23b,23a](#),
 S. Crépe-Renaudin [id60](#), F. Crescioli [id128](#), M. Cristinziani [id142](#), M. Cristoforetti [id78a,78b](#), V. Croft [id115](#),
 J.E. Crosby [id122](#), G. Crosetti [id43b,43a](#), A. Cueto [id100](#), Z. Cui [id7](#), W.R. Cunningham [id59](#), F. Curcio [id164](#),
 J.R. Curran [id52](#), P. Czodrowski [id36](#), M.M. Czurylo [id36](#), M.J. Da Cunha Sargedas De Sousa [id57b,57a](#),
 J.V. Da Fonseca Pinto [id83b](#), C. Da Via [id102](#), W. Dabrowski [id86a](#), T. Dado [id49](#), S. Dahbi [id149](#),
 T. Dai [id107](#), D. Dal Santo [id19](#), C. Dallapiccola [id104](#), M. Dam [id42](#), G. D'amen [id29](#), V. D'Amico [id110](#),
 J. Damp [id101](#), J.R. Dandoy [id34](#), D. Dannheim [id36](#), M. Danninger [id143](#), V. Dao [id36](#), G. Darbo [id57b](#),
 S.J. Das [id29,af](#), F. Dattola [id48](#), S. D'Auria [id71a,71b](#), A. D'avanzo [id72a,72b](#), C. David [id33a](#), T. Davidek [id134](#),
 I. Dawson [id95](#), H.A. Day-hall [id133](#), K. De [id8](#), R. De Asmundis [id72a](#), N. De Biase [id48](#),
 S. De Castro [id23b,23a](#), N. De Groot [id114](#), P. de Jong [id115](#), H. De la Torre [id116](#), A. De Maria [id14c](#),
 A. De Salvo [id75a](#), U. De Sanctis [id76a,76b](#), F. De Santis [id70a,70b](#), A. De Santo [id147](#),
 J.B. De Vivie De Regie [id60](#), D.V. Dedovich [id38](#), J. Degens [id93](#), A.M. Deiana [id44](#), F. Del Corso [id23b,23a](#),
 J. Del Peso [id100](#), F. Del Rio [id63a](#), L. Delagrangue [id128](#), F. Deliot [id136](#), C.M. Delitzsch [id49](#),
 M. Della Pietra [id72a,72b](#), D. Della Volpe [id56](#), A. Dell'Acqua [id36](#), L. Dell'Asta [id71a,71b](#), M. Delmastro [id4](#),
 P.A. Delsart [id60](#), S. Demers [id173](#), M. Demichev [id38](#), S.P. Denisov [id37](#), L. D'Eramo [id40](#),
 D. Derendarz [id87](#), F. Derue [id128](#), P. Dervan [id93](#), K. Desch [id24](#), C. Deutsch [id24](#), F.A. Di Bello [id57b,57a](#),
 A. Di Ciaccio [id76a,76b](#), L. Di Ciaccio [id4](#), A. Di Domenico [id75a,75b](#), C. Di Donato [id72a,72b](#),
 A. Di Girolamo [id36](#), G. Di Gregorio [id36](#), A. Di Luca [id78a,78b](#), B. Di Micco [id77a,77b](#), R. Di Nardo [id77a,77b](#),
 M. Diamantopoulou [id34](#), F.A. Dias [id115](#), T. Dias Do Vale [id143](#), M.A. Diaz [id138a,138b](#),
 F.G. Diaz Capriles [id24](#), M. Didenko [id164](#), E.B. Diehl [id107](#), S. Díez Cornell [id48](#), C. Diez Pardos [id142](#),
 C. Dimitriadi [id162,24](#), A. Dimitrievska [id20](#), J. Dingfelder [id24](#), I-M. Dinu [id27b](#), S.J. Dittmeier [id63b](#),
 F. Dittus [id36](#), M. Divisek [id134](#), F. Djama [id103](#), T. Djobava [id150b](#), C. Doglioni [id102,99](#),
 A. Dohnalova [id28a](#), J. Dolejsi [id134](#), Z. Dolezal [id134](#), K. Domijan [id86a](#), K.M. Dona [id39](#),
 M. Donadelli [id83c](#), B. Dong [id108](#), J. Donini [id40](#), A. D'Onofrio [id72a,72b](#), M. D'Onofrio [id93](#),
 J. Dopke [id135](#), A. Doria [id72a](#), N. Dos Santos Fernandes [id131a](#), P. Dougan [id102](#), M.T. Dova [id91](#),
 A.T. Doyle [id59](#), M.A. Draguet [id127](#), E. Dreyer [id170](#), I. Drivas-koulouris [id10](#), M. Drnevich [id118](#),
 M. Drozdova [id56](#), D. Du [id62a](#), T.A. du Pree [id115](#), F. Dubinin [id37](#), M. Dubovsky [id28a](#), E. Duchovni [id170](#),
 G. Duckeck [id110](#), O.A. Ducu [id27b](#), D. Duda [id52](#), A. Dudarev [id36](#), E.R. Duden [id26](#), M. D'uffizi [id102](#),
 L. DufLOT [id66](#), M. Dührssen [id36](#), I. Duminica [id27g](#), A.E. Dumitriu [id27b](#), M. Dunford [id63a](#), S. Dungs [id49](#),
 K. Dunne [id47a,47b](#), A. Duperrin [id103](#), H. Duran Yildiz [id3a](#), M. Düren [id58](#), A. Durglishvili [id150b](#),
 B.L. Dwyer [id116](#), G.I. Dyckes [id17a](#), M. Dyndal [id86a](#), B.S. Dziedzic [id36](#), Z.O. Earnshaw [id147](#),
 G.H. Eberwein [id127](#), B. Eckerova [id28a](#), S. Eggebrecht [id55](#), E. Egidio Purcino De Souza [id128](#),
 L.F. Ehrke [id56](#), G. Eigen [id16](#), K. Einsweiler [id17a](#), T. Ekelof [id162](#), P.A. Ekman [id99](#), S. El Farkh [id35b](#),
 Y. El Ghazali [id35b](#), H. El Jarrari [id36](#), A. El Moussaouy [id109](#), V. Ellajosyula [id162](#), M. Ellert [id162](#),
 F. Ellinghaus [id172](#), N. Ellis [id36](#), J. Elmsheuser [id29](#), M. Elsayy [id117a](#), M. Elsing [id36](#),
 D. Emel'yanov [id135](#), Y. Enari [id154](#), I. Ene [id17a](#), S. Epari [id13](#), P.A. Erland [id87](#), M. Errenst [id172](#),
 M. Escalier [id66](#), C. Escobar [id164](#), E. Etzion [id152](#), G. Evans [id131a](#), H. Evans [id68](#), L.S. Evans [id96](#),
 A. Ezhilov [id37](#), S. Ezzarqtouni [id35a](#), F. Fabbri [id23b,23a](#), L. Fabbri [id23b,23a](#), G. Facini [id97](#),

V. Fadeyev ¹³⁷, R.M. Fakhruddinov ³⁷, D. Fakoudis ¹⁰¹, S. Falciano ^{75a},
 L.F. Falda Ulhoa Coelho ³⁶, F. Fallavollita ¹¹¹, J. Faltova ¹³⁴, C. Fan ¹⁶³, Y. Fan ^{14a},
 Y. Fang ^{14a,14e}, M. Fanti ^{71a,71b}, M. Faraj ^{69a,69b}, Z. Farazpay ⁹⁸, A. Farbin ⁸, A. Farilla ^{77a},
 T. Farooque ¹⁰⁸, S.M. Farrington ⁵², F. Fassi ^{35e}, D. Fassouliotis ⁹, M. Faucci Giannelli ^{76a,76b},
 W.J. Fawcett ³², L. Fayard ⁶⁶, P. Federic ¹³⁴, P. Federicova ¹³², O.L. Fedin ^{37,a}, M. Feickert ¹⁷¹,
 L. Feligioni ¹⁰³, D.E. Fellers ¹²⁴, C. Feng ^{62b}, M. Feng ^{14b}, Z. Feng ¹¹⁵, M.J. Fenton ¹⁶⁰,
 L. Ferencz ⁴⁸, R.A.M. Ferguson ⁹², S.I. Fernandez Luengo ^{138f}, P. Fernandez Martinez ¹³,
 M.J.V. Fernoux ¹⁰³, J. Ferrando ⁹², A. Ferrari ¹⁶², P. Ferrari ^{115,114}, R. Ferrari ^{73a}, D. Ferrere ⁵⁶,
 C. Ferretti ¹⁰⁷, F. Fiedler ¹⁰¹, P. Fiedler ¹³³, A. Filipčič ⁹⁴, E.K. Filmer ¹, F. Filthaut ¹¹⁴,
 M.C.N. Fiolhais ^{131a,131c,c}, L. Fiorini ¹⁶⁴, W.C. Fisher ¹⁰⁸, T. Fitschen ¹⁰², P.M. Fitzhugh ¹³⁶,
 I. Fleck ¹⁴², P. Fleischmann ¹⁰⁷, T. Flick ¹⁷², M. Flores ^{33d,aa}, L.R. Flores Castillo ^{64a},
 L. Flores Sanz De Acedo ³⁶, F.M. Follega ^{78a,78b}, N. Fomin ¹⁶, J.H. Foo ¹⁵⁶, A. Formica ¹³⁶,
 A.C. Forti ¹⁰², E. Fortin ³⁶, A.W. Fortman ^{17a}, M.G. Foti ^{17a}, L. Fountas ^{9,i}, D. Fournier ⁶⁶,
 H. Fox ⁹², P. Francavilla ^{74a,74b}, S. Francescato ⁶¹, S. Franchellucci ⁵⁶, M. Franchini ^{23b,23a},
 S. Franchino ^{63a}, D. Francis ³⁶, L. Franco ¹¹⁴, V. Franco Lima ³⁶, L. Franconi ⁴⁸, M. Franklin ⁶¹,
 G. Frattari ²⁶, Y.Y. Frid ¹⁵², J. Friend ⁵⁹, N. Fritzsche ⁵⁰, A. Froch ⁵⁴, D. Froidevaux ³⁶,
 J.A. Frost ¹²⁷, Y. Fu ^{62a}, S. Fuenzalida Garrido ^{138f}, M. Fujimoto ¹⁰³, K.Y. Fung ^{64a},
 E. Furtado De Simas Filho ^{83e}, M. Furukawa ¹⁵⁴, J. Fuster ¹⁶⁴, A. Gabrielli ^{23b,23a},
 A. Gabrielli ¹⁵⁶, P. Gadow ³⁶, G. Gagliardi ^{57b,57a}, L.G. Gagnon ^{17a}, S. Gaid ¹⁶¹,
 S. Galantzan ¹⁵², E.J. Gallas ¹²⁷, B.J. Gallop ¹³⁵, K.K. Gan ¹²⁰, S. Ganguly ¹⁵⁴, Y. Gao ⁵²,
 F.M. Garay Walls ^{138a,138b}, B. Garcia ²⁹, C. García ¹⁶⁴, A. Garcia Alonso ¹¹⁵,
 A.G. Garcia Caffaro ¹⁷³, J.E. García Navarro ¹⁶⁴, M. Garcia-Sciveres ^{17a}, G.L. Gardner ¹²⁹,
 R.W. Gardner ³⁹, N. Garelli ¹⁵⁹, D. Garg ⁸⁰, R.B. Garg ¹⁴⁴, J.M. Gargan ⁵², C.A. Garner ¹⁵⁶,
 C.M. Garvey ^{33a}, V.K. Gassmann ¹⁵⁹, G. Gaudio ^{73a}, V. Gautam ¹³, P. Gauzzi ^{75a,75b},
 I.L. Gavrilenko ³⁷, A. Gavrilyuk ³⁷, C. Gay ¹⁶⁵, G. Gaycken ⁴⁸, E.N. Gazis ¹⁰, A.A. Geanta ^{27b},
 C.M. Gee ¹³⁷, A. Gekow ¹²⁰, C. Gemme ^{57b}, M.H. Genest ⁶⁰, A.D. Gentry ¹¹³, S. George ⁹⁶,
 W.F. George ²⁰, T. Geralis ⁴⁶, P. Gessinger-Befurt ³⁶, M.E. Geyik ¹⁷², M. Ghani ¹⁶⁸,
 K. Ghorbanian ⁹⁵, A. Ghosal ¹⁴², A. Ghosh ¹⁶⁰, A. Ghosh ⁷, B. Giacobbe ^{23b}, S. Giagu ^{75a,75b},
 T. Giani ¹¹⁵, P. Giannetti ^{74a}, A. Giannini ^{62a}, S.M. Gibson ⁹⁶, M. Gignac ¹³⁷, D.T. Gil ^{86b},
 A.K. Gilbert ^{86a}, B.J. Gilbert ⁴¹, D. Gillberg ³⁴, G. Gilles ¹¹⁵, L. Ginabat ¹²⁸,
 D.M. Gingrich ^{2,ad}, M.P. Giordani ^{69a,69c}, P.F. Giraud ¹³⁶, G. Giugliarelli ^{69a,69c}, D. Giugni ^{71a},
 F. Giuli ³⁶, I. Gkialas ^{9,i}, L.K. Gladilin ³⁷, C. Glasman ¹⁰⁰, G.R. Gledhill ¹²⁴, G. Glemža ⁴⁸,
 M. Glisic ¹²⁴, I. Gnesi ^{43b,e}, Y. Go ²⁹, M. Goblirsch-Kolb ³⁶, B. Gocke ⁴⁹, D. Godin ¹⁰⁹,
 B. Gokturk ^{21a}, S. Goldfarb ¹⁰⁶, T. Golling ⁵⁶, M.G.D. Gololo ^{33g}, D. Golubkov ³⁷,
 J.P. Gombas ¹⁰⁸, A. Gomes ^{131a,131b}, G. Gomes Da Silva ¹⁴², A.J. Gomez Delegido ¹⁶⁴,
 R. Gonçalves ^{131a}, L. Gonella ²⁰, A. Gongadze ^{150c}, F. Gonnella ²⁰, J.L. Gonski ¹⁴⁴,
 R.Y. González Andana ⁵², S. González de la Hoz ¹⁶⁴, R. Gonzalez Lopez ⁹³,
 C. Gonzalez Renteria ^{17a}, M.V. Gonzalez Rodrigues ⁴⁸, R. Gonzalez Suarez ¹⁶²,
 S. Gonzalez-Sevilla ⁵⁶, L. Goossens ³⁶, B. Gorini ³⁶, E. Gorini ^{70a,70b}, A. Gorišek ⁹⁴,
 T.C. Gosart ¹²⁹, A.T. Goshaw ⁵¹, M.I. Gostkin ³⁸, S. Goswami ¹²², C.A. Gottardo ³⁶,
 S.A. Gotz ¹¹⁰, M. Gouighri ^{35b}, V. Goumarre ⁴⁸, A.G. Goussiou ¹³⁹, N. Govender ^{33c},
 I. Grabowska-Bold ^{86a}, K. Graham ³⁴, E. Gramstad ¹²⁶, S. Grancagnolo ^{70a,70b}, C.M. Grant ^{1,136},
 P.M. Gravila ^{27f}, F.G. Gravili ^{70a,70b}, H.M. Gray ^{17a}, M. Greco ^{70a,70b}, C. Grefe ²⁴,
 A.S. Grefsrud ¹⁶, I.M. Gregor ⁴⁸, K.T. Greif ¹⁶⁰, P. Grenier ¹⁴⁴, S.G. Grewe ¹¹¹, A.A. Grillo ¹³⁷,
 K. Grimm ³¹, S. Grinstein ^{13,r}, J.-F. Grivaz ⁶⁶, E. Gross ¹⁷⁰, J. Grosse-Knetter ⁵⁵,
 J.C. Grundy ¹²⁷, L. Guan ¹⁰⁷, J.G.R. Guerrero Rojas ¹⁶⁴, G. Guerrieri ^{69a,69c}, F. Guescini ¹¹¹,
 R. Gugel ¹⁰¹, J.A.M. Guhit ¹⁰⁷, A. Guida ¹⁸, E. Guilloton ¹⁶⁸, S. Guindon ³⁶, F. Guo ^{14a,14e},

J. Guo ^{62c}, L. Guo ⁴⁸, Y. Guo ¹⁰⁷, R. Gupta ¹³⁰, S. Gurbuz ²⁴, S.S. Gurdasani ⁵⁴,
 G. Gustavino ³⁶, M. Guth ⁵⁶, P. Gutierrez ¹²¹, L.F. Gutierrez Zagazeta ¹²⁹, M. Gutsche ⁵⁰,
 C. Gutschow ⁹⁷, C. Gwenlan ¹²⁷, C.B. Gwilliam ⁹³, E.S. Haaland ¹²⁶, A. Haas ¹¹⁸,
 M. Habedank ⁴⁸, C. Haber ^{17a}, H.K. Hadavand ⁸, A. Hadeef ⁵⁰, S. Hadzic ¹¹¹, A.I. Hagan ⁹²,
 J.J. Hahn ¹⁴², E.H. Haines ⁹⁷, M. Haleem ¹⁶⁷, J. Haley ¹²², J.J. Hall ¹⁴⁰, G.D. Hallewell ¹⁰³,
 L. Halser ¹⁹, K. Hamano ¹⁶⁶, M. Hamer ²⁴, G.N. Hamity ⁵², E.J. Hampshire ⁹⁶, J. Han ^{62b},
 K. Han ^{62a}, L. Han ^{14c}, L. Han ^{62a}, S. Han ^{17a}, Y.F. Han ¹⁵⁶, K. Hanagaki ⁸⁴, M. Hance ¹³⁷,
 D.A. Hangal ⁴¹, H. Hanif ¹⁴³, M.D. Hank ¹²⁹, J.B. Hansen ⁴², P.H. Hansen ⁴², K. Hara ¹⁵⁸,
 D. Harada ⁵⁶, T. Harenberg ¹⁷², S. Harkusha ³⁷, M.L. Harris ¹⁰⁴, Y.T. Harris ¹²⁷, J. Harrison ¹³,
 N.M. Harrison ¹²⁰, P.F. Harrison ¹⁶⁸, N.M. Hartman ¹¹¹, N.M. Hartmann ¹¹⁰, R.Z. Hasan ^{96,135},
 Y. Hasegawa ¹⁴¹, S. Hassan ¹⁶, R. Hauser ¹⁰⁸, C.M. Hawkes ²⁰, R.J. Hawkings ³⁶,
 Y. Hayashi ¹⁵⁴, S. Hayashida ¹¹², D. Hayden ¹⁰⁸, C. Hayes ¹⁰⁷, R.L. Hayes ¹¹⁵, C.P. Hays ¹²⁷,
 J.M. Hays ⁹⁵, H.S. Hayward ⁹³, F. He ^{62a}, M. He ^{14a,14e}, Y. He ¹⁵⁵, Y. He ⁴⁸, Y. He ⁹⁷,
 N.B. Heatley ⁹⁵, V. Hedberg ⁹⁹, A.L. Heggelund ¹²⁶, N.D. Hehir ^{95,*}, C. Heidegger ⁵⁴,
 K.K. Heidegger ⁵⁴, W.D. Heidorn ⁸¹, J. Heilman ³⁴, S. Heim ⁴⁸, T. Heim ^{17a}, J.G. Heinlein ¹²⁹,
 J.J. Heinrich ¹²⁴, L. Heinrich ^{111,ab}, J. Hejbal ¹³², A. Held ¹⁷¹, S. Hellesund ¹⁶,
 C.M. Helling ¹⁶⁵, S. Hellman ^{47a,47b}, R.C.W. Henderson ⁹², L. Henkelmann ³²,
 A.M. Henriques Correia ³⁶, H. Herde ⁹⁹, Y. Hernández Jiménez ¹⁴⁶, L.M. Herrmann ²⁴,
 T. Herrmann ⁵⁰, G. Herten ⁵⁴, R. Hertenberger ¹¹⁰, L. Hervas ³⁶, M.E. Hesping ¹⁰¹,
 N.P. Hessey ^{157a}, M. Hidaoui ^{35b}, E. Hill ¹⁵⁶, S.J. Hillier ²⁰, J.R. Hinds ¹⁰⁸, F. Hinterkeuser ²⁴,
 M. Hirose ¹²⁵, S. Hirose ¹⁵⁸, D. Hirschbuehl ¹⁷², T.G. Hitchings ¹⁰², B. Hiti ⁹⁴, J. Hobbs ¹⁴⁶,
 R. Hobincu ^{27e}, N. Hod ¹⁷⁰, M.C. Hodgkinson ¹⁴⁰, B.H. Hodgkinson ¹²⁷, A. Hoecker ³⁶,
 D.D. Hofer ¹⁰⁷, J. Hofer ⁴⁸, T. Holm ²⁴, M. Holzbock ¹¹¹, L.B.A.H. Hommels ³²,
 B.P. Honan ¹⁰², J.J. Hong ⁶⁸, J. Hong ^{62c}, T.M. Hong ¹³⁰, B.H. Hooberman ¹⁶³,
 W.H. Hopkins ⁶, M.C. Hoppesch ¹⁶³, Y. Horii ¹¹², S. Hou ¹⁴⁹, A.S. Howard ⁹⁴, J. Howarth ⁵⁹,
 J. Hoya ⁶, M. Hrabovsky ¹²³, A. Hrynevich ⁴⁸, T. Hryn'ova ⁴, P.J. Hsu ⁶⁵, S.-C. Hsu ¹³⁹,
 T. Hsu ⁶⁶, M. Hu ^{17a}, Q. Hu ^{62a}, S. Huang ^{64b}, X. Huang ^{14a,14e}, Y. Huang ¹⁴⁰, Y. Huang ¹⁰¹,
 Y. Huang ^{14a}, Z. Huang ¹⁰², Z. Hubacek ¹³³, M. Huebner ²⁴, F. Hugging ²⁴, T.B. Huffman ¹²⁷,
 C.A. Hugli ⁴⁸, M. Huhtinen ³⁶, S.K. Huiberts ¹⁶, R. Hulsken ¹⁰⁵, N. Huseynov ¹², J. Huston ¹⁰⁸,
 J. Huth ⁶¹, R. Hyneman ¹⁴⁴, G. Iacobucci ⁵⁶, G. Iakovidis ²⁹, L. Iconomidou-Fayard ⁶⁶,
 J.P. Iddon ³⁶, P. Iengo ^{72a,72b}, R. Iguchi ¹⁵⁴, T. Iizawa ¹²⁷, Y. Ikegami ⁸⁴, N. Ilic ¹⁵⁶,
 H. Imam ^{35a}, M. Ince Lezki ⁵⁶, T. Ingebretsen Carlson ^{47a,47b}, G. Introzzi ^{73a,73b}, M. Iodice ^{77a},
 V. Ippolito ^{75a,75b}, R.K. Irwin ⁹³, M. Ishino ¹⁵⁴, W. Islam ¹⁷¹, C. Issever ^{18,48}, S. Istin ^{21a,ah},
 H. Ito ¹⁶⁹, R. Iuppa ^{78a,78b}, A. Ivina ¹⁷⁰, J.M. Izen ⁴⁵, V. Izzo ^{72a}, P. Jacka ¹³², P. Jackson ¹,
 C.S. Jagfeld ¹¹⁰, G. Jain ^{157a}, P. Jain ⁴⁸, K. Jakobs ⁵⁴, T. Jakoubek ¹⁷⁰, J. Jamieson ⁵⁹,
 M. Javurkova ¹⁰⁴, L. Jeanty ¹²⁴, J. Jejelava ^{150a,y}, P. Jenni ^{54,f}, C.E. Jessiman ³⁴, C. Jia ^{62b},
 J. Jia ¹⁴⁶, X. Jia ⁶¹, X. Jia ^{14a,14e}, Z. Jia ^{14c}, C. Jiang ⁵², S. Jiggins ⁴⁸, J. Jimenez Pena ¹³,
 S. Jin ^{14c}, A. Jinaru ^{27b}, O. Jinnouchi ¹⁵⁵, P. Johansson ¹⁴⁰, K.A. Johns ⁷, J.W. Johnson ¹³⁷,
 D.M. Jones ¹⁴⁷, E. Jones ⁴⁸, P. Jones ³², R.W.L. Jones ⁹², T.J. Jones ⁹³, H.L. Joos ^{55,36},
 R. Joshi ¹²⁰, J. Jovicevic ¹⁵, X. Ju ^{17a}, J.J. Junggeburth ¹⁰⁴, T. Junkermann ^{63a},
 A. Juste Rozas ^{13,r}, M.K. Juzek ⁸⁷, S. Kabana ^{138e}, A. Kaczmarek ⁸⁷, M. Kado ¹¹¹,
 H. Kagan ¹²⁰, M. Kagan ¹⁴⁴, A. Kahn ¹²⁹, C. Kahra ¹⁰¹, T. Kaji ¹⁵⁴, E. Kajomovitz ¹⁵¹,
 N. Kakati ¹⁷⁰, I. Kalaitzidou ⁵⁴, C.W. Kalderon ²⁹, N.J. Kang ¹³⁷, D. Kar ^{33g}, K. Karava ¹²⁷,
 M.J. Kareem ^{157b}, E. Karentzos ⁵⁴, O. Karkout ¹¹⁵, S.N. Karpov ³⁸, Z.M. Karpova ³⁸,
 V. Kartvelishvili ⁹², A.N. Karyukhin ³⁷, E. Kasimi ¹⁵³, J. Katzy ⁴⁸, S. Kaur ³⁴, K. Kawade ¹⁴¹,
 M.P. Kawale ¹²¹, C. Kawamoto ⁸⁸, T. Kawamoto ^{62a}, E.F. Kay ³⁶, F.I. Kaya ¹⁵⁹, S. Kazakos ¹⁰⁸,
 V.F. Kazanin ³⁷, Y. Ke ¹⁴⁶, J.M. Keaveney ^{33a}, R. Keeler ¹⁶⁶, G.V. Kehris ⁶¹, J.S. Keller ³⁴,

A.S. Kelly⁹⁷, J.J. Kempster¹⁴⁷, P.D. Kennedy¹⁰¹, O. Kepka¹³², B.P. Kerridge¹³⁵, S. Kersten¹⁷², B.P. Kerševan⁹⁴, L. Keszeghova^{28a}, S. Ketabchi Haghighat¹⁵⁶, R.A. Khan¹³⁰, A. Khanov¹²², A.G. Kharlamov³⁷, T. Kharlamova³⁷, E.E. Khoda¹³⁹, M. Kholodenko³⁷, T.J. Khoo¹⁸, G. Khorauli¹⁶⁷, J. Khubua^{150b}, Y.A.R. Khwaira¹²⁸, B. Kibirige^{33g}, D.W. Kim^{47a,47b}, Y.K. Kim³⁹, N. Kimura⁹⁷, M.K. Kingston⁵⁵, A. Kirchhoff⁵⁵, C. Kirfel²⁴, F. Kirfel²⁴, J. Kirk¹³⁵, A.E. Kiryunin¹¹¹, C. Kitsaki¹⁰, O. Kivernyk²⁴, M. Klassen¹⁵⁹, C. Klein³⁴, L. Klein¹⁶⁷, M.H. Klein⁴⁴, S.B. Klein⁵⁶, U. Klein⁹³, P. Klimek³⁶, A. Klimentov²⁹, T. Klioutchnikova³⁶, P. Kluit¹¹⁵, S. Kluth¹¹¹, E. Kneringer⁷⁹, T.M. Knight¹⁵⁶, A. Knue⁴⁹, R. Kobayashi⁸⁸, D. Kobylanskii¹⁷⁰, S.F. Koch¹²⁷, M. Kocian¹⁴⁴, P. Kodyš¹³⁴, D.M. Koeck¹²⁴, P.T. Koenig²⁴, T. Koffas³⁴, O. Kolay⁵⁰, I. Koletsou⁴, T. Komarek¹²³, K. Köneke⁵⁴, A.X.Y. Kong¹, T. Kono¹¹⁹, N. Konstantinidis⁹⁷, P. Kontaxakis⁵⁶, B. Konya⁹⁹, R. Kopeliansky⁴¹, S. Koperny^{86a}, K. Korcyl⁸⁷, K. Kordas^{153,d}, A. Korn⁹⁷, S. Korn⁵⁵, I. Korolkov¹³, N. Korotkova³⁷, B. Kortman¹¹⁵, O. Kortner¹¹¹, S. Kortner¹¹¹, W.H. Kostecka¹¹⁶, V.V. Kostyukhin¹⁴², A. Kotsokechagia¹³⁶, A. Koulouris³⁶, A. Kourkoumeli-Charalampidi^{73a,73b}, C. Kourkoumelis⁹, E. Kourlitis^{111,ab}, O. Kovanda¹²⁴, R. Kowalewski¹⁶⁶, W. Kozanecki¹³⁶, A.S. Kozhin³⁷, V.A. Kramarenko³⁷, G. Kramberger⁹⁴, P. Kramer¹⁰¹, M.W. Krasny¹²⁸, A. Krasznahorkay³⁶, J.W. Kraus¹⁷², J.A. Kremer⁴⁸, T. Kresse⁵⁰, J. Kretschmar⁹³, K. Kreul¹⁸, P. Krieger¹⁵⁶, S. Krishnamurthy¹⁰⁴, M. Krivos¹³⁴, K. Krizka²⁰, K. Kroeninger⁴⁹, H. Kroha¹¹¹, J. Kroll¹³², J. Kroll¹²⁹, K.S. Krowpman¹⁰⁸, U. Kruchonak³⁸, H. Krüger²⁴, N. Krumnack⁸¹, M.C. Kruse⁵¹, O. Kuchinskaia³⁷, S. Kудay^{3a}, S. Kuehn³⁶, R. Kuesters⁵⁴, T. Kuhl⁴⁸, V. Kukhtin³⁸, Y. Kulchitsky^{37,a}, S. Kuleshov^{138d,138b}, M. Kumar^{33g}, N. Kumari⁴⁸, P. Kumari^{157b}, A. Kupco¹³², T. Kupfer⁴⁹, A. Kupich³⁷, O. Kuprash⁵⁴, H. Kurashige⁸⁵, L.L. Kurchaninov^{157a}, O. Kurdysh⁶⁶, Y.A. Kurochkin³⁷, A. Kurova³⁷, M. Kuze¹⁵⁵, A.K. Kvam¹⁰⁴, J. Kvita¹²³, T. Kwan¹⁰⁵, N.G. Kyriacou¹⁰⁷, L.A.O. Laatu¹⁰³, C. Lacasta¹⁶⁴, F. Lacava^{75a,75b}, H. Lacker¹⁸, D. Lacour¹²⁸, N.N. Lad⁹⁷, E. Ladygin³⁸, A. Lafarge⁴⁰, B. Laforge¹²⁸, T. Lagouri¹⁷³, F.Z. Lahbabi^{35a}, S. Lai⁵⁵, J.E. Lambert¹⁶⁶, S. Lammers⁶⁸, W. Lampl⁷, C. Lampoudis^{153,d}, G. Lamprinoudis¹⁰¹, A.N. Lancaster¹¹⁶, E. Lançon²⁹, U. Landgraf⁵⁴, M.P.J. Landon⁹⁵, V.S. Lang⁵⁴, O.K.B. Langrekken¹²⁶, A.J. Lankford¹⁶⁰, F. Lanni³⁶, K. Lantzsck²⁴, A. Lanza^{73a}, J.F. Laporte¹³⁶, T. Lari^{71a}, F. Lasagni Manghi^{23b}, M. Lassnig³⁶, V. Latonova¹³², A. Laudrain¹⁰¹, A. Laurier¹⁵¹, S.D. Lawlor¹⁴⁰, Z. Lawrence¹⁰², R. Lazaridou¹⁶⁸, M. Lazzaroni^{71a,71b}, B. Le¹⁰², E.M. Le Boulicaut⁵¹, L.T. Le Pottier^{17a}, B. Leban^{23b,23a}, A. Lebedev⁸¹, M. LeBlanc¹⁰², F. Ledroit-Guillon⁶⁰, S.C. Lee¹⁴⁹, S. Lee^{47a,47b}, T.F. Lee⁹³, L.L. Leeuw^{33c}, H.P. Lefebvre⁹⁶, M. Lefebvre¹⁶⁶, C. Leggett^{17a}, G. Lehmann Miotto³⁶, M. Leigh⁵⁶, W.A. Leight¹⁰⁴, W. Leinonen¹¹⁴, A. Leisos^{153,q}, M.A.L. Leite^{83c}, C.E. Leitgeb¹⁸, R. Leitner¹³⁴, K.J.C. Leney⁴⁴, T. Lenz²⁴, S. Leone^{74a}, C. Leonidopoulos⁵², A. Leopold¹⁴⁵, C. Leroy¹⁰⁹, R. Les¹⁰⁸, C.G. Lester³², M. Levchenko³⁷, J. Levêque⁴, L.J. Levinson¹⁷⁰, G. Levrini^{23b,23a}, M.P. Lewicki⁸⁷, C. Lewis¹³⁹, D.J. Lewis⁴, A. Li⁵, B. Li^{62b}, C. Li^{62a}, C-Q. Li¹¹¹, H. Li^{62a}, H. Li^{62b}, H. Li^{14c}, H. Li^{14b}, H. Li^{62b}, J. Li^{62c}, K. Li¹³⁹, L. Li^{62c}, M. Li^{14a,14e}, S. Li^{14a,14e}, S. Li^{62d,62c}, T. Li⁵, X. Li¹⁰⁵, Z. Li¹²⁷, Z. Li¹⁰⁵, Z. Li^{14a,14e}, S. Liang^{14a,14e}, Z. Liang^{14a}, M. Liberatore¹³⁶, B. Liberti^{76a}, K. Lie^{64c}, J. Lieber Marin^{83e}, H. Lien⁶⁸, H. Lin¹⁰⁷, K. Lin¹⁰⁸, R.E. Lindley⁷, J.H. Lindon², E. Lipeles¹²⁹, A. Lipniacka¹⁶, A. Lister¹⁶⁵, J.D. Little⁶⁸, B. Liu^{14a}, B.X. Liu^{14d}, D. Liu^{62d,62c}, E.H.L. Liu²⁰, J.B. Liu^{62a}, J.K.K. Liu³², K. Liu^{62d}, K. Liu^{62d,62c}, M. Liu^{62a}, M.Y. Liu^{62a}, P. Liu^{14a}, Q. Liu^{62d,139,62c}, X. Liu^{62a}, X. Liu^{62b}, Y. Liu^{14d,14e}, Y.L. Liu^{62b}, Y.W. Liu^{62a}, J. Llorente Merino¹⁴³, S.L. Lloyd⁹⁵, E.M. Lobodzinska⁴⁸, P. Loch⁷, T. Lohse¹⁸, K. Lohwasser¹⁴⁰, E. Loiacono⁴⁸,

M. Lokajicek ^{132,*}, J.D. Lomas ²⁰, J.D. Long ¹⁶³, I. Longarini ¹⁶⁰, R. Longo ¹⁶³,
I. Lopez Paz ⁶⁷, A. Lopez Solis ⁴⁸, N. Lorenzo Martinez ⁴, A.M. Lory ¹¹⁰, M. Losada ^{117a},
G. Löschcke Centeno ¹⁴⁷, O. Loseva ³⁷, X. Lou ^{47a,47b}, X. Lou ^{14a,14e}, A. Lounis ⁶⁶,
P.A. Love ⁹², G. Lu ^{14a,14e}, M. Lu ⁶⁶, S. Lu ¹²⁹, Y.J. Lu ⁶⁵, H.J. Lubatti ¹³⁹, C. Luci ^{75a,75b},
F.L. Lucio Alves ^{14c}, F. Luehring ⁶⁸, I. Luise ¹⁴⁶, O. Lukianchuk ⁶⁶, O. Lundberg ¹⁴⁵,
B. Lund-Jensen ¹⁴⁵, N.A. Luongo ⁶, M.S. Lutz ³⁶, A.B. Lux ²⁵, D. Lynn ²⁹, R. Lysak ¹³²,
E. Lytken ⁹⁹, V. Lyubushkin ³⁸, T. Lyubushkina ³⁸, M.M. Lyukova ¹⁴⁶, M.Firdaus M. Soberi ⁵²,
H. Ma ²⁹, K. Ma ^{62a}, L.L. Ma ^{62b}, W. Ma ^{62a}, Y. Ma ¹²², G. Maccarrone ⁵³, J.C. MacDonald ¹⁰¹,
P.C. Machado De Abreu Farias ^{83e}, R. Madar ⁴⁰, T. Madula ⁹⁷, J. Maeda ⁸⁵, T. Maeno ²⁹,
H. Maguire ¹⁴⁰, V. Maiboroda ¹³⁶, A. Maio ^{131a,131b,131d}, K. Maj ^{86a}, O. Majersky ⁴⁸,
S. Majewski ¹²⁴, N. Makovec ⁶⁶, V. Maksimovic ¹⁵, B. Malaescu ¹²⁸, Pa. Malecki ⁸⁷,
V.P. Maleev ³⁷, F. Malek ^{60,m}, M. Mali ⁹⁴, D. Malito ⁹⁶, U. Mallik ⁸⁰, S. Maltezos ¹⁰,
S. Malyukov ³⁸, J. Mamuzic ¹³, G. Mancini ⁵³, M.N. Mancini ²⁶, G. Manco ^{73a,73b},
J.P. Mandalia ⁹⁵, I. Mandić ⁹⁴, L. Manhaes de Andrade Filho ^{83a}, I.M. Maniatis ¹⁷⁰,
J. Manjarres Ramos ⁹⁰, D.C. Mankad ¹⁷⁰, A. Mann ¹¹⁰, S. Manzoni ³⁶, L. Mao ^{62c},
X. Mapekula ^{33c}, A. Marantis ^{153,q}, G. Marchiori ⁵, M. Marcisovsky ¹³², C. Marcon ^{71a},
M. Marinescu ²⁰, S. Marium ⁴⁸, M. Marjanovic ¹²¹, A. Markhoos ⁵⁴, M. Markovitch ⁶⁶,
E.J. Marshall ⁹², Z. Marshall ^{17a}, S. Marti-Garcia ¹⁶⁴, T.A. Martin ¹³⁵, V.J. Martin ⁵²,
B. Martin dit Latour ¹⁶, L. Martinelli ^{75a,75b}, M. Martinez ^{13,r}, P. Martinez Agullo ¹⁶⁴,
V.I. Martinez Outschoorn ¹⁰⁴, P. Martinez Suarez ¹³, S. Martin-Haugh ¹³⁵, G. Martinovicova ¹³⁴,
V.S. Martoiu ^{27b}, A.C. Martyniuk ⁹⁷, A. Marzin ³⁶, D. Mascione ^{78a,78b}, L. Masetti ¹⁰¹,
T. Mashimo ¹⁵⁴, J. Masik ¹⁰², A.L. Maslennikov ³⁷, P. Massarotti ^{72a,72b}, P. Mastrandrea ^{74a,74b},
A. Mastroberardino ^{43b,43a}, T. Masubuchi ¹⁵⁴, T. Mathisen ¹⁶², J. Matousek ¹³⁴, N. Matsuzawa ¹⁵⁴,
J. Maurer ^{27b}, A.J. Maury ⁶⁶, B. Maček ⁹⁴, D.A. Maximov ³⁷, A.E. May ¹⁰², R. Mazini ¹⁴⁹,
I. Maznas ¹¹⁶, M. Mazza ¹⁰⁸, S.M. Mazza ¹³⁷, E. Mazzeo ^{71a,71b}, C. Mc Ginn ²⁹,
J.P. Mc Gowan ¹⁶⁶, S.P. Mc Kee ¹⁰⁷, C.C. McCracken ¹⁶⁵, E.F. McDonald ¹⁰⁶,
A.E. McDougall ¹¹⁵, J.A. Mcfayden ¹⁴⁷, R.P. McGovern ¹²⁹, G. Mchedlidze ^{150b},
R.P. Mckenzie ^{33g}, T.C. Mclachlan ⁴⁸, D.J. McLaughlin ⁹⁷, S.J. McMahon ¹³⁵,
C.M. Mcpartland ⁹³, R.A. McPherson ^{166,v}, S. Mehlhase ¹¹⁰, A. Mehta ⁹³, D. Melini ¹⁶⁴,
B.R. Mellado Garcia ^{33g}, A.H. Melo ⁵⁵, F. Meloni ⁴⁸, A.M. Mendes Jacques Da Costa ¹⁰²,
H.Y. Meng ¹⁵⁶, L. Meng ⁹², S. Menke ¹¹¹, M. Mentink ³⁶, E. Meoni ^{43b,43a}, G. Mercado ¹¹⁶,
S. Merianos ¹⁵³, C. Merlassino ^{69a,69c}, L. Merola ^{72a,72b}, C. Meroni ^{71a,71b}, J. Metcalfe ⁶,
A.S. Mete ⁶, E. Meuser ¹⁰¹, C. Meyer ⁶⁸, J-P. Meyer ¹³⁶, R.P. Middleton ¹³⁵, L. Mijović ⁵²,
G. Mikenberg ¹⁷⁰, M. Mikestikova ¹³², M. Mikuž ⁹⁴, H. Mildner ¹⁰¹, A. Milic ³⁶,
D.W. Miller ³⁹, E.H. Miller ¹⁴⁴, L.S. Miller ³⁴, A. Milov ¹⁷⁰, D.A. Milstead ^{47a,47b}, T. Min ^{14c},
A.A. Minaenko ³⁷, I.A. Minashvili ^{150b}, L. Mince ⁵⁹, A.I. Mincer ¹¹⁸, B. Mindur ^{86a},
M. Mineev ³⁸, Y. Mino ⁸⁸, L.M. Mir ¹³, M. Miralles Lopez ⁵⁹, M. Mironova ^{17a}, A. Mishima ¹⁵⁴,
M.C. Missio ¹¹⁴, A. Mitra ¹⁶⁸, V.A. Mitsou ¹⁶⁴, Y. Mitsumori ¹¹², O. Miu ¹⁵⁶,
P.S. Miyagawa ⁹⁵, T. Mkrtychyan ^{63a}, M. Mlinarevic ⁹⁷, T. Mlinarevic ⁹⁷, M. Mlynarikova ³⁶,
S. Mobius ¹⁹, P. Mogg ¹¹⁰, M.H. Mohamed Farook ¹¹³, A.F. Mohammed ^{14a,14e}, S. Mohapatra ⁴¹,
G. Mokgatitswane ^{33g}, L. Moleri ¹⁷⁰, B. Mondal ¹⁴², S. Mondal ¹³³, K. Mönig ⁴⁸,
E. Monnier ¹⁰³, L. Monsonis Romero ¹⁶⁴, J. Montejo Berlingen ¹³, M. Montella ¹²⁰,
F. Montekali ^{77a,77b}, F. Monticelli ⁹¹, S. Monzani ^{69a,69c}, N. Morange ⁶⁶,
A.L. Moreira De Carvalho ⁴⁸, M. Moreno Llácer ¹⁶⁴, C. Moreno Martinez ⁵⁶, P. Morettini ^{57b},
S. Morgenstern ³⁶, M. Morii ⁶¹, M. Morinaga ¹⁵⁴, F. Morodei ^{75a,75b}, L. Morvaj ³⁶,
P. Moschovakos ³⁶, B. Moser ³⁶, M. Mosidze ^{150b}, T. Moskalets ⁵⁴, P. Moskvitina ¹¹⁴,
J. Moss ^{31,j}, P. Moszkowicz ^{86a}, A. Moussa ^{35d}, E.J.W. Moyse ¹⁰⁴, O. Mtintsilana ^{33g},

S. Muanza ¹⁰³, J. Mueller ¹³⁰, D. Muenstermann ⁹², R. Müller ¹⁹, G.A. Mullier ¹⁶², A.J. Mullin³², J.J. Mullin¹²⁹, D.P. Mungo ¹⁵⁶, D. Munoz Perez ¹⁶⁴, F.J. Munoz Sanchez ¹⁰², M. Murin ¹⁰², W.J. Murray ^{168,135}, M. Muškinja ⁹⁴, C. Mwewa ²⁹, A.G. Myagkov ^{37,a}, A.J. Myers ⁸, G. Myers ¹⁰⁷, M. Myska ¹³³, B.P. Nachman ^{17a}, O. Nackenhorst ⁴⁹, K. Nagai ¹²⁷, K. Nagano ⁸⁴, J.L. Nagle ^{29,af}, E. Nagy ¹⁰³, A.M. Nairz ³⁶, Y. Nakahama ⁸⁴, K. Nakamura ⁸⁴, K. Nakkalil ⁵, H. Nanjo ¹²⁵, E.A. Narayanan ¹¹³, I. Naryshkin ³⁷, L. Nasella ^{71a,71b}, M. Naseri ³⁴, S. Nasri ^{117b}, C. Nass ²⁴, G. Navarro ^{22a}, J. Navarro-Gonzalez ¹⁶⁴, R. Nayak ¹⁵², A. Nayaz ¹⁸, P.Y. Nechaeva ³⁷, S. Nechaeva ^{23b,23a}, F. Nechansky ⁴⁸, L. Nedic ¹²⁷, T.J. Neep ²⁰, A. Negri ^{73a,73b}, M. Negrini ^{23b}, C. Nellist ¹¹⁵, C. Nelson ¹⁰⁵, K. Nelson ¹⁰⁷, S. Nemecek ¹³², M. Nessi ^{36,g}, M.S. Neubauer ¹⁶³, F. Neuhaus ¹⁰¹, J. Neundorf ⁴⁸, P.R. Newman ²⁰, C.W. Ng ¹³⁰, Y.W.Y. Ng ⁴⁸, B. Ngair ^{117a}, H.D.N. Nguyen ¹⁰⁹, R.B. Nickerson ¹²⁷, R. Nicolaidou ¹³⁶, J. Nielsen ¹³⁷, M. Niemeyer ⁵⁵, J. Niermann ⁵⁵, N. Nikiforou ³⁶, V. Nikolaenko ^{37,a}, I. Nikolic-Audit ¹²⁸, K. Nikolopoulos ²⁰, P. Nilsson ²⁹, I. Ninca ⁴⁸, G. Ninio ¹⁵², A. Nisati ^{75a}, N. Nishu ², R. Nisius ¹¹¹, J-E. Nitschke ⁵⁰, E.K. Nkadimeng ^{33g}, T. Nobe ¹⁵⁴, T. Nommensen ¹⁴⁸, M.B. Norfolk ¹⁴⁰, R.R.B. Norisam ⁹⁷, B.J. Norman ³⁴, M. Noury ^{35a}, J. Novak ⁹⁴, T. Novak ⁹⁴, L. Novotny ¹³³, R. Novotny ¹¹³, L. Nozka ¹²³, K. Ntekas ¹⁶⁰, N.M.J. Nunes De Moura Junior ^{83b}, J. Ocariz ¹²⁸, A. Ochi ⁸⁵, I. Ochoa ^{131a}, S. Oerdek ^{48,s}, J.T. Offermann ³⁹, A. Ogrodnik ¹³⁴, A. Oh ¹⁰², C.C. Ohm ¹⁴⁵, H. Oide ⁸⁴, R. Oishi ¹⁵⁴, M.L. Ojeda ⁴⁸, Y. Okumura ¹⁵⁴, L.F. Oleiro Seabra ^{131a}, S.A. Olivares Pino ^{138d}, G. Oliveira Correa ¹³, D. Oliveira Damazio ²⁹, D. Oliveira Goncalves ^{83a}, J.L. Oliver ¹⁶⁰, Ö.O. Öncel ⁵⁴, A.P. O'Neill ¹⁹, A. Onofre ^{131a,131e}, P.U.E. Onyisi ¹¹, M.J. Oreglia ³⁹, G.E. Orellana ⁹¹, D. Orestano ^{77a,77b}, N. Orlando ¹³, R.S. Orr ¹⁵⁶, V. O'Shea ⁵⁹, L.M. Osojnak ¹²⁹, R. Ospanov ^{62a}, G. Otero y Garzon ³⁰, H. Otono ⁸⁹, P.S. Ott ^{63a}, G.J. Ottino ^{17a}, M. Ouchrif ^{35d}, F. Ould-Saada ¹²⁶, T. Ovsiannikova ¹³⁹, M. Owen ⁵⁹, R.E. Owen ¹³⁵, V.E. Ozcan ^{21a}, F. Ozturk ⁸⁷, N. Ozturk ⁸, S. Ozturk ⁸², H.A. Pacey ¹²⁷, A. Pacheco Pages ¹³, C. Padilla Aranda ¹³, G. Padovano ^{75a,75b}, S. Pagan Griso ^{17a}, G. Palacino ⁶⁸, A. Palazzo ^{70a,70b}, J. Pampel ²⁴, J. Pan ¹⁷³, T. Pan ^{64a}, D.K. Panchal ¹¹, C.E. Pandini ¹¹⁵, J.G. Panduro Vazquez ¹³⁵, H.D. Pandya ¹, H. Pang ^{14b}, P. Pani ⁴⁸, G. Panizzo ^{69a,69c}, L. Panwar ¹²⁸, L. Paolozzi ⁵⁶, S. Parajuli ¹⁶³, A. Paramonov ⁶, C. Paraskevopoulos ⁵³, D. Paredes Hernandez ^{64b}, A. Pareti ^{73a,73b}, K.R. Park ⁴¹, T.H. Park ¹⁵⁶, M.A. Parker ³², F. Parodi ^{57b,57a}, E.W. Parrish ¹¹⁶, V.A. Parrish ⁵², J.A. Parsons ⁴¹, U. Parzefall ⁵⁴, B. Pascual Dias ¹⁰⁹, L. Pascual Dominguez ¹⁰⁰, E. Pasqualucci ^{75a}, S. Passaggio ^{57b}, F. Pastore ⁹⁶, P. Patel ⁸⁷, U.M. Patel ⁵¹, J.R. Pater ¹⁰², T. Pauly ³⁶, C.I. Pazos ¹⁵⁹, J. Pearkes ¹⁴⁴, M. Pedersen ¹²⁶, R. Pedro ^{131a}, S.V. Peleganchuk ³⁷, O. Penc ³⁶, E.A. Pender ⁵², G.D. Penn ¹⁷³, K.E. Pensi ¹¹⁰, M. Penzin ³⁷, B.S. Peralva ^{83d}, A.P. Pereira Peixoto ¹³⁹, L. Pereira Sanchez ¹⁴⁴, D.V. Perepelitsa ^{29,af}, E. Perez Codina ^{157a}, M. Perganti ¹⁰, H. Pernegger ³⁶, S. Perrella ^{75a,75b}, O. Perrin ⁴⁰, K. Peters ⁴⁸, R.F.Y. Peters ¹⁰², B.A. Petersen ³⁶, T.C. Petersen ⁴², E. Petit ¹⁰³, V. Petousis ¹³³, C. Petridou ^{153,d}, T. Petru ¹³⁴, A. Petrukhin ¹⁴², M. Pettee ^{17a}, N.E. Pettersson ³⁶, A. Petukhov ³⁷, K. Petukhova ¹³⁴, R. Pezoa ^{138f}, L. Pezzotti ³⁶, G. Pezzullo ¹⁷³, T.M. Pham ¹⁷¹, T. Pham ¹⁰⁶, P.W. Phillips ¹³⁵, G. Piacquadio ¹⁴⁶, E. Pianori ^{17a}, F. Piazza ¹²⁴, R. Piegai ³⁰, D. Pietreanu ^{27b}, A.D. Pilkington ¹⁰², M. Pinamonti ^{69a,69c}, J.L. Pinfeld ², B.C. Pinheiro Pereira ^{131a}, A.E. Pinto Pinoargote ^{136,136}, L. Pintucci ^{69a,69c}, K.M. Piper ¹⁴⁷, A. Pirttikoski ⁵⁶, D.A. Pizzi ³⁴, L. Pizzimento ^{64b}, A. Pizzini ¹¹⁵, M.-A. Pleier ²⁹, V. Pleskot ¹³⁴, E. Plotnikova³⁸, G. Poddar ⁹⁵, R. Poettgen ⁹⁹, L. Poggioli ¹²⁸, I. Pokharel ⁵⁵, S. Polacek ¹³⁴, G. Polesello ^{73a}, A. Poley ^{143,157a}, A. Polini ^{23b}, C.S. Pollard ¹⁶⁸, Z.B. Pollock ¹²⁰, E. Pompa Pacchi ^{75a,75b}, N.I. Pond ⁹⁷, D. Ponomarenko ¹¹⁴, L. Pontecorvo ³⁶, S. Popa ^{27a}, G.A. Popeneciu ^{27d}, A. Poreba ³⁶,

D.M. Portillo Quintero [ID157a](#), S. Pospisil [ID133](#), M.A. Postill [ID140](#), P. Postolache [ID27c](#), K. Potamianos [ID168](#),
 P.A. Potepa [ID86a](#), I.N. Potrap [ID38](#), C.J. Potter [ID32](#), H. Potti [ID1](#), J. Poveda [ID164](#), M.E. Pozo Astigarraga [ID36](#),
 A. Prades Ibanez [ID164](#), J. Pretel [ID54](#), D. Price [ID102](#), M. Primavera [ID70a](#), M.A. Principe Martin [ID100](#),
 R. Privara [ID123](#), T. Procter [ID59](#), M.L. Proffitt [ID139](#), N. Proklova [ID129](#), K. Prokofiev [ID64c](#), G. Proto [ID111](#),
 J. Proudfoot [ID6](#), M. Przybycien [ID86a](#), W.W. Przygoda [ID86b](#), A. Psallidas [ID46](#), J.E. Puddefoot [ID140](#),
 D. Pudzha [ID37](#), D. Pyatiizbyantseva [ID37](#), J. Qian [ID107](#), D. Qichen [ID102](#), Y. Qin [ID13](#), T. Qiu [ID52](#),
 A. Quadt [ID55](#), M. Queitsch-Maitland [ID102](#), G. Quetant [ID56](#), R.P. Quinn [ID165](#), G. Rabanal Bolanos [ID61](#),
 D. Rafanoharana [ID54](#), F. Raffaelli [ID76a,76b](#), F. Ragusa [ID71a,71b](#), J.L. Rainbolt [ID39](#), J.A. Raine [ID56](#),
 S. Rajagopalan [ID29](#), E. Ramakoti [ID37](#), I.A. Ramirez-Berend [ID34](#), K. Ran [ID48,14e](#), N.P. Rapheeha [ID33g](#),
 H. Rasheed [ID27b](#), V. Raskina [ID128](#), D.F. Rassloff [ID63a](#), A. Rastogi [ID17a](#), S. Rave [ID101](#), B. Ravina [ID55](#),
 I. Ravinovich [ID170](#), M. Raymond [ID36](#), A.L. Read [ID126](#), N.P. Readioff [ID140](#), D.M. Rebutzi [ID73a,73b](#),
 G. Redlinger [ID29](#), A.S. Reed [ID111](#), K. Reeves [ID26](#), J.A. Reidelsturz [ID172](#), D. Reikher [ID152](#), A. Rej [ID49](#),
 C. Rembser [ID36](#), M. Renda [ID27b](#), M.B. Rendel [ID111](#), F. Renner [ID48](#), A.G. Rennie [ID160](#), A.L. Rescia [ID48](#),
 S. Resconi [ID71a](#), M. Ressegotti [ID57b,57a](#), S. Rettie [ID36](#), J.G. Reyes Rivera [ID108](#), E. Reynolds [ID17a](#),
 O.L. Rezanova [ID37](#), P. Reznicek [ID134](#), H. Riani [ID35d](#), N. Ribaric [ID92](#), E. Ricci [ID78a,78b](#), R. Richter [ID111](#),
 S. Richter [ID47a,47b](#), E. Richter-Was [ID86b](#), M. Ridel [ID128](#), S. Ridouani [ID35d](#), P. Rieck [ID118](#), P. Riedler [ID36](#),
 E.M. Riefel [ID47a,47b](#), J.O. Rieger [ID115](#), M. Rijssenbeek [ID146](#), M. Rimoldi [ID36](#), L. Rinaldi [ID23b,23a](#),
 T.T. Rinn [ID29](#), M.P. Rinnagel [ID110](#), G. Ripellino [ID162](#), I. Riu [ID13](#), J.C. Rivera Vergara [ID166](#),
 F. Rizatdinova [ID122](#), E. Rizvi [ID95](#), B.R. Roberts [ID17a](#), S.H. Robertson [ID105,v](#), D. Robinson [ID32](#),
 C.M. Robles Gajardo [ID138f](#), M. Robles Manzano [ID101](#), A. Robson [ID59](#), A. Rocchi [ID76a,76b](#), C. Roda [ID74a,74b](#),
 S. Rodriguez Bosca [ID36](#), Y. Rodriguez Garcia [ID22a](#), A. Rodriguez Rodriguez [ID54](#),
 A.M. Rodríguez Vera [ID116](#), S. Roe [ID36](#), J.T. Roemer [ID160](#), A.R. Roepe-Gier [ID137](#), J. Roggel [ID172](#),
 O. Røhne [ID126](#), R.A. Rojas [ID104](#), C.P.A. Roland [ID128](#), J. Roloff [ID29](#), A. Romaniouk [ID37](#),
 E. Romano [ID73a,73b](#), M. Romano [ID23b](#), A.C. Romero Hernandez [ID163](#), N. Rompotis [ID93](#), L. Roos [ID128](#),
 S. Rosati [ID75a](#), B.J. Rosser [ID39](#), E. Rossi [ID127](#), E. Rossi [ID72a,72b](#), L.P. Rossi [ID61](#), L. Rossini [ID54](#),
 R. Rosten [ID120](#), M. Rotaru [ID27b](#), B. Rottler [ID54](#), C. Rougier [ID90](#), D. Rousseau [ID66](#), D. Rouso [ID48](#),
 A. Roy [ID163](#), S. Roy-Garand [ID156](#), A. Rozanov [ID103](#), Z.M.A. Rozario [ID59](#), Y. Rozen [ID151](#),
 A. Rubio Jimenez [ID164](#), A.J. Ruby [ID93](#), V.H. Ruelas Rivera [ID18](#), T.A. Ruggeri [ID1](#), A. Ruggiero [ID127](#),
 A. Ruiz-Martinez [ID164](#), A. Rummler [ID36](#), Z. Rurikova [ID54](#), N.A. Rusakovich [ID38](#), H.L. Russell [ID166](#),
 G. Russo [ID75a,75b](#), J.P. Rutherford [ID7](#), S. Rutherford Colmenares [ID32](#), M. Rybar [ID134](#), E.B. Rye [ID126](#),
 A. Ryzhov [ID44](#), J.A. Sabater Iglesias [ID56](#), P. Sabatini [ID164](#), H.F.W. Sadrozinski [ID137](#),
 F. Safai Tehrani [ID75a](#), B. Safarzadeh Samani [ID135](#), S. Saha [ID1](#), M. Sahinsoy [ID111](#), A. Saibel [ID164](#),
 M. Saimpert [ID136](#), M. Saito [ID154](#), T. Saito [ID154](#), A. Sala [ID71a,71b](#), D. Salamani [ID36](#), A. Salnikov [ID144](#),
 J. Salt [ID164](#), A. Salvador Salas [ID152](#), D. Salvatore [ID43b,43a](#), F. Salvatore [ID147](#), A. Salzburger [ID36](#),
 D. Sammel [ID54](#), E. Sampson [ID92](#), D. Sampsonidis [ID153,d](#), D. Sampsonidou [ID124](#), J. Sánchez [ID164](#),
 V. Sanchez Sebastian [ID164](#), H. Sandaker [ID126](#), C.O. Sander [ID48](#), J.A. Sandesara [ID104](#), M. Sandhoff [ID172](#),
 C. Sandoval [ID22b](#), L. Sanfilippo [ID63a](#), D.P.C. Sankey [ID135](#), T. Sano [ID88](#), A. Sansoni [ID53](#), L. Santi [ID75a,75b](#),
 C. Santoni [ID40](#), H. Santos [ID131a,131b](#), A. Santra [ID170](#), E. Sanzani [ID23b,23a](#), K.A. Saoucha [ID161](#),
 J.G. Saraiva [ID131a,131d](#), J. Sardain [ID7](#), O. Sasaki [ID84](#), K. Sato [ID158](#), C. Sauer [ID63b](#), E. Sauvan [ID4](#),
 P. Savard [ID156,ad](#), R. Sawada [ID154](#), C. Sawyer [ID135](#), L. Sawyer [ID98](#), C. Sbarra [ID23b](#), A. Sbrizzi [ID23b,23a](#),
 T. Scanlon [ID97](#), J. Schaarschmidt [ID139](#), U. Schäfer [ID101](#), A.C. Schaffer [ID66,44](#), D. Schaile [ID110](#),
 R.D. Schamberger [ID146](#), C. Scharf [ID18](#), M.M. Schefer [ID19](#), V.A. Schegelsky [ID37](#), D. Scheirich [ID134](#),
 M. Schernau [ID160](#), C. Scheulen [ID55](#), C. Schiavi [ID57b,57a](#), M. Schioppa [ID43b,43a](#), B. Schlag [ID144,1](#),
 K.E. Schleicher [ID54](#), S. Schlenker [ID36](#), J. Schmeing [ID172](#), M.A. Schmidt [ID172](#), K. Schmieden [ID101](#),
 C. Schmitt [ID101](#), N. Schmitt [ID101](#), S. Schmitt [ID48](#), L. Schoeffel [ID136](#), A. Schoening [ID63b](#),
 P.G. Scholer [ID34](#), E. Schopf [ID127](#), M. Schott [ID24](#), J. Schovancova [ID36](#), S. Schramm [ID56](#), T. Schroer [ID56](#),
 H-C. Schultz-Coulon [ID63a](#), M. Schumacher [ID54](#), B.A. Schumm [ID137](#), Ph. Schune [ID136](#), A.J. Schuy [ID139](#),

H.R. Schwartz [id137](#), A. Schwartzman [id144](#), T.A. Schwarz [id107](#), Ph. Schwemling [id136](#),
 R. Schwienhorst [id108](#), A. Sciandra [id29](#), G. Sciolla [id26](#), F. Scuri [id74a](#), C.D. Sebastiani [id93](#),
 K. Sedlaczek [id116](#), S.C. Seidel [id113](#), A. Seiden [id137](#), B.D. Seidlitz [id41](#), C. Seitz [id48](#), J.M. Seixas [id83b](#),
 G. Sekhniaidze [id72a](#), L. Selem [id60](#), N. Semprini-Cesari [id23b,23a](#), D. Sengupta [id56](#), V. Senthilkumar [id164](#),
 L. Serin [id66](#), M. Sessa [id76a,76b](#), H. Severini [id121](#), F. Sforza [id57b,57a](#), A. Sfyrta [id56](#), Q. Sha [id14a](#),
 E. Shabalina [id55](#), A.H. Shah [id32](#), R. Shaheen [id145](#), J.D. Shahinian [id129](#), D. Shaked Renous [id170](#),
 L.Y. Shan [id14a](#), M. Shapiro [id17a](#), A. Sharma [id36](#), A.S. Sharma [id165](#), P. Sharma [id80](#), P.B. Shatalov [id37](#),
 K. Shaw [id147](#), S.M. Shaw [id102](#), Q. Shen [id62c,5](#), D.J. Sheppard [id143](#), P. Sherwood [id97](#), L. Shi [id97](#),
 X. Shi [id14a](#), C.O. Shimmin [id173](#), J.D. Shinner [id96](#), I.P.J. Shipsey [id127](#), S. Shirabe [id89](#),
 M. Shiyakova [id38,t](#), M.J. Shochet [id39](#), J. Shojaii [id106](#), D.R. Shope [id126](#), B. Shrestha [id121](#),
 S. Shrestha [id120,ag](#), M.J. Shroff [id166](#), P. Sicho [id132](#), A.M. Sickles [id163](#), E. Sideras Haddad [id33g](#),
 A.C. Sidley [id115](#), A. Sidoti [id23b](#), F. Siegert [id50](#), Dj. Sijacki [id15](#), F. Sili [id91](#), J.M. Silva [id52](#),
 M.V. Silva Oliveira [id29](#), S.B. Silverstein [id47a](#), S. Simion [id66](#), R. Simoniello [id36](#), E.L. Simpson [id102](#),
 H. Simpson [id147](#), L.R. Simpson [id107](#), N.D. Simpson [id99](#), S. Simsek [id82](#), S. Sindhu [id55](#), P. Sinervo [id156](#),
 S. Singh [id156](#), S. Sinha [id48](#), S. Sinha [id102](#), M. Sioli [id23b,23a](#), I. Siral [id36](#), E. Sitnikova [id48](#),
 J. Sjölin [id47a,47b](#), A. Skaf [id55](#), E. Skorda [id20](#), P. Skubic [id121](#), M. Slawinska [id87](#), V. Smakhtin [id170](#),
 B.H. Smart [id135](#), S.Yu. Smirnov [id37](#), Y. Smirnov [id37](#), L.N. Smirnova [id37,a](#), O. Smirnova [id99](#),
 A.C. Smith [id41](#), D.R. Smith [id160](#), E.A. Smith [id39](#), H.A. Smith [id127](#), J.L. Smith [id102](#), R. Smith [id144](#),
 M. Smizanska [id92](#), K. Smolek [id133](#), A.A. Snesarev [id37](#), S.R. Snider [id156](#), H.L. Snoek [id115](#),
 S. Snyder [id29](#), R. Sobie [id166,v](#), A. Soffer [id152](#), C.A. Solans Sanchez [id36](#), E.Yu. Soldatov [id37](#),
 U. Soldevila [id164](#), A.A. Solodkov [id37](#), S. Solomon [id26](#), A. Soloshenko [id38](#), K. Solovieva [id54](#),
 O.V. Solovyanov [id40](#), P. Sommer [id36](#), A. Sonay [id13](#), W.Y. Song [id157b](#), A. Sopczak [id133](#), A.L. Soppio [id97](#),
 F. Sopkova [id28b](#), J.D. Sorenson [id113](#), I.R. Sotarriva Alvarez [id155](#), V. Sothilingam [id63a](#),
 O.J. Soto Sandoval [id138c,138b](#), S. Sottocornola [id68](#), R. Soualah [id161](#), Z. Soumami [id35e](#), D. South [id48](#),
 N. Soybelman [id170](#), S. Spagnolo [id70a,70b](#), M. Spalla [id111](#), D. Sperlich [id54](#), G. Spigo [id36](#), S. Spinali [id92](#),
 D.P. Spiteri [id59](#), M. Spousta [id134](#), E.J. Staats [id34](#), R. Stamen [id63a](#), A. Stampeki [id20](#), M. Standke [id24](#),
 E. Stanecka [id87](#), W. Stanek-Maslouska [id48](#), M.V. Stange [id50](#), B. Stanislaus [id17a](#), M.M. Stanitzki [id48](#),
 B. Stapf [id48](#), E.A. Starchenko [id37](#), G.H. Stark [id137](#), J. Stark [id90](#), P. Staroba [id132](#), P. Starovoitov [id63a](#),
 S. Stärz [id105](#), R. Staszewski [id87](#), G. Stavropoulos [id46](#), J. Steentoft [id162](#), P. Steinberg [id29](#),
 B. Stelzer [id143,157a](#), H.J. Stelzer [id130](#), O. Stelzer-Chilton [id157a](#), H. Stenzel [id58](#), T.J. Stevenson [id147](#),
 G.A. Stewart [id36](#), J.R. Stewart [id122](#), M.C. Stockton [id36](#), G. Stoicea [id27b](#), M. Stolarski [id131a](#),
 S. Stonjek [id111](#), A. Straessner [id50](#), J. Strandberg [id145](#), S. Strandberg [id47a,47b](#), M. Stratmann [id172](#),
 M. Strauss [id121](#), T. Streblor [id103](#), P. Strizenc [id28b](#), R. Ströhmer [id167](#), D.M. Strom [id124](#),
 R. Stroynowski [id44](#), A. Strubig [id47a,47b](#), S.A. Stucci [id29](#), B. Stugu [id16](#), J. Stupak [id121](#), N.A. Styles [id48](#),
 D. Su [id144](#), S. Su [id62a](#), W. Su [id62d](#), X. Su [id62a](#), D. Suchy [id28a](#), K. Sugizaki [id154](#), V.V. Sulin [id37](#),
 M.J. Sullivan [id93](#), D.M.S. Sultan [id127](#), L. Sultanaliyeva [id37](#), S. Sultansoy [id3b](#), T. Sumida [id88](#),
 S. Sun [id107](#), S. Sun [id171](#), O. Sunneborn Gudnadottir [id162](#), N. Sur [id103](#), M.R. Sutton [id147](#),
 H. Suzuki [id158](#), M. Svatos [id132](#), M. Swiatlowski [id157a](#), T. Swirski [id167](#), I. Sykora [id28a](#), M. Sykora [id134](#),
 T. Sykora [id134](#), D. Ta [id101](#), K. Tackmann [id48,s](#), A. Taffard [id160](#), R. Tafirout [id157a](#),
 J.S. Tafoya Vargas [id66](#), Y. Takubo [id84](#), M. Talby [id103](#), A.A. Talyshev [id37](#), K.C. Tam [id64b](#),
 N.M. Tamir [id152](#), A. Tanaka [id154](#), J. Tanaka [id154](#), R. Tanaka [id66](#), M. Tanasini [id146](#), Z. Tao [id165](#),
 S. Tapia Araya [id138f](#), S. Tapprogge [id101](#), A. Tarek Abouelfadl Mohamed [id108](#), S. Tarem [id151](#),
 K. Tariq [id14a](#), G. Tarna [id27b](#), G.F. Tartarelli [id71a](#), M.J. Tartarin [id90](#), P. Tas [id134](#), M. Tasevsky [id132](#),
 E. Tassi [id43b,43a](#), A.C. Tate [id163](#), G. Tateno [id154](#), Y. Tayalati [id35e,u](#), G.N. Taylor [id106](#), W. Taylor [id157b](#),
 A.S. Tee [id171](#), R. Teixeira De Lima [id144](#), P. Teixeira-Dias [id96](#), J.J. Teoh [id156](#), K. Terashi [id154](#),
 J. Terron [id100](#), S. Terzo [id13](#), M. Testa [id53](#), R.J. Teuscher [id156,v](#), A. Thaler [id79](#), O. Theiner [id56](#),
 N. Themistokleous [id52](#), T. Thevenaux-Pelzer [id103](#), O. Thielmann [id172](#), D.W. Thomas [id96](#),

J.P. Thomas ²⁰, E.A. Thompson ^{17a}, P.D. Thompson ²⁰, E. Thomson ¹²⁹, R.E. Thornberry⁴⁴, C. Tian ^{62a}, Y. Tian ⁵⁵, V. Tikhomirov ^{37,a}, Yu.A. Tikhonov ³⁷, S. Timoshenko³⁷, D. Timoshyn ¹³⁴, E.X.L. Ting ¹, P. Tipton ¹⁷³, A. Tishelman-Charny ²⁹, S.H. Tlou ^{33g}, K. Todome ¹⁵⁵, S. Todorova-Nova ¹³⁴, S. Todt⁵⁰, L. Toffolin ^{69a,69c}, M. Togawa ⁸⁴, J. Tojo ⁸⁹, S. Tokár ^{28a}, K. Tokushuku ⁸⁴, O. Toldaiev ⁶⁸, R. Tombs ³², M. Tomoto ^{84,112}, L. Tompkins ^{144,1}, K.W. Topolnicki ^{86b}, E. Torrence ¹²⁴, H. Torres ⁹⁰, E. Torró Pastor ¹⁶⁴, M. Toscani ³⁰, C. Tosciri ³⁹, M. Tost ¹¹, D.R. Tovey ¹⁴⁰, A. Traeet¹⁶, I.S. Trandafir ^{27b}, T. Trefzger ¹⁶⁷, A. Tricoli ²⁹, I.M. Trigger ^{157a}, S. Trincaz-Duvoid ¹²⁸, D.A. Trischuk ²⁶, B. Trocmé ⁶⁰, L. Truong ^{33c}, M. Trzebinski ⁸⁷, A. Trzupiek ⁸⁷, F. Tsai ¹⁴⁶, M. Tsai ¹⁰⁷, A. Tsiamis ^{153,d}, P.V. Tsiareshka³⁷, S. Tsigaridas ^{157a}, A. Tsigotis ^{153,q}, V. Tsiskaridze ¹⁵⁶, E.G. Tskhadadze ^{150a}, M. Tsopoulou ¹⁵³, Y. Tsujikawa ⁸⁸, I.I. Tsukerman ³⁷, V. Tsulaia ^{17a}, S. Tsuno ⁸⁴, K. Tsuru ¹¹⁹, D. Tsybychev ¹⁴⁶, Y. Tu ^{64b}, A. Tudorache ^{27b}, V. Tudorache ^{27b}, A.N. Tuna ⁶¹, S. Turchikhin ^{57b,57a}, I. Turk Cakir ^{3a}, R. Turra ^{71a}, T. Turtuvshin ^{38,w}, P.M. Tuts ⁴¹, S. Tzamarias ^{153,d}, E. Tzovara ¹⁰¹, F. Ukegawa ¹⁵⁸, P.A. Ulloa Poblete ^{138c,138b}, E.N. Umaka ²⁹, G. Unal ³⁶, A. Undrus ²⁹, G. Unel ¹⁶⁰, J. Urban ^{28b}, P. Urrejola ^{138a}, G. Usai ⁸, R. Ushioda ¹⁵⁵, M. Usman ¹⁰⁹, Z. Uysal ⁸², V. Vacek ¹³³, B. Vachon ¹⁰⁵, T. Vafeiadis ³⁶, A. Vaitkus ⁹⁷, C. Valderanis ¹¹⁰, E. Valdes Santurio ^{47a,47b}, M. Valente ^{157a}, S. Valentinetti ^{23b,23a}, A. Valero ¹⁶⁴, E. Valiente Moreno ¹⁶⁴, A. Vallier ⁹⁰, J.A. Valls Ferrer ¹⁶⁴, D.R. Van Arneeman ¹¹⁵, T.R. Van Daalen ¹³⁹, A. Van Der Graaf ⁴⁹, P. Van Gemmeren ⁶, M. Van Rijnbach ³⁶, S. Van Stroud ⁹⁷, I. Van Vulpen ¹¹⁵, P. Vana ¹³⁴, M. Vanadia ^{76a,76b}, W. Vandelli ³⁶, E.R. Vandewall ¹²², D. Vannicola ¹⁵², L. Vannoli ⁵³, R. Vari ^{75a}, E.W. Varnes ⁷, C. Varni ^{17b}, T. Varol ¹⁴⁹, D. Varouchas ⁶⁶, L. Variiale ¹⁶⁴, K.E. Varvell ¹⁴⁸, M.E. Vasile ^{27b}, L. Vaslin⁸⁴, G.A. Vasquez ¹⁶⁶, A. Vasyukov ³⁸, R. Vavricka¹⁰¹, T. Vazquez Schroeder ³⁶, J. Veatch ³¹, V. Vecchio ¹⁰², M.J. Veen ¹⁰⁴, I. Veliscek ²⁹, L.M. Veloce ¹⁵⁶, F. Veloso ^{131a,131c}, S. Veneziano ^{75a}, A. Ventura ^{70a,70b}, S. Ventura Gonzalez ¹³⁶, A. Verbytskyi ¹¹¹, M. Verducci ^{74a,74b}, C. Vergis ⁹⁵, M. Verissimo De Araujo ^{83b}, W. Verkerke ¹¹⁵, J.C. Vermeulen ¹¹⁵, C. Vernieri ¹⁴⁴, M. Vessella ¹⁰⁴, M.C. Vetterli ^{143,ad}, A. Vgenopoulos ^{153,d}, N. Viaux Maira ^{138f}, T. Vickey ¹⁴⁰, O.E. Vickey Boeriu ¹⁴⁰, G.H.A. Viehhauser ¹²⁷, L. Vigani ^{63b}, M. Villa ^{23b,23a}, M. Villaplana Perez ¹⁶⁴, E.M. Villhauer⁵², E. Vilucchi ⁵³, M.G. Vincter ³⁴, A. Visibile¹¹⁵, C. Vittori ³⁶, I. Vivarelli ^{23b,23a}, E. Voevodina ¹¹¹, F. Vogel ¹¹⁰, J.C. Voigt ⁵⁰, P. Vokac ¹³³, Yu. Volkotrub ^{86b}, J. Von Ahnen ⁴⁸, E. Von Toerne ²⁴, B. Vormwald ³⁶, V. Vorobel ¹³⁴, K. Vorobev ³⁷, M. Vos ¹⁶⁴, K. Voss ¹⁴², M. Vozak ¹¹⁵, L. Vozdecky ¹²¹, N. Vranjes ¹⁵, M. Vranjes Milosavljevic ¹⁵, M. Vreeswijk ¹¹⁵, N.K. Vu ^{62d,62c}, R. Vuillermet ³⁶, O. Vujinovic ¹⁰¹, I. Vukotic ³⁹, S. Wada ¹⁵⁸, C. Wagner¹⁰⁴, J.M. Wagner ^{17a}, W. Wagner ¹⁷², S. Wahdan ¹⁷², H. Wahlberg ⁹¹, M. Wakida ¹¹², J. Walder ¹³⁵, R. Walker ¹¹⁰, W. Walkowiak ¹⁴², A. Wall ¹²⁹, E.J. Wallin ⁹⁹, T. Wamorkar ⁶, A.Z. Wang ¹³⁷, C. Wang ¹⁰¹, C. Wang ¹¹, H. Wang ^{17a}, J. Wang ^{64c}, R. Wang ⁶¹, R. Wang ⁶, S.M. Wang ¹⁴⁹, S. Wang ^{62b}, S. Wang ^{14a}, T. Wang ^{62a}, W.T. Wang ⁸⁰, W. Wang ^{14a}, X. Wang ^{14c}, X. Wang ¹⁶³, X. Wang ^{62c}, Y. Wang ^{62d}, Y. Wang ^{14c}, Z. Wang ¹⁰⁷, Z. Wang ^{62d,51,62c}, Z. Wang ¹⁰⁷, A. Warburton ¹⁰⁵, R.J. Ward ²⁰, N. Warrack ⁵⁹, S. Waterhouse ⁹⁶, A.T. Watson ²⁰, H. Watson ⁵⁹, M.F. Watson ²⁰, E. Watton ^{59,135}, G. Watts ¹³⁹, B.M. Waugh ⁹⁷, J.M. Webb ⁵⁴, C. Weber ²⁹, H.A. Weber ¹⁸, M.S. Weber ¹⁹, S.M. Weber ^{63a}, C. Wei ^{62a}, Y. Wei ⁵⁴, A.R. Weidberg ¹²⁷, E.J. Weik ¹¹⁸, J. Weingarten ⁴⁹, C. Weiser ⁵⁴, C.J. Wells ⁴⁸, T. Wenaus ²⁹, B. Wendland ⁴⁹, T. Wengler ³⁶, N.S. Wenke¹¹¹, N. Wermes ²⁴, M. Wessels ^{63a}, A.M. Wharton ⁹², A.S. White ⁶¹, A. White ⁸, M.J. White ¹, D. Whiteson ¹⁶⁰, L. Wickremasinghe ¹²⁵, W. Wiedenmann ¹⁷¹, M. Wielers ¹³⁵, C. Wiglesworth ⁴², D.J. Wilbern¹²¹, H.G. Wilkens ³⁶, J.J.H. Wilkinson ³², D.M. Williams ⁴¹, H.H. Williams¹²⁹, S. Williams ³², S. Willocq ¹⁰⁴, B.J. Wilson ¹⁰², P.J. Windischhofer ³⁹,

F.I. Winkel ³⁰, F. Winklmeier ¹²⁴, B.T. Winter ⁵⁴, J.K. Winter ¹⁰², M. Wittgen ¹⁴⁴, M. Wobisch ⁹⁸, T. Wojtkowski ⁶⁰, Z. Wolffs ¹¹⁵, J. Wollrath ¹⁶⁰, M.W. Wolter ⁸⁷, H. Wolters ^{131a,131c}, M.C. Wong ¹³⁷, E.L. Woodward ⁴¹, S.D. Worm ⁴⁸, B.K. Wosiek ⁸⁷, K.W. Woźniak ⁸⁷, S. Wozniowski ⁵⁵, K. Wraight ⁵⁹, C. Wu ²⁰, M. Wu ^{14d}, M. Wu ¹¹⁴, S.L. Wu ¹⁷¹, X. Wu ⁵⁶, Y. Wu ^{62a}, Z. Wu ⁴, J. Wuerzinger ^{111,ab}, T.R. Wyatt ¹⁰², B.M. Wynne ⁵², S. Xella ⁴², L. Xia ^{14c}, M. Xia ^{14b}, J. Xiang ^{64c}, M. Xie ^{62a}, S. Xin ^{14a,14e}, A. Xiong ¹²⁴, J. Xiong ^{17a}, D. Xu ^{14a}, H. Xu ^{62a}, L. Xu ^{62a}, R. Xu ¹²⁹, T. Xu ¹⁰⁷, Y. Xu ^{14b}, Z. Xu ⁵², Z. Xu ^{14c}, B. Yabsley ¹⁴⁸, S. Yacoob ^{33a}, Y. Yamaguchi ¹⁵⁵, E. Yamashita ¹⁵⁴, H. Yamauchi ¹⁵⁸, T. Yamazaki ^{17a}, Y. Yamazaki ⁸⁵, J. Yan ^{62c}, S. Yan ⁵⁹, Z. Yan ¹⁰⁴, H.J. Yang ^{62c,62d}, H.T. Yang ^{62a}, S. Yang ^{62a}, T. Yang ^{64c}, X. Yang ³⁶, X. Yang ^{14a}, Y. Yang ⁴⁴, Y. Yang ^{62a}, Z. Yang ^{62a}, W-M. Yao ^{17a}, H. Ye ^{14c}, H. Ye ⁵⁵, J. Ye ^{14a}, S. Ye ²⁹, X. Ye ^{62a}, Y. Yeh ⁹⁷, I. Yeletsikh ³⁸, B.K. Yeo ^{17b}, M.R. Yexley ⁹⁷, T.P. Yildirim ¹²⁷, P. Yin ⁴¹, K. Yorita ¹⁶⁹, S. Younas ^{27b}, C.J.S. Young ³⁶, C. Young ¹⁴⁴, C. Yu ^{14a,14e}, Y. Yu ^{62a}, M. Yuan ¹⁰⁷, R. Yuan ^{62d,62c}, L. Yue ⁹⁷, M. Zaazoua ^{62a}, B. Zabinski ⁸⁷, E. Zaid ⁵², Z.K. Zak ⁸⁷, T. Zakareishvili ¹⁶⁴, N. Zakharchuk ³⁴, S. Zambito ⁵⁶, J.A. Zamora Saa ^{138d,138b}, J. Zang ¹⁵⁴, D. Zanzi ⁵⁴, O. Zaplatilek ¹³³, C. Zeitnitz ¹⁷², H. Zeng ^{14a}, J.C. Zeng ¹⁶³, D.T. Zenger Jr ²⁶, O. Zenin ³⁷, T. Ženiš ^{28a}, S. Zenz ⁹⁵, S. Zerradi ^{35a}, D. Zerwas ⁶⁶, M. Zhai ^{14a,14e}, D.F. Zhang ¹⁴⁰, J. Zhang ^{62b}, J. Zhang ⁶, K. Zhang ^{14a,14e}, L. Zhang ^{62a}, L. Zhang ^{14c}, P. Zhang ^{14a,14e}, R. Zhang ¹⁷¹, S. Zhang ¹⁰⁷, S. Zhang ⁹⁰, T. Zhang ¹⁵⁴, X. Zhang ^{62c}, X. Zhang ^{62b}, Y. Zhang ^{62c}, Y. Zhang ⁹⁷, Y. Zhang ^{14c}, Z. Zhang ^{17a}, Z. Zhang ^{62b}, Z. Zhang ⁶⁶, H. Zhao ¹³⁹, T. Zhao ^{62b}, Y. Zhao ¹³⁷, Z. Zhao ^{62a}, Z. Zhao ^{62a}, A. Zhemchugov ³⁸, J. Zheng ^{14c}, K. Zheng ¹⁶³, X. Zheng ^{62a}, Z. Zheng ¹⁴⁴, D. Zhong ¹⁶³, B. Zhou ¹⁰⁷, H. Zhou ⁷, N. Zhou ^{62c}, Y. Zhou ^{14b}, Y. Zhou ^{14c}, Y. Zhou ⁷, C.G. Zhu ^{62b}, J. Zhu ¹⁰⁷, X. Zhu ^{62d}, Y. Zhu ^{62c}, Y. Zhu ^{62a}, X. Zhuang ^{14a}, K. Zhukov ³⁷, N.I. Zimine ³⁸, J. Zinsser ^{63b}, M. Ziolkowski ¹⁴², L. Živković ¹⁵, A. Zoccoli ^{23b,23a}, K. Zoch ⁶¹, T.G. Zorbas ¹⁴⁰, O. Zormpa ⁴⁶, W. Zou ⁴¹, L. Zwalinski ³⁶.

¹Department of Physics, University of Adelaide, Adelaide; Australia.

²Department of Physics, University of Alberta, Edmonton AB; Canada.

^{3(a)}Department of Physics, Ankara University, Ankara; ^(b)Division of Physics, TOBB University of Economics and Technology, Ankara; Türkiye.

⁴LAPP, Université Savoie Mont Blanc, CNRS/IN2P3, Annecy; France.

⁵APC, Université Paris Cité, CNRS/IN2P3, Paris; France.

⁶High Energy Physics Division, Argonne National Laboratory, Argonne IL; United States of America.

⁷Department of Physics, University of Arizona, Tucson AZ; United States of America.

⁸Department of Physics, University of Texas at Arlington, Arlington TX; United States of America.

⁹Physics Department, National and Kapodistrian University of Athens, Athens; Greece.

¹⁰Physics Department, National Technical University of Athens, Zografou; Greece.

¹¹Department of Physics, University of Texas at Austin, Austin TX; United States of America.

¹²Institute of Physics, Azerbaijan Academy of Sciences, Baku; Azerbaijan.

¹³Institut de Física d'Altes Energies (IFAE), Barcelona Institute of Science and Technology, Barcelona; Spain.

^{14(a)}Institute of High Energy Physics, Chinese Academy of Sciences, Beijing; ^(b)Physics Department, Tsinghua University, Beijing; ^(c)Department of Physics, Nanjing University, Nanjing; ^(d)School of Science, Shenzhen Campus of Sun Yat-sen University; ^(e)University of Chinese Academy of Science (UCAS), Beijing; China.

¹⁵Institute of Physics, University of Belgrade, Belgrade; Serbia.

¹⁶Department for Physics and Technology, University of Bergen, Bergen; Norway.

- ¹⁷(*a*) Physics Division, Lawrence Berkeley National Laboratory, Berkeley CA; (*b*) University of California, Berkeley CA; United States of America.
- ¹⁸Institut für Physik, Humboldt Universität zu Berlin, Berlin; Germany.
- ¹⁹Albert Einstein Center for Fundamental Physics and Laboratory for High Energy Physics, University of Bern, Bern; Switzerland.
- ²⁰School of Physics and Astronomy, University of Birmingham, Birmingham; United Kingdom.
- ²¹(*a*) Department of Physics, Bogazici University, Istanbul; (*b*) Department of Physics Engineering, Gaziantep University, Gaziantep; (*c*) Department of Physics, Istanbul University, Istanbul; Türkiye.
- ²²(*a*) Facultad de Ciencias y Centro de Investigaciones, Universidad Antonio Nariño, Bogotá; (*b*) Departamento de Física, Universidad Nacional de Colombia, Bogotá; Colombia.
- ²³(*a*) Dipartimento di Fisica e Astronomia A. Righi, Università di Bologna, Bologna; (*b*) INFN Sezione di Bologna; Italy.
- ²⁴Physikalisches Institut, Universität Bonn, Bonn; Germany.
- ²⁵Department of Physics, Boston University, Boston MA; United States of America.
- ²⁶Department of Physics, Brandeis University, Waltham MA; United States of America.
- ²⁷(*a*) Transilvania University of Brasov, Brasov; (*b*) Horia Hulubei National Institute of Physics and Nuclear Engineering, Bucharest; (*c*) Department of Physics, Alexandru Ioan Cuza University of Iasi, Iasi; (*d*) National Institute for Research and Development of Isotopic and Molecular Technologies, Physics Department, Cluj-Napoca; (*e*) National University of Science and Technology Politehnica, Bucharest; (*f*) West University in Timisoara, Timisoara; (*g*) Faculty of Physics, University of Bucharest, Bucharest; Romania.
- ²⁸(*a*) Faculty of Mathematics, Physics and Informatics, Comenius University, Bratislava; (*b*) Department of Subnuclear Physics, Institute of Experimental Physics of the Slovak Academy of Sciences, Kosice; Slovak Republic.
- ²⁹Physics Department, Brookhaven National Laboratory, Upton NY; United States of America.
- ³⁰Universidad de Buenos Aires, Facultad de Ciencias Exactas y Naturales, Departamento de Física, y CONICET, Instituto de Física de Buenos Aires (IFIBA), Buenos Aires; Argentina.
- ³¹California State University, CA; United States of America.
- ³²Cavendish Laboratory, University of Cambridge, Cambridge; United Kingdom.
- ³³(*a*) Department of Physics, University of Cape Town, Cape Town; (*b*) iThemba Labs, Western Cape; (*c*) Department of Mechanical Engineering Science, University of Johannesburg, Johannesburg; (*d*) National Institute of Physics, University of the Philippines Diliman (Philippines); (*e*) University of South Africa, Department of Physics, Pretoria; (*f*) University of Zululand, KwaDlangezwa; (*g*) School of Physics, University of the Witwatersrand, Johannesburg; South Africa.
- ³⁴Department of Physics, Carleton University, Ottawa ON; Canada.
- ³⁵(*a*) Faculté des Sciences Ain Chock, Réseau Universitaire de Physique des Hautes Energies - Université Hassan II, Casablanca; (*b*) Faculté des Sciences, Université Ibn-Tofail, Kénitra; (*c*) Faculté des Sciences Semlalia, Université Cadi Ayyad, LPHEA-Marrakech; (*d*) LPMR, Faculté des Sciences, Université Mohamed Premier, Oujda; (*e*) Faculté des sciences, Université Mohammed V, Rabat; (*f*) Institute of Applied Physics, Mohammed VI Polytechnic University, Ben Guerir; Morocco.
- ³⁶CERN, Geneva; Switzerland.
- ³⁷Affiliated with an institute covered by a cooperation agreement with CERN.
- ³⁸Affiliated with an international laboratory covered by a cooperation agreement with CERN.
- ³⁹Enrico Fermi Institute, University of Chicago, Chicago IL; United States of America.
- ⁴⁰LPC, Université Clermont Auvergne, CNRS/IN2P3, Clermont-Ferrand; France.
- ⁴¹Nevis Laboratory, Columbia University, Irvington NY; United States of America.
- ⁴²Niels Bohr Institute, University of Copenhagen, Copenhagen; Denmark.
- ⁴³(*a*) Dipartimento di Fisica, Università della Calabria, Rende; (*b*) INFN Gruppo Collegato di Cosenza,

Laboratori Nazionali di Frascati; Italy.

⁴⁴Physics Department, Southern Methodist University, Dallas TX; United States of America.

⁴⁵Physics Department, University of Texas at Dallas, Richardson TX; United States of America.

⁴⁶National Centre for Scientific Research "Demokritos", Agia Paraskevi; Greece.

⁴⁷(^a) Department of Physics, Stockholm University; (^b) Oskar Klein Centre, Stockholm; Sweden.

⁴⁸Deutsches Elektronen-Synchrotron DESY, Hamburg and Zeuthen; Germany.

⁴⁹Fakultät Physik, Technische Universität Dortmund, Dortmund; Germany.

⁵⁰Institut für Kern- und Teilchenphysik, Technische Universität Dresden, Dresden; Germany.

⁵¹Department of Physics, Duke University, Durham NC; United States of America.

⁵²SUPA - School of Physics and Astronomy, University of Edinburgh, Edinburgh; United Kingdom.

⁵³INFN e Laboratori Nazionali di Frascati, Frascati; Italy.

⁵⁴Physikalisches Institut, Albert-Ludwigs-Universität Freiburg, Freiburg; Germany.

⁵⁵II. Physikalisches Institut, Georg-August-Universität Göttingen, Göttingen; Germany.

⁵⁶Département de Physique Nucléaire et Corpusculaire, Université de Genève, Genève; Switzerland.

⁵⁷(^a) Dipartimento di Fisica, Università di Genova, Genova; (^b) INFN Sezione di Genova; Italy.

⁵⁸II. Physikalisches Institut, Justus-Liebig-Universität Giessen, Giessen; Germany.

⁵⁹SUPA - School of Physics and Astronomy, University of Glasgow, Glasgow; United Kingdom.

⁶⁰LPSC, Université Grenoble Alpes, CNRS/IN2P3, Grenoble INP, Grenoble; France.

⁶¹Laboratory for Particle Physics and Cosmology, Harvard University, Cambridge MA; United States of America.

⁶²(^a) Department of Modern Physics and State Key Laboratory of Particle Detection and Electronics, University of Science and Technology of China, Hefei; (^b) Institute of Frontier and Interdisciplinary Science and Key Laboratory of Particle Physics and Particle Irradiation (MOE), Shandong University, Qingdao; (^c) School of Physics and Astronomy, Shanghai Jiao Tong University, Key Laboratory for Particle Astrophysics and Cosmology (MOE), SKLPPC, Shanghai; (^d) Tsung-Dao Lee Institute, Shanghai; (^e) School of Physics and Microelectronics, Zhengzhou University; China.

⁶³(^a) Kirchhoff-Institut für Physik, Ruprecht-Karls-Universität Heidelberg, Heidelberg; (^b) Physikalisches Institut, Ruprecht-Karls-Universität Heidelberg, Heidelberg; Germany.

⁶⁴(^a) Department of Physics, Chinese University of Hong Kong, Shatin, N.T., Hong Kong; (^b) Department of Physics, University of Hong Kong, Hong Kong; (^c) Department of Physics and Institute for Advanced Study, Hong Kong University of Science and Technology, Clear Water Bay, Kowloon, Hong Kong; China.

⁶⁵Department of Physics, National Tsing Hua University, Hsinchu; Taiwan.

⁶⁶IJCLab, Université Paris-Saclay, CNRS/IN2P3, 91405, Orsay; France.

⁶⁷Centro Nacional de Microelectrónica (IMB-CNM-CSIC), Barcelona; Spain.

⁶⁸Department of Physics, Indiana University, Bloomington IN; United States of America.

⁶⁹(^a) INFN Gruppo Collegato di Udine, Sezione di Trieste, Udine; (^b) ICTP, Trieste; (^c) Dipartimento Politecnico di Ingegneria e Architettura, Università di Udine, Udine; Italy.

⁷⁰(^a) INFN Sezione di Lecce; (^b) Dipartimento di Matematica e Fisica, Università del Salento, Lecce; Italy.

⁷¹(^a) INFN Sezione di Milano; (^b) Dipartimento di Fisica, Università di Milano, Milano; Italy.

⁷²(^a) INFN Sezione di Napoli; (^b) Dipartimento di Fisica, Università di Napoli, Napoli; Italy.

⁷³(^a) INFN Sezione di Pavia; (^b) Dipartimento di Fisica, Università di Pavia, Pavia; Italy.

⁷⁴(^a) INFN Sezione di Pisa; (^b) Dipartimento di Fisica E. Fermi, Università di Pisa, Pisa; Italy.

⁷⁵(^a) INFN Sezione di Roma; (^b) Dipartimento di Fisica, Sapienza Università di Roma, Roma; Italy.

⁷⁶(^a) INFN Sezione di Roma Tor Vergata; (^b) Dipartimento di Fisica, Università di Roma Tor Vergata, Roma; Italy.

⁷⁷(^a) INFN Sezione di Roma Tre; (^b) Dipartimento di Matematica e Fisica, Università Roma Tre, Roma; Italy.

- ⁷⁸(*a*) INFN-TIFPA; (*b*) Università degli Studi di Trento, Trento; Italy.
- ⁷⁹Universität Innsbruck, Department of Astro and Particle Physics, Innsbruck; Austria.
- ⁸⁰University of Iowa, Iowa City IA; United States of America.
- ⁸¹Department of Physics and Astronomy, Iowa State University, Ames IA; United States of America.
- ⁸²Istinye University, Sariyer, Istanbul; Türkiye.
- ⁸³(*a*) Departamento de Engenharia Elétrica, Universidade Federal de Juiz de Fora (UFJF), Juiz de Fora; (*b*) Universidade Federal do Rio De Janeiro COPPE/EE/IF, Rio de Janeiro; (*c*) Instituto de Física, Universidade de São Paulo, São Paulo; (*d*) Rio de Janeiro State University, Rio de Janeiro; (*e*) Federal University of Bahia, Bahia; Brazil.
- ⁸⁴KEK, High Energy Accelerator Research Organization, Tsukuba; Japan.
- ⁸⁵Graduate School of Science, Kobe University, Kobe; Japan.
- ⁸⁶(*a*) AGH University of Krakow, Faculty of Physics and Applied Computer Science, Krakow; (*b*) Marian Smoluchowski Institute of Physics, Jagiellonian University, Krakow; Poland.
- ⁸⁷Institute of Nuclear Physics Polish Academy of Sciences, Krakow; Poland.
- ⁸⁸Faculty of Science, Kyoto University, Kyoto; Japan.
- ⁸⁹Research Center for Advanced Particle Physics and Department of Physics, Kyushu University, Fukuoka ; Japan.
- ⁹⁰L2IT, Université de Toulouse, CNRS/IN2P3, UPS, Toulouse; France.
- ⁹¹Instituto de Física La Plata, Universidad Nacional de La Plata and CONICET, La Plata; Argentina.
- ⁹²Physics Department, Lancaster University, Lancaster; United Kingdom.
- ⁹³Oliver Lodge Laboratory, University of Liverpool, Liverpool; United Kingdom.
- ⁹⁴Department of Experimental Particle Physics, Jožef Stefan Institute and Department of Physics, University of Ljubljana, Ljubljana; Slovenia.
- ⁹⁵School of Physics and Astronomy, Queen Mary University of London, London; United Kingdom.
- ⁹⁶Department of Physics, Royal Holloway University of London, Egham; United Kingdom.
- ⁹⁷Department of Physics and Astronomy, University College London, London; United Kingdom.
- ⁹⁸Louisiana Tech University, Ruston LA; United States of America.
- ⁹⁹Fysiska institutionen, Lunds universitet, Lund; Sweden.
- ¹⁰⁰Departamento de Física Teórica C-15 and CIAFF, Universidad Autónoma de Madrid, Madrid; Spain.
- ¹⁰¹Institut für Physik, Universität Mainz, Mainz; Germany.
- ¹⁰²School of Physics and Astronomy, University of Manchester, Manchester; United Kingdom.
- ¹⁰³CPPM, Aix-Marseille Université, CNRS/IN2P3, Marseille; France.
- ¹⁰⁴Department of Physics, University of Massachusetts, Amherst MA; United States of America.
- ¹⁰⁵Department of Physics, McGill University, Montreal QC; Canada.
- ¹⁰⁶School of Physics, University of Melbourne, Victoria; Australia.
- ¹⁰⁷Department of Physics, University of Michigan, Ann Arbor MI; United States of America.
- ¹⁰⁸Department of Physics and Astronomy, Michigan State University, East Lansing MI; United States of America.
- ¹⁰⁹Group of Particle Physics, University of Montreal, Montreal QC; Canada.
- ¹¹⁰Fakultät für Physik, Ludwig-Maximilians-Universität München, München; Germany.
- ¹¹¹Max-Planck-Institut für Physik (Werner-Heisenberg-Institut), München; Germany.
- ¹¹²Graduate School of Science and Kobayashi-Maskawa Institute, Nagoya University, Nagoya; Japan.
- ¹¹³Department of Physics and Astronomy, University of New Mexico, Albuquerque NM; United States of America.
- ¹¹⁴Institute for Mathematics, Astrophysics and Particle Physics, Radboud University/Nikhef, Nijmegen; Netherlands.
- ¹¹⁵Nikhef National Institute for Subatomic Physics and University of Amsterdam, Amsterdam;

Netherlands.

¹¹⁶Department of Physics, Northern Illinois University, DeKalb IL; United States of America.

¹¹⁷(^a)New York University Abu Dhabi, Abu Dhabi;(^b)United Arab Emirates University, Al Ain; United Arab Emirates.

¹¹⁸Department of Physics, New York University, New York NY; United States of America.

¹¹⁹Ochanomizu University, Otsuka, Bunkyo-ku, Tokyo; Japan.

¹²⁰Ohio State University, Columbus OH; United States of America.

¹²¹Homer L. Dodge Department of Physics and Astronomy, University of Oklahoma, Norman OK; United States of America.

¹²²Department of Physics, Oklahoma State University, Stillwater OK; United States of America.

¹²³Palacký University, Joint Laboratory of Optics, Olomouc; Czech Republic.

¹²⁴Institute for Fundamental Science, University of Oregon, Eugene, OR; United States of America.

¹²⁵Graduate School of Science, Osaka University, Osaka; Japan.

¹²⁶Department of Physics, University of Oslo, Oslo; Norway.

¹²⁷Department of Physics, Oxford University, Oxford; United Kingdom.

¹²⁸LPNHE, Sorbonne Université, Université Paris Cité, CNRS/IN2P3, Paris; France.

¹²⁹Department of Physics, University of Pennsylvania, Philadelphia PA; United States of America.

¹³⁰Department of Physics and Astronomy, University of Pittsburgh, Pittsburgh PA; United States of America.

¹³¹(^a)Laboratório de Instrumentação e Física Experimental de Partículas - LIP, Lisboa;(^b)Departamento de Física, Faculdade de Ciências, Universidade de Lisboa, Lisboa;(^c)Departamento de Física, Universidade de Coimbra, Coimbra;(^d)Centro de Física Nuclear da Universidade de Lisboa, Lisboa;(^e)Departamento de Física, Universidade do Minho, Braga;(^f)Departamento de Física Teórica y del Cosmos, Universidad de Granada, Granada (Spain);(^g)Departamento de Física, Instituto Superior Técnico, Universidade de Lisboa, Lisboa; Portugal.

¹³²Institute of Physics of the Czech Academy of Sciences, Prague; Czech Republic.

¹³³Czech Technical University in Prague, Prague; Czech Republic.

¹³⁴Charles University, Faculty of Mathematics and Physics, Prague; Czech Republic.

¹³⁵Particle Physics Department, Rutherford Appleton Laboratory, Didcot; United Kingdom.

¹³⁶IRFU, CEA, Université Paris-Saclay, Gif-sur-Yvette; France.

¹³⁷Santa Cruz Institute for Particle Physics, University of California Santa Cruz, Santa Cruz CA; United States of America.

¹³⁸(^a)Departamento de Física, Pontificia Universidad Católica de Chile, Santiago;(^b)Millennium Institute for Subatomic physics at high energy frontier (SAPHIR), Santiago;(^c)Instituto de Investigación Multidisciplinario en Ciencia y Tecnología, y Departamento de Física, Universidad de La Serena;(^d)Universidad Andres Bello, Department of Physics, Santiago;(^e)Instituto de Alta Investigación, Universidad de Tarapacá, Arica;(^f)Departamento de Física, Universidad Técnica Federico Santa María, Valparaíso; Chile.

¹³⁹Department of Physics, University of Washington, Seattle WA; United States of America.

¹⁴⁰Department of Physics and Astronomy, University of Sheffield, Sheffield; United Kingdom.

¹⁴¹Department of Physics, Shinshu University, Nagano; Japan.

¹⁴²Department Physik, Universität Siegen, Siegen; Germany.

¹⁴³Department of Physics, Simon Fraser University, Burnaby BC; Canada.

¹⁴⁴SLAC National Accelerator Laboratory, Stanford CA; United States of America.

¹⁴⁵Department of Physics, Royal Institute of Technology, Stockholm; Sweden.

¹⁴⁶Departments of Physics and Astronomy, Stony Brook University, Stony Brook NY; United States of America.

- ¹⁴⁷Department of Physics and Astronomy, University of Sussex, Brighton; United Kingdom.
- ¹⁴⁸School of Physics, University of Sydney, Sydney; Australia.
- ¹⁴⁹Institute of Physics, Academia Sinica, Taipei; Taiwan.
- ¹⁵⁰^(a)E. Andronikashvili Institute of Physics, Iv. Javakhishvili Tbilisi State University, Tbilisi; ^(b)High Energy Physics Institute, Tbilisi State University, Tbilisi; ^(c)University of Georgia, Tbilisi; Georgia.
- ¹⁵¹Department of Physics, Technion, Israel Institute of Technology, Haifa; Israel.
- ¹⁵²Raymond and Beverly Sackler School of Physics and Astronomy, Tel Aviv University, Tel Aviv; Israel.
- ¹⁵³Department of Physics, Aristotle University of Thessaloniki, Thessaloniki; Greece.
- ¹⁵⁴International Center for Elementary Particle Physics and Department of Physics, University of Tokyo, Tokyo; Japan.
- ¹⁵⁵Department of Physics, Tokyo Institute of Technology, Tokyo; Japan.
- ¹⁵⁶Department of Physics, University of Toronto, Toronto ON; Canada.
- ¹⁵⁷^(a)TRIUMF, Vancouver BC; ^(b)Department of Physics and Astronomy, York University, Toronto ON; Canada.
- ¹⁵⁸Division of Physics and Tomonaga Center for the History of the Universe, Faculty of Pure and Applied Sciences, University of Tsukuba, Tsukuba; Japan.
- ¹⁵⁹Department of Physics and Astronomy, Tufts University, Medford MA; United States of America.
- ¹⁶⁰Department of Physics and Astronomy, University of California Irvine, Irvine CA; United States of America.
- ¹⁶¹University of Sharjah, Sharjah; United Arab Emirates.
- ¹⁶²Department of Physics and Astronomy, University of Uppsala, Uppsala; Sweden.
- ¹⁶³Department of Physics, University of Illinois, Urbana IL; United States of America.
- ¹⁶⁴Instituto de Física Corpuscular (IFIC), Centro Mixto Universidad de Valencia - CSIC, Valencia; Spain.
- ¹⁶⁵Department of Physics, University of British Columbia, Vancouver BC; Canada.
- ¹⁶⁶Department of Physics and Astronomy, University of Victoria, Victoria BC; Canada.
- ¹⁶⁷Fakultät für Physik und Astronomie, Julius-Maximilians-Universität Würzburg, Würzburg; Germany.
- ¹⁶⁸Department of Physics, University of Warwick, Coventry; United Kingdom.
- ¹⁶⁹Waseda University, Tokyo; Japan.
- ¹⁷⁰Department of Particle Physics and Astrophysics, Weizmann Institute of Science, Rehovot; Israel.
- ¹⁷¹Department of Physics, University of Wisconsin, Madison WI; United States of America.
- ¹⁷²Fakultät für Mathematik und Naturwissenschaften, Fachgruppe Physik, Bergische Universität Wuppertal, Wuppertal; Germany.
- ¹⁷³Department of Physics, Yale University, New Haven CT; United States of America.
- ^a Also Affiliated with an institute covered by a cooperation agreement with CERN.
- ^b Also at An-Najah National University, Nablus; Palestine.
- ^c Also at Borough of Manhattan Community College, City University of New York, New York NY; United States of America.
- ^d Also at Center for Interdisciplinary Research and Innovation (CIRI-AUTH), Thessaloniki; Greece.
- ^e Also at Centro Studi e Ricerche Enrico Fermi; Italy.
- ^f Also at CERN, Geneva; Switzerland.
- ^g Also at Département de Physique Nucléaire et Corpusculaire, Université de Genève, Genève; Switzerland.
- ^h Also at Departament de Física de la Universitat Autònoma de Barcelona, Barcelona; Spain.
- ⁱ Also at Department of Financial and Management Engineering, University of the Aegean, Chios; Greece.
- ^j Also at Department of Physics, California State University, Sacramento; United States of America.
- ^k Also at Department of Physics, King's College London, London; United Kingdom.
- ^l Also at Department of Physics, Stanford University, Stanford CA; United States of America.

- m* Also at Department of Physics, Stellenbosch University; South Africa.
- n* Also at Department of Physics, University of Fribourg, Fribourg; Switzerland.
- o* Also at Department of Physics, University of Thessaly; Greece.
- p* Also at Department of Physics, Westmont College, Santa Barbara; United States of America.
- q* Also at Hellenic Open University, Patras; Greece.
- r* Also at Institutio Catalana de Recerca i Estudis Avancats, ICREA, Barcelona; Spain.
- s* Also at Institut für Experimentalphysik, Universität Hamburg, Hamburg; Germany.
- t* Also at Institute for Nuclear Research and Nuclear Energy (INRNE) of the Bulgarian Academy of Sciences, Sofia; Bulgaria.
- u* Also at Institute of Applied Physics, Mohammed VI Polytechnic University, Ben Guerir; Morocco.
- v* Also at Institute of Particle Physics (IPP); Canada.
- w* Also at Institute of Physics and Technology, Mongolian Academy of Sciences, Ulaanbaatar; Mongolia.
- x* Also at Institute of Physics, Azerbaijan Academy of Sciences, Baku; Azerbaijan.
- y* Also at Institute of Theoretical Physics, Ilia State University, Tbilisi; Georgia.
- z* Also at Lawrence Livermore National Laboratory, Livermore; United States of America.
- aa* Also at National Institute of Physics, University of the Philippines Diliman (Philippines); Philippines.
- ab* Also at Technical University of Munich, Munich; Germany.
- ac* Also at The Collaborative Innovation Center of Quantum Matter (CICQM), Beijing; China.
- ad* Also at TRIUMF, Vancouver BC; Canada.
- ae* Also at Università di Napoli Parthenope, Napoli; Italy.
- af* Also at University of Colorado Boulder, Department of Physics, Colorado; United States of America.
- ag* Also at Washington College, Chestertown, MD; United States of America.
- ah* Also at Yeditepe University, Physics Department, Istanbul; Türkiye.
- * Deceased